UC Davis
UC Davis Electronic Theses and Dissertations

Title

Agricultural Externalities in Interconnected Systems: Causal Evidence from Hydrological Networks and Global Commodity Markets

Permalink

https://escholarship.org/uc/item/4h0244tg

ISBN

9798193262473

Author

Chen, Tzu-Hui J.

Publication Date

2026-09-08

Peer reviewed|Thesis/dissertation

eScholarship.org Powered by the California Digital Library
University of California

Agricultural Externalities in Interconnected Systems: Causal Evidence from Hydrological Networks and Global Commodity Markets

By

TZU-HUI CHEN

DISSERTATION

Submitted in partial satisfaction of the requirements for the degree of

DOCTOR OF PHILOSOPHY

in

Agricultural and Resource Economics

in the

OFFICE OF GRADUATE STUDIES

of the

UNIVERSITY OF CALIFORNIA

DAVIS

Approved:

Aaron Smith, Co-Chair

Richard J. Sexton, Co-Chair

Kevin Novan

Committee in Charge

2026

Abstract

Agriculture provides food, fiber, and energy that are fundamental to human well-being. Yet agricultural production and policies can generate externalities, including health risks from chemical use and environmental damages from land-use change. These impacts often extend far beyond the locations where agricultural decisions are made, transmitted through interconnected natural and economic systems. This dissertation examines how hydrological networks and global commodity markets propagate agricultural externalities across space, creating consequences for populations and ecosystems far removed from production and consumption sites.

One essay in the dissertation investigates the health impacts of agricultural water pollution by examining glyphosate, the world's most widely used herbicide. Leveraging hydrological flow patterns and variations in upstream glyphosate use across watersheds and time to identify causal effects, I show that glyphosate affects populations far downstream from application sites through waterborne transmission. Using a panel dataset in the US Corn Belt from 2001 to 2014, the results suggest that a 10 kg/km^2 increase in upstream glyphosate use increases neonatal mortality by 4.6 percent in lower-income areas, with no observed effects in higher-income regions. The research design also exploits variations in spatial distance, seasonal exposure patterns, and rainfall data to isolate the effects of glyphosate contamination. Additional evidence suggests that water treatment and avoidance behaviors may mitigate exposure risks and contribute to the observed heterogeneity.

Another essay examines the global environmental consequences of biomass-based diesel (BBD) policies, highlighting how market-mediated spillovers can undermine sustainability goals. Although biofuels are intended to reduce greenhouse gas emissions from transportation, their climate benefits may be offset by indirect land-use change. Vegetable oils, including palm oil, are the main feedstock of BBD. Combining high-resolution satellite data with a causal econometric framework, this study estimates that global BBD demand from 2002 to 2018 induced the conversion of 1.7 million hectares of forest, primarily natural forests, to oil palm plantations in Indonesia and Malaysia. By modeling the global vegetable oil market, the study further shows that vegetable oils are highly substitutable. Increased demand for non-palm oils in BBD production raises palm oil demand indirectly. This expansion, driven by biomass-based diesel-induced increases in palm oil prices, accounts for approximately one-fifth of regional forest-to-palm conversion during the study period.

The resulting land-use change released more than one gigaton of CO_2, implying a higher carbon intensity for biomass-based diesel than for fossil diesel. The findings highlight how market linkages across vegetable oils transmit the effects of biofuel policies globally, causing environmental damage far from the regions where biofuels are consumed.

Collectively, this dissertation demonstrates that accounting for spatial spillovers transmitted through both natural and economic networks is essential for designing agricultural and environmental policies that fully incorporate their unintended consequences.

Acknowledgments

To my co-chairs, Rich and Aaron, I feel incredibly fortunate to have had both of you as my advisors. Throughout graduate school, your mentorship, trust, and unwavering support helped me navigate not only academic challenges but also crucial career decisions. I have learned from you what it means to be a great mentor.

I am thankful to Aaron, who has graciously taken the time to work with me. Whenever I encountered a research hurdle, his sharp intuition and knowledge of econometrics helped me navigate a way forward, and our regular discussions shaped the way I think about empirical research. Just as importantly, he never made academic work feel overwhelming. Whenever I worried that I was stuck, he would remind me that these challenges were a normal part of the process and patiently work through them with me. His confidence in me, together with his steady reassurance, gave me the confidence to keep growing.

I am grateful to Rich, whose mentorship has shaped me in ways that extend beyond research. He sees not only the big picture in economics, but also the people behind the work. Time and again, he offered support before I even knew how to ask for it—whether by creating opportunities for my research or checking in when he sensed I was struggling. I have also always been amazed by his ability to view ideas through an economic lens that reveals far more nuance than I initially saw. That combination of intellectual depth and genuine kindness is something I will carry with me throughout my career.

I am also thankful to Kevin for serving on my committee and for his invaluable guidance over the years. Kevin has a remarkable ability to explain complex concepts with clarity and simplicity, and I have benefited enormously from his insights and teaching. Beyond my committee, I am grateful to Matt, Kristin, Jamie, Steve, and Eric. Through classes, seminars, and conversations at the ARE Student Café, you have all contributed significantly to my growth as a researcher, teacher, and scholar.

I am deeply grateful to the ARE community, my classmates, officemates, the IT team, and many others, for creating such a supportive environment that nurtured my research and allowed me to grow in a warm and encouraging setting. I am also thankful to my therapist and my fellow

graduate students in group therapy; the PhD journey can be challenging, and your support gave me the strength to keep moving forward.

To my Taiwanese friends, thank you for walking with me through all these years. It has meant the world to have you by my side. I am especially grateful to Han-Ju; I feel fortunate that we navigated our PhD journeys at the same time, sharing both the highs and the lows. May we all find a place where we can feel settled and at peace.

Finally, to my mom and dad, my sisters Karen, Ivy, and Jennifer, and my boyfriend, Nick: thank you for being my foundation. Thank you to my Pum-Pum family for giving me a home filled with boundless love and unwavering support. This home, rich in love and a deep care for society, has been the driving force that keeps me moving forward. And to Nick, thank you for always being by my side. In moments of anxiety, frustration, and doubt, you have been my sanctuary. Thank you for holding me through moments of fear, for your smile and your hugs, and for sharing both the difficulties and the joys of this journey. I cannot imagine completing this PhD without all of you. While this path has not always been easy, your love has made it profoundly meaningful.

Contents

List of Figures viii

List of Tables ix

Chapter 1. Introduction 1

1.1 Overview and Framework 1

1.2 Empirical and Data Challenges 2

1.3 Using hydrological networks and a quasi-experimental design to identify the causal effects of glyphosate water pollution 3

1.4 Using empirical approaches and remote sensing data to reveal the environmental impacts of "green" biofuels 4

Chapter 2. Glyphosate Use, Water Contamination, and Neonatal Health in the United States 6

2.1 Background 11

2.1.1 Glyphosate use in the US 11

2.1.2 Glyphosate and Water 12

2.1.3 Glyphosate and Birth Outcomes 14

2.2 Methods 15

2.2.1 Identification Strategy 15

2.2.2 Data 16

2.2.3 Descriptive Statistics 20

2.3 Results 22

2.3.1 Internal Validity and other birth outcomes 24

2.3.2 Water Contamination 27

2.3.3 Agricultural Glyphosate Use 29

2.3.4 Other robustness checks 33
2.3.5 Potential Mechanisms 34
2.4 Conclusion 35
2A Appendix 37

Chapter 3. Using vegetable oils for biofuel accelerates tropical deforestation and increases carbon emissions 61
3.1 Results 63
3.1.1 Effects of BBD on palm oil prices 63
3.1.2 Effect of palm price on deforestation 65
3.1.3 Effects of BBD use on carbon emissions 68
3.2 Conclusion and discussion 70
3.3 Materials and Methods 71
3S Supplementary Materials 77

Bibliography 101

List of Figures

2.1 Main pesticide use in the US Corn Belt, 2001-2014 8

2.2 Fertilizer use in the US, 2001-2014 8

2.3 Illustrating the concepts of upstream, downstream, and local areas using Sully County, SD as an example 17

2A.1 Average glyphosate concentration by month, 2001-2014 38

2A.2 Average per capita income by income groups 56

2A.3 Change in upstream glyphosate use by income groups 56

2A.4 Average MCL violation coverage by income groups 57

2A.5 Average MR violation coverage by income groups 57

2A.6 Average annual flow rate (QA) by income groups 58

2A.7 Average annual flow rate (QC) by income groups 58

2A.8 Average annual flow rate (QE) by income groups 59

2A.9 Timeline of glyphosate exposure and birth months 60

3.1 Global use of vegetable oils for biomass-based diesel and resulting land use change and carbon emissions 63

3.2 Estimated demand and supply responses to palm oil prices 64

3.3 Effects of attainable revenue on deforestation area 67

3S.1 Real prices of major vegetable oils (2010 USD), 1960–2022 88

3S.2 Observed and BAU palm oil prices and land-use changes 88

3S.3 Correlations of yield shocks for the top two exporters of each oil crop 89

List of Tables

2.1 Descriptive Statistics 21

2.2 Glyphosate effects on neonatal mortality rate 23

2.3 Glyphosate on other birth outcomes 25

2.4 Placebo test: Downstream glyphosate effects on neonatal mortality rate 27

2.5 Glyphosate effects on neonatal mortality rate by distance 28

2.6 Glyphosate effects on neonatal mortality rate using different year definitions 30

2.7 Rainfall and seasonal heterogeneous effects on neonatal mortality rate 31

2.8 Testing the effects of overall agricultural chemicals on neonatal mortality rates 32

2.9 Robustness checks on neonatal mortality rate by different outlier definitions 34

2A.1 Relationship between glyphosate concentrations and upstream glyphosate applications 39

2A.2 Relationship between glyphosate concentrations and downstream glyphosate applications 39

2A.3 Relationship between glyphosate concentrations and upstream glyphosate applications by distances 40

2A.4 Heterogeneity in glyphosate concentrations and upstream glyphosate applications 41

2A.5 Heterogeneity in glyphosate concentrations by precipitation 41

2A.6 Nearby glyphosate effects on neonatal mortality rate 43

2A.7 Correlations between glyphosate and farm/non-farm economic conditions 43

2A.8 Correlations of water quality measures and glyphosate 45

2A.9 Glyphosate impacts on neonatal mortality with agricultural chemical controls 46

2A.10 EPA-Regulated Drinking Water Contaminants by Category 48

2A.11 Heterogeneous glyphosate effects on neonatal mortality rate by mother's demographics, private water sources, and flow rates 50

2A.12 Regression of neonatal mortality on violations 52

2A.13 Regression of local glyphosate and upstream glyphosate on covariates 53

2A.14 Glyphosate effects on neonatal mortality rate using different FE and controls 54

2A.15 Neonatal mortality effects of glyphosate: HUC4-clustered standard errors 55

2A.16 Upstream glyphosate effects on neonatal mortality: gestational length specifications 55

3.1 Carbon emissions from land-use change due to oil palm expansion 69

3S.1 Inverse palm oil demand: alternative flexible time trend specifications 90

3S.2 Inverse palm oil demand: separating oil crops with alternative flexible time trend specifications 91

3S.3 Comparison of supply elasticities and demand flexibility across time periods 92

3S.4 ADF test statistics for the log price series of major vegetable oils 93

3S.5 Long-run relationships: log palm oil and vegetable oil prices 93

3S.6 Long-run supply elasticity: competing oil crops 94

3S.7 Long-run supply elasticity of oil palm 94

3S.8 Price effects on deforestation area for palm 95

3S.9 Reverse causality check: excluding high palm-share cells 95

3S.10 Price effects on deforestation area for palm controlling for weather 96

3S.11 Attainable yield confounders: sensitivity analysis 96

3S.12 Palm price effects on deforestation: alternative price periods 97

3S.13 Palm price deviation effects on deforestation area for palm 97

3S.14 Comparison of carbon emission estimates (Mg CO_2e/ha) from land-use change across studies 98

3S.15 Demand flexibility: yield shock sensitivity checks 99

3S.16 Short-run supply elasticity (palm): yield shock sensitivity 99

3S.17 Short-run supply elasticity (other oil crops): yield shock sensitivity 99

3S.18 Long-run supply elasticity (palm): yield shock sensitivity 100

3S.19 Long-run supply elasticity (other oil crops): yield shock sensitivity 100

CHAPTER 1

Introduction

1.1. Overview and Framework

Agriculture is fundamental to human well-being, providing food, fiber, and increasingly, renewable energy. At the same time, agricultural production and policies could generate substantial externalities, including water pollution, biodiversity loss, greenhouse gas emissions, and adverse health outcomes (Kim et al., 2017; Pendrill et al., 2022; Yang et al., 2024). These effects could extend far beyond the immediate sites of production and consumption because agricultural systems are embedded within interconnected natural and economic networks that transmit impacts across geographic boundaries. Through biophysical systems, such as hydrological pathways, agricultural pollutants can travel long distances and affect connected communities and ecosystems. Through global commodity markets, policies designed to promote renewable energy can alter production and land-use incentives not only for targeted feedstocks but also for related crops in distant regions. Quantifying these externalities, including the indirect effects transmitted through physical and economic networks, is essential for understanding how the costs and benefits of agricultural production are distributed across populations and ecosystems. Such knowledge is critical for designing agricultural and environmental policies that promote both productivity and sustainability.

Chapter 2 of this dissertation examines how agricultural pollutants transmitted through hydrological networks affect human health. The analysis focuses on glyphosate and neonatal mortality. Glyphosate is the world's most widely used herbicide, and its use has increased dramatically following the adoption of glyphosate-tolerant genetically modified crops. Glyphosate can enter water systems through runoff and leaching, potentially exposing populations far from application sites. Despite its widespread use, empirical evidence on glyphosate's health effects remains limited, and the chemical continues to be the subject of intense scientific and policy debate. For example, the United States maintains that current exposure levels do not pose significant health risks, whereas the

European Union's drinking water standard for glyphosate is 7,000 times stricter. These contrasting regulatory approaches, together with growing calls to reevaluate glyphosate's toxicity (Myers et al., 2016), underscore the need for robust causal evidence on its health impacts.

Chapter 3 examines how biofuel policies transmitted through global commodity markets affect tropical deforestation and carbon emissions. The analysis focuses on biomass-based diesel (BBD), a rapidly growing substitute for petroleum diesel that primarily relies on vegetable oils as feedstocks. Although biofuel policies are designed to reduce greenhouse gas emissions, expanding demand for vegetable oils may induce indirect land-use change (ILUC) by increasing crop prices and incentivizing cropland expansion in distant regions. Because vegetable oils are close substitutes in global markets (Declerck et al., 2023; Hinrichsen, 2016), biofuel policies that rely on non-palm feedstocks could still increase palm oil prices and accelerate deforestation in major palm-producing countries. These market linkages highlight the importance of accounting for spillovers across related commodities, rather than evaluating policies solely through the lens of individual crops.

1.2. Empirical and Data Challenges

Identifying the causal effects of agricultural externalities poses several empirical challenges, chief among them endogeneity. In the context of pollution, exposure and health outcomes are often confounded by unobserved socioeconomic factors (Chay and Greenstone, 2005). For example, agricultural chemical use is closely linked to local agricultural development, infrastructure, and regional economic conditions, which may independently influence public health outcomes (Osawa et al., 2016; Useche et al., 2009; Wang et al., 2017). Quantifying effects transmitted through global commodity markets introduces an additional source of endogeneity: the simultaneous determination of prices and production decisions (Roberts and Schlenker, 2013). Disentangling these overlapping causal pathways requires isolating exogenous variation within both physical transport systems and market networks.

Beyond these identification challenges, empirical research in this area is constrained by data limitations. Sparse monitoring of chemical contaminants in water systems has left water pollution both understudied and underregulated (Keiser and Shapiro, 2019). Likewise, traditional administrative data often lack the spatial resolution and temporal coverage needed to accurately measure

land-use change and deforestation (Burgess et al., 2012). Because the environmental and social consequences of agricultural activities vary substantially across locations, high-resolution spatial data are essential for measuring these externalities and understanding their heterogeneous effects.

To address these challenges, this dissertation leverages quasi-experimental research designs and advances in spatial data availability, combining information from hydrological networks, administrative records, and high-resolution remote sensing datasets. The following sections preview the methodologies and findings of the dissertation's two central questions: how agricultural pollution affects infant health and how biofuel policies shape land-use change. Together, these chapters demonstrate how natural and economic networks propagate agricultural externalities across space, highlighting the importance of accounting for distant and unintended consequences in agricultural and environmental policymaking.

1.3. Using hydrological networks and a quasi-experimental design to identify the causal effects of glyphosate water pollution

Estimating the health effects of glyphosate exposure is challenging because both exposure and health outcomes are correlated with local socioeconomic conditions, while direct measures of glyphosate contamination in water systems are limited. To address these challenges, Chapter 2 exploits hydrological flow patterns to identify the causal effects of upstream glyphosate use on downstream birth outcomes. Using a panel dataset covering counties in the US Corn Belt from 2001 to 2014, I combine information on watershed connectivity, pesticide applications, birth outcomes, and socioeconomic characteristics. This research design mitigates endogeneity concerns by leveraging variation in upstream glyphosate use that is plausibly exogenous to downstream socioeconomic conditions. Additional variation in spatial distance, seasonal exposure timing, and rainfall patterns helps isolate the effects of waterborne glyphosate contamination from localized socioeconomic confounders.

The results indicate that a 10 kg/km^2 increase in upstream glyphosate use increases neonatal mortality by 4.6 percent in lower-income areas, with no detectable effects in higher-income regions. Based on average application rates and birth counts during the study period, glyphosate use is estimated to contribute to 87.6 additional neonatal deaths annually in lower-income communities

across the US Corn Belt. Additional analyses suggest that water treatment infrastructure and avoidance behaviors may contribute to the observed heterogeneity.

This chapter provides new evidence on the health impacts of glyphosate exposure through water systems and advances understanding of heterogeneous effects and their underlying mechanisms. The findings contribute to the environmental justice literature by demonstrating that lower-income communities bear a disproportionate share of the health burden from agricultural pollution and offer insights for policy design by highlighting potential mitigation strategies. More broadly, this chapter contributes to the economics literature on water pollution, an area that remains relatively understudied due in part to data constraints (Keiser and Shapiro, 2019). By examining the effects of glyphosate application rather than localized measures of glyphosate concentration, this study overcomes key data limitations and provides evidence of an important agricultural externality.

1.4. Using empirical approaches and remote sensing data to reveal the environmental impacts of "green" biofuels

Chapter 3 examines the environmental consequences of biomass-based diesel (BBD) through indirect land-use change (ILUC). Existing evidence on biofuel-induced ILUC relies largely on ex-ante modeling frameworks, which yield highly divergent estimates (Broch et al., 2013; Cui and Martin, 2017; Taheripour and Tyner, 2020; Warner et al., 2014). Many of these models do not account for unmanaged land or accurately predict where land-use change occurs, introducing uncertainty into carbon emission estimates (Berry et al., 2024; Warner et al., 2014). Their results are also sensitive to assumptions regarding consumer behavior, yield responses, and substitution across agricultural commodities (Berry et al., 2024; Daioglou et al., 2020). Consequently, the carbon intensity values derived from these models, which are widely used in policy design, often differentiate biofuels by feedstock while overlooking cross-commodity market substitutions that ultimately drive land-use change.

To address these limitations and empirically quantify market-mediated spillovers, this chapter integrates econometric analysis with high-resolution remote sensing data. We first estimate how global BBD demand affects palm oil prices through supply and demand interactions among major vegetable oils, using exogenous yield shocks to identify the supply and demand models. We then

use panel data on forest-to-palm conversion across 32,305 grid cells in Indonesia and Malaysia from 2002 to 2018 to identify the causal effects of palm oil prices on deforestation. Finally, the analysis combines these estimates and integrates spatial information on forest cover, biomass, peatlands, and plantation expansion to estimate the carbon emissions associated with BBD-induced deforestation.

This empirical approach reduces reliance on ex-ante assumptions by directly observing historical land-use change. The use of remote sensing data improves the accuracy of emission estimates, captures heterogeneity in environmental values across landscapes, and overcomes limitations of administrative data, including the incomplete reporting of illegal deforestation.

Our results indicate that global BBD demand from 2002 to 2018 induced the conversion of approximately 1.7 million hectares of forest to oil palm plantations in Indonesia and Malaysia. Because palm oil and other vegetable oils are close substitutes, policies that rely on non-palm vegetable oil feedstocks can still increase palm oil prices and indirectly drive deforestation. This policy-driven land-use change primarily occurred in natural forests and released more than one gigaton of CO_2 emissions, implying a higher net carbon intensity for BBD than for fossil diesel. These findings demonstrate how global commodity markets transmit the environmental consequences of biofuel policies across commodities and regions and underscore the importance of accounting for indirect land-use change when designing renewable energy policies.

The remainder of this dissertation is organized as follows. Chapter 2 presents the empirical analysis of upstream glyphosate use and downstream neonatal health outcomes in the US Corn Belt. Chapter 3 evaluates the global market-mediated impacts of biomass-based diesel policies on tropical deforestation and carbon emissions.

CHAPTER 2

Glyphosate Use, Water Contamination, and Neonatal Health in the United States

Herbicides are widely used in modern agriculture, with glyphosate—commonly known by its trade name, Roundup—being the most extensively applied worldwide. Since the introduction of genetically modified (GM) glyphosate-tolerant crops in 1996, global glyphosate use has surged fifteenfold (Benbrook, 2016). As of 2024, more than 90 percent of soybeans and corn grown in the US are GM herbicide-tolerant crops, with most treated with glyphosate. By providing an easy method for weed control, glyphosate has contributed to food production (Duke and Powles, 2008). However, despite its widespread use and agricultural benefits, research on its potential health risks remains largely limited to animal and laboratory studies. Ongoing debates over glyphosate's effects on human health continue to fuel scientific and regulatory discussions (Tiramani et al., 2017; Mendez et al., 2022).

This study provides empirical evidence of glyphosate's health impacts on the general population through its presence in water systems. Glyphosate can be transported to surface and groundwater through mechanisms such as rainfall and leaching, potentially affecting populations far from the application sites. In the United States, which uses nearly 20 percent of the world's glyphosate, the Environmental Protection Agency (EPA) has assessed that current usage levels do not pose significant health risks. In contrast, some countries have adopted more stringent regulations. For example, the European Union's standards for glyphosate in drinking water are 7,000 times stricter than those in the US. Over the past decade, studies have also called for a reevaluation of its toxicity (Myers et al., 2016).

A version of this material has been published as: Chen (2026). "Glyphosate use, water contamination, and neonatal health in the united states." *Journal of the Association of Environmental and Resource Economists*, 13(3):755–790.

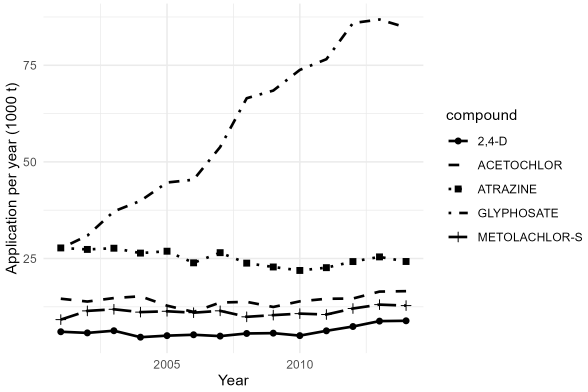
Investigating glyphosate's causal health effects presents challenges typical of pollution studies. Pollution levels and outcomes often correlate with unobserved socioeconomic factors, leading to endogeneity issues (Chay and Greenstone, 2005). For instance, factors such as land use, genetically modified crops, and glyphosate use decisions may not be independent of local agricultural development and socioeconomic conditions (Osawa et al., 2016), such as land ownership, farm sizes (Wang et al., 2017), income, and attitudes towards pesticide and genetically modified crops (Useche et al., 2009). These conditions can also influence health outcomes. Given the impossibility of randomly assigning glyphosate to humans, causal evidence on its health effects remains limited.

To address this identification challenge, this study employs a quasi-experimental framework using water flow mechanisms to investigate the effects of upstream glyphosate on downstream birth outcomes. This approach builds on the work of previous studies, such as those by Dias et al. (2023) and Skidmore et al. (2023). This design mitigates endogeneity concerns, as the correlation between socioeconomic factors of each county and upstream pesticide use is low. I construct a panel dataset covering 13 states from 2001 to 2014 in the US Corn Belt. The US is a major glyphosate user in the world, with the Corn Belt accounting for two-thirds of its glyphosate use.

The study also takes advantage of the distinct rise in glyphosate use during the sample period. Figure 2.1 illustrates trends in major pesticide use, while Figure 2.2 depicts fertilizer use. While glyphosate use increased dramatically during the study period, the use of other agricultural chemicals remained relatively stable. This sharp variation in glyphosate use, combined with water flow data, allows for the isolation of its effects, making it unlikely that other socioeconomic factors or chemicals confound the results. The research design further incorporates variations in spatial distances, seasonal exposure patterns, and rainfall data to ensure that the observed health impacts are attributable to glyphosate water contamination rather than coincidental factors.

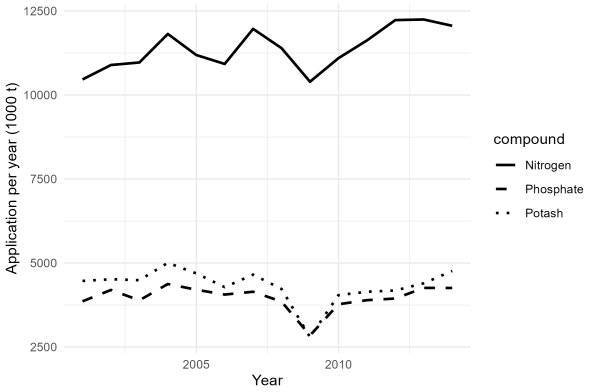
This quasi-experimental design reveals that a 10 kg/km^2 increase in glyphosate use in upstream watersheds within 200km leads to 0.153 neonatal deaths per thousand births or a 4.6 percent neonatal mortality rate increase in lower-income areas, with no discernible effects in higher-income areas. Considering that annual glyphosate use upstream on average is 23.46 kg/km^2 from 2001 to 2014 and the average annual number of newborns is 243,645 in the lower-income areas of the Corn Belt, glyphosate use in the study period corresponds to 87.6 annual neonatal deaths (90%

FIGURE 2.1. Main pesticide use in the US Corn Belt, 2001-2014



Source: USGS

FIGURE 2.2. Fertilizer use in the US, 2001-2014



Source: USDA

confidence interval [32.2, 142.9]). The effects are more pronounced in areas with younger, less educated mothers, higher proportions of white residents, and greater reliance on private wells, but are weaker in areas with timely water system violation notifications. These findings suggest that avoidance behaviors and water treatment may mitigate glyphosate's health impacts. Additionally, the results suggest that glyphosate leads to a higher preterm birth rate. It's worth noting that this study focuses solely on glyphosate's impact on infants and does not consider its effects on older individuals, implying that the overall health impacts may be larger than indicated by the aforementioned numbers.

Prior studies have sought to understand glyphosate's health impacts. However, beyond laboratory experiments, most studies only investigate correlations between glyphosate and birth outcomes, rather than establishing causation (Lacroix and Kurrasch, 2023). These studies primarily examine the relationship between urinary glyphosate concentrations and birth outcomes in humans, often relying on small, regional samples with limited diversity in racial/ethnic and socioeconomic characteristics. The non-random nature of glyphosate exposure makes it challenging to address confounders and provide causal evidence, while the lack of sample diversity limits the ability to explore heterogeneous effects (Parvez et al., 2018; Silver et al., 2021; Gerona et al., 2022; Lesseur et al., 2022).

One exception is Dias et al. (2023), who leverage water flow patterns in Brazil to identify a causal effect: 10 kg/km^2 of upstream glyphosate use in Brazil results in 0.39 additional infant

deaths per 1,000 births. Building on their foundation, this study examines the health impacts of glyphosate in the US and further explores heterogeneous effects across socioeconomic contexts. The effects in US low-income areas are smaller than the average effects in Brazil, and the effects are insignificant in US high-income areas.

Studying waterborne glyphosate's impact in a developed country such as the US, as well as its heterogeneous effects, has several important implications. First, the health impacts of pollution are likely to highly depend on government regulations and individual behaviors. Differences in the magnitude of glyphosate's effects across and within countries not only add to our understanding of environmental justice but also shed light on the underlying mechanisms and potential mitigation strategies. Prior research shows that pollution disproportionately affects low-income and minority communities (Banzhaf et al., 2019). This study contributes to this body of knowledge by demonstrating that glyphosate more negatively impacts lower-income areas in the US, despite these areas experiencing lower levels of upstream glyphosate use. Intermediate factors, such as water treatment infrastructure and avoidance behaviors, may play critical roles in explaining these heterogeneous effects, and improving them could mitigate the health impacts.

Second, glyphosate remains at the center of political and scientific debates. Uncovering evidence of glyphosate's impacts across multiple countries reinforces the potential widespread effects, while disentangling exposure mechanisms is essential for effective regulation and targeted mitigation. Although few studies offer causal evidence on glyphosate's health effects, most focus on developing countries (Camacho and Mejía, 2017; Dias et al., 2023; Skidmore et al., 2023). An exception is Reynier and Rubin (2025), who estimate that local glyphosate use reduces birthweight and gestational length in rural US counties using an instrumental variables strategy. However, their analysis does not isolate specific exposure pathways-it remains unclear whether the observed effects result from direct contact, drift, or waterborne transmission. In an appendix, they attempt to assess waterborne exposure using machine learning-predicted glyphosate concentrations, but the predictions have limited accuracy.[1] In contrast, my study directly links upstream glyphosate application to downstream birth outcomes using hydrological flow, providing a more transparent

[1]Reynier and Rubin (2025)'s out-of-sample R^2 values are 0.59 (random forest) and 0.31 (LASSO), indicating some degree of noise in predicted glyphosate concentrations. They find no significant waterborne effects on birthweight-consistent with my results-and do not examine glyphosate water exposure effects on other birth outcomes.

and policy-relevant proxy for waterborne exposure. This approach allows me to isolate the health effects of glyphosate transmitted through water and to focus on neonatal mortality—an outcome not examined in Reynier and Rubin (2025).

Third, developed countries such as the US typically have better-quality data than developing countries. This study benefits from access to fine-grained glyphosate usage data, whereas Dias et al. (2023) imputed local usage from national-level glyphosate use and relied on estimated potential yield gains from the adoption of genetically modified seeds to correct measurement errors. The availability of more precise data in this study allows for a more direct link between glyphosate exposure and health outcomes.

Beyond the literature on health impacts and environmental justice, this study makes two specific economic contributions. First, it advances the economics of water pollution, a field often constrained by limited data on chemical concentrations in water (Keiser and Shapiro, 2019). By focusing on glyphosate application rather than concentration, I identify agricultural externalities that would otherwise remain undetectable due to sparse monitoring data. Second, this study refines the cost-benefit analysis of GM crop and biofuel policies. GM crops and biofuel production are significant sources of glyphosate use. While previous research emphasizes the benefits of these technologies for farm income and rural development (Qaim, 2009; Ali and Abdulai, 2010), the paper highlights an important uncounted cost. The results suggest that glyphosate-induced adverse birth outcomes constitute a significant negative externality that must be weighed against the economic benefits of these policies.

The remainder of this paper is structured as follows: Section 2.1 provides the changes in glyphosate use in the US, and elucidates the mechanism linking glyphosate contamination to infant health via water sources. Section 2.2 elaborates on the identification strategies, empirical model, and the dataset employed in the analysis. Section 2.3 presents the findings and includes detailed robustness checks. Finally, Section 2.4 discusses the implications and limitations of the study's findings and offers concluding remarks.

2.1. Background

This section outlines the relationship between glyphosate usage in the US, water contamination, and potential health impacts, providing background and supporting evidence for this study.

2.1.1. Glyphosate use in the US

Glyphosate serves as a broad-spectrum herbicide used for weed control. The US is a major glyphosate user, accounting for nearly 20 percent of global usage. Since its introduction in 1974, over 1.6 billion kilograms of glyphosate have been used in the US. The introduction and adoption of GM glyphosate-resistant seeds accelerated glyphosate usage starting in 1996. Approximately 67 percent of the total glyphosate used in the US from 1974 to 2014 was applied in the last 10 years of that period (Benbrook, 2016). Glyphosate is mainly sprayed on corn and soybeans, which are predominantly planted in the Corn Belt. In 2014, glyphosate comprised over 40 percent of all pesticide use in the Corn Belt, according to the USGS. The Corn Belt accounts for about two-thirds of glyphosate use in the US. The expansion of the Renewable Fuel Standard in 2007 led to a marked increase in demand for corn ethanol, resulting in more land being planted with corn and further driving up glyphosate use. Figure 2.1 displays the top-utilized pesticides in the US Corn Belt. It reveals that glyphosate use surged with the adoption of GM crops and had an additional increase around 2007 due to the expansion of corn-based biofuels.

Glyphosate application primarily occurs from April to September. The planting season for corn in the Corn Belt is from April to early June, while for soybeans it spans from May to early July (USDA, 2010). For corn, glyphosate is recommended to be broadcast on the top of the corn plants until they reach 30 inches in height, and applied using drop nozzles when the plants are between 30 and 48 inches tall, typically within 60 days after planting (Ransom and Endres, 2020; Bayer Crop Science, 2020; Bayer Crop Science, 2024). For soybeans, it is generally advised to apply no later than the second reproductive stage, typically within 46 to 83 days after planting (Jhala, 2017; Naeve, 2018; Endres and Kandel, 2021).

2.1.2. Glyphosate and Water

Glyphosate has been increasingly detected in water sources. Several studies have examined the connection between agricultural activities and glyphosate concentrations in water (Aparicio et al., 2013; Medalie et al., 2020). For instance, Coupe et al. (2012) identified glyphosate in water within agricultural basins such as Iowa and Mississippi, noting that concentrations align with crop application patterns. Although glyphosate monitoring has been infrequent and limited in spatial coverage, its detection in US water systems has risen since the 2000s (Battaglin et al., 2014; Shoda et al., 2020). The Water Quality Portal (WQP) compiles glyphosate data from agencies including the US Geological Survey (USGS), the USDA Agricultural Research Service (ARS), and the EPA. Appendix Figure 2A.1 shows a clear seasonal pattern in glyphosate concentrations in natural water systems, and Tables 2A.1–2A.3 demonstrate strong correlations between these concentrations and upstream agricultural use. Glyphosate's half-life in water varies between 2 to 91 days, averaging around 40 days (Coupe et al., 2012; Battaglin et al., 2014), depending on factors such as light exposure, microbial activity, and soil absorption (Mallat and Barcelo, 1998).

When glyphosate enters water systems, it can contaminate drinking water (Rendon-von Osten and Dzul-Caamal, 2017; Lima et al., 2022; Brown and Farenhorst, 2024). The US EPA regulates glyphosate, along with over 90 other chemicals, in drinking water.[2] Since 1992, the maximum contamination level (MCL) for glyphosate has been set at 700 $\mu g/L$, compared to 500 $\mu g/L$ in Brazil, 280 $\mu g/L$ in Canada, and 0.1 $\mu g/L$ in the European Union. Public water systems are required to monitor glyphosate once or twice every three years after the initial compliance period, depending on the population served.[3] No public water system exceeded the MCL during the study period, and systems are not obligated to publicly report if detections are below this threshold, leaving exact contamination data for drinking water unavailable.

States are responsible for enforcing water regulations and can adopt stricter standards. However, enforcement stringency varies due to factors such as state budgets, congressional voting patterns, and community characteristics (Sigman, 2005; Grant and Grooms, 2017; Elrod et al., 2019). Public water systems can apply for waivers to reduce monitoring requirements.

[2]Appendix 2A.4 provides detailed information on monitoring procedures and the full list of regulated chemicals.
[3]Title 40: Code of Federal Regulations, Chapter I, Subchapter D, Part 141, Subpart C, §141.24.

Water systems may treat water through various treatments. Studies suggest that methods like adsorption, advanced oxidation processes, and filtration can reduce glyphosate in water supplies (Jönsson et al., 2013; Espinoza-Montero et al., 2020). However, in 2006, about 31 percent of public water systems, or 17 percent of those using their own sources, did not treat their water. Approximately 75 percent of systems rely on groundwater, with nearly half using only disinfection (EPA, 2009). Drinking water quality remains a major environmental concern in the US (Keiser and Shapiro, 2019). Violations among public water systems are prevalent, particularly in lower-income, rural, and non-white communities (Allaire et al., 2018; Mueller and Gasteyer, 2021; Teodoro et al., 2018) and in smaller water systems (Rubin, 2013; EPA, 2014).

Public water systems are required to notify residents about violations. While violations may signal poor water quality, they can also prompt information and potentially trigger avoidance behaviors. For Maximum Contaminant Level (MCL) violations, notifications must be sent within 30 days—or within 24 hours for certain chemicals. In contrast, Monitoring and Reporting (MR) violations only require notification within one year. Marcus (2022) finds that immediate notifications (within 24 hours) of coliform MCL violations increase bottled water consumption and mitigate adverse health impacts. Hadachek (2024) observes higher bottled water consumption and even reduced infant mortality rates following nitrate MCL violations, particularly in areas with lower poverty rates. The finding suggests that public notifications can lead some individuals to consume safer water, improving health outcomes.

On the other hand, some Americans rely on private water sources rather than public water supplies. According to USGS estimates, from 2000 to 2015, approximately 18.5 percent of the population across the thirteen Corn Belt states primarily sourced their water from private wells. These sources are not regulated by the EPA under the Safe Drinking Water Act (Pieper et al., 2015; Malecki et al., 2017), making private owners responsible for their water quality. Studies suggest private water quality could be poor, though wealthier individuals tend to test and treat their water more frequently and effectively, resulting in better water quality (Smith et al., 2014; Flanagan et al., 2015; Malecki et al., 2017).

2.1.3. Glyphosate and Birth Outcomes

Through drinking water, glyphosate can affect people far from its application sites. Curwin et al. (2006) and Connolly et al. (2022) detected glyphosate in human urine, finding it not only among farmers and workers directly involved in its application but also among the general population. Grau et al. (2022) found lower glyphosate detection associated with filtered water consumption. In a study by Ospina et al. (2022), glyphosate was quantified in urine samples from 2,310 individuals in the US during 2013-2014, with glyphosate detected in 81 percent of the samples. Moreover, glyphosate exposure extends to pregnant women. Several studies found that more than 90 percent of urine samples from pregnant women in the Midwest and other regions of the US contained glyphosate residues (Gerona et al., 2022; Parvez et al., 2018; Lesseur et al., 2022). Some studies tracking human exposure to glyphosate over time have reported increasing proportions of individuals with detectable levels of glyphosate in their urine (Mills et al., 2017; Gillezeau et al., 2019).

Glyphosate can reach pregnant women and ultimately affect the fetus. Studies have detected glyphosate in the serum of pregnant women at childbirth and in umbilical cord serum (Kongtip et al., 2017) and shown that glyphosate can cross the placental barrier (Mose et al., 2008; Poulsen et al., 2009). In vitro experiments show that glyphosate exposure can trigger apoptosis and necrosis in embryonic and placental cells (Benachour et al., 2007; Tajai et al., 2023), even at concentrations far lower than typical agricultural use and corresponding to levels of indirect exposure (Richard et al., 2005; Benachour and Séralini, 2009). Additionally, glyphosate exposure could induce oxidative stress and inflammation, potentially leading to preterm births (Lesseur et al., 2022).

In summary, this background section underscores the nexus between glyphosate usage, water contamination, and potential health implications, notably regarding birth outcomes. The following section on methodologies will detail the analytical approaches I employ to investigate the causal link between glyphosate exposure and neonatal health outcomes.

2.2. Methods

2.2.1. Identification Strategy

To construct an empirical model for identifying the birth impacts of glyphosate, I leverage the glyphosate use changes observed in the 13 states comprising the Corn Belt from 2001 to 2014.[4] Glyphosate use in the Corn Belt drastically increased during the study period. The use of glyphosate in 2014 was three times the amount in 2001. Over this period, these 13 Corn Belt states collectively used 822.4 million kilograms of glyphosate active ingredient, accounting for 66 percent of the total glyphosate use in the United States.

Estimating the impact of glyphosate on health outcomes requires addressing endogeneity issues, as socioeconomic factors often influence planting and pesticide choices. I leverage water flows to examine the effects of upstream pesticide use changes on downstream health outcomes, following Dias et al. (2023) and Skidmore et al. (2023). This design mitigates endogeneity concerns as upstream pesticide adoption is less likely to correlate with socioeconomic factors in downstream areas. Specifically, I use the following equation to identify glyphosate's impact on birth outcomes:

$$Y_{it} = \theta up_gly_{it} + \boldsymbol{X_{it}'}\boldsymbol{\beta} + \alpha_i + \delta_{st} + \mu_{it}. \tag{2.1}$$

where Y_{it} denotes a specific birth outcome in county i in year t, up_gly captures the amount of glyphosate use upstream from county i, $\boldsymbol{X_{it}}$ is a set of time-varying control variables, and α_i and δ_{st} denote county and state-year fixed effects, respectively. The base model uses state-year fixed effects because states implement and determine the stringency of water regulations, which may change over time. The Appendix Table 2A.14 provides estimates using year fixed effects. To further address endogeneity concerns, the model includes a comprehensive set of time-varying controls. These controls encompass demographics (mother's age, race, marital status, country of origin, hypertension, and diabetes ratios), economic factors (including income, unemployment rate, poverty rate, and agricultural employment share), industrial water pollution, and medical resources

[4]These states include Illinois, Indiana, Iowa, Kansas, Kentucky, Michigan, Minnesota, Missouri, Nebraska, North Dakota, Ohio, South Dakota, and Wisconsin. This timeframe was selected based on data availability and to capture a balanced period before and after the 2007 RFS expansion.

(hospital beds, other health providers per thousand population, and per square kilometer). This study not only considers medical resources per capita but also their density, as spatial distances are also a factor affecting birth outcomes (Blondel et al., 2011; Daysal et al., 2015).

Given potential heteroskedasticity—where the variance of the error term may differ across counties due to differences in population size—regressions are weighted by the mean number of newborns in each county over the study period. Counties with fewer births tend to exhibit greater variability in neonatal mortality rates because of small sample sizes. Weighting helps transform heteroskedastic errors into homoskedastic ones (Smith and Taylor, 2017) and make the regression close to the population target (Angrist and Pischke, 2009). Furthermore, because glyphosate exposure from upstream sources tends to be spatially correlated within watersheds, I apply robust standard errors clustered at the watershed level.

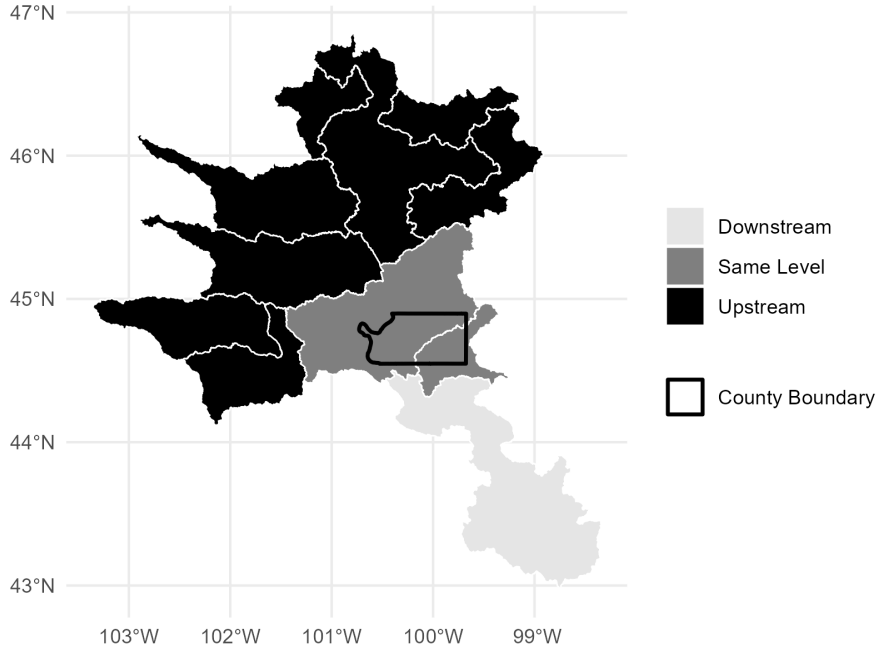
2.2.2. Data

To conduct the analysis, I compiled detailed data on glyphosate use, socioeconomic factors, medical resource metrics, and birth outcomes from 2001 to 2014. Below, I outline the sources of data and the methods used to construct variables.

Glyphosate and Watersheds County-level annual glyphosate usage estimates from 2001 to 2014 are sourced from the US Geological Survey (USGS). To identify glyphosate applied upstream, I connect the glyphosate use data with the Watershed Boundary Dataset (WBD) and Mainstem Rivers of the Conterminous United States (ver. 2.0, Feb 2023) from the USGS.

The WBD provides hydrologic units (HUs) that define drainage areas to streams and rivers based on topographic, hydrologic, and relevant landscape characteristics without regard for administrative or political boundaries. Six levels of HUs, ranging from 2- to 12-digit codes, constitute the hierarchical dataset. Two-unit hydrologic unit codes (HUC2) identify the highest level of drainage areas and are further divided into HUC4, HUC6, HUC8, HUC10, and HUC12. Mainstem Rivers of the Conterminous United States (ver. 2.0, Feb 2023) provides information on the hydrologic unit network, defining the upstream and downstream of each unit. HU8 is the smallest level with complete information, and this study employs HU8 units to define the upstream of each county.

FIGURE 2.3. Illustrating the concepts of upstream, downstream, and local areas using Sully County, SD as an example



In total, 496 HU8s cover the counties in the Corn Belt, with an average area of 4,539.9 square kilometers and a median of 3,665.0 square kilometers.

Figure 2.3 illustrates the upstream and downstream concepts. To determine the hydrologic unit to which each county belongs, I overlay county boundaries with HU8 boundaries. HU8s that intersect with county boundaries are considered the same level for each county and are shown in dark gray. The upstream and downstream HU8s of the intersected HU8 represent the upstream and downstream areas relative to each county and are shown in black and light gray, respectively. This study primarily focuses on upstream areas defined as HU8s within a 200 km radius from the centroid of each county and HU8. Section 2.3.2 examines alternative definitions of upstream areas based on different distances.

Glyphosate use in each county's upstream is computed using the amount of glyphosate applied per square kilometer (tonne/km^2) in its upstream HU8s. I determine the glyphosate use for each HU8 by the amount applied per square kilometer across all intersecting counties, weighted by the proportion of the intersection area. I also incorporate the amount of glyphosate per square kilometer applied within each county as locally applied glyphosate, serving as a control.

Birth Outcomes Birth outcomes are extracted from the US National Center for Health Statistics (NCHS) vital statistics. The dataset comprises birth records with county-level geographical identifiers and comprehensive maternal information. The main focus is on the neonatal mortality rate (NMR), but I also investigate other birth outcomes, including infant mortality rate (IMR), preterm birth rates (PTBR), term birth weight, and low birth weight rate of term births (LBWR).

NMR is defined as the ratio of neonatal deaths before one week due to health causes per thousand newborns. I exclude deaths caused by external factors like accidents or assaults, as glyphosate is unlikely to influence these external deaths. However, I also examine external NMR for internal validity. IMR considers infant deaths due to health causes up to one year after birth. PTBR is the ratio of babies born alive before 37 weeks of pregnancy completion per 1,000 newborns. Term birth is defined as births occurring between 37 weeks and 41 weeks, and LBWR is the ratio of term birth babies weighing less than 2,500 g per thousand term births.

I calculate birth outcome variables using births conceived within the same calendar year to better match glyphosate exposure, as using birth years would misalign births with minimal exposure to glyphosate in that year. Since glyphosate affects unborn children in utero and most birth outcomes are measured at or shortly after birth, infants born early in a year are more exposed to glyphosate use from the previous year. Therefore, I compute birth outcomes using a conception-year approach, averaging the outcomes for births occurring from September of one year through August of the following year.[5] I also explore averaging the outcomes across different months and report the results in Section 2.3.3.

The dataset includes demographic information on the mother's age, marital status, race, education, birth country, health conditions (hypertension and diabetes), and details about newborns, such as birth order and plurality (single, twin, triplet, etc.). I use this information as controls.

Other Variables To control additional socioeconomic factors and consider regional health service availability, I incorporate data from the Bureau of Economic Analysis (BEA), the Bureau of Labor Statistics (BLS), and the Health Resources & Services Administration's (HRSA) Area

[5]Appendix Figure 2A.9 illustrates the timeline of glyphosate application, birth month, and conception month, showing how using conception year better matches births to the glyphosate application than using birth year. I also consider constructing the conception year using birth month and gestational length. However, since most counties have some missing data on gestational lengths, using only the counties with complete information results in missing observations. Relying solely on births with recorded gestational lengths can lead to inaccurate variables, especially when there are missing data in mortality files.

Health Resource Files (AHRF) sourced from Griffith et al. (2021). These data provide information on the number of hospital beds, health providers other than hospitals, income, poverty rate, unemployment rate, and agricultural employment ratios at the county level. Income is deflated using the GDP deflator sourced from BEA.

Industrial water pollution serves as an important control to eliminate the possibility of health impacts from other pollutants besides glyphosate. The data are from the EPA's Risk-Screening Environmental Indicators (RSEI), which integrates information from the Toxics Release Inventory (TRI). TRI records toxic chemical releases reported by industrial and federal facilities, regulated by the EPA due to significant adverse health effects. EPA constructs the RSEI and calculates toxicity-weighted water pollution concentrations for each flowline in the US based on TRI data along with the chemical's fate and transport through the environment.[6] To estimate county-level industrial water pollution, this study averaged concentrations across flowlines, weighted by flowline length. I exclude outlier flowlines with a concentration exceeding the 99.99th percentile to address potential reliability issues with self-reported TRI data.[7] Table 2.9 shows the consideration of various outlier thresholds. Additionally, I examine other top pesticides used and corn and soybean areas in the Corn Belt to ensure the observed effects stem from glyphosate. I source pesticide data from the USGS and area data from the USDA. I compute the upstream use of each pesticide and upstream corn and soybean area using the same methods outlined in Section 2.2.2 for upstream glyphosate estimates.

Violation records of public water systems are sourced from the Safe Drinking Water Information System (SDWIS) of the EPA. This dataset encompasses basic information about all public water systems in the US. Information regarding water sources, specifically the percentage of people using private water sources, is obtained from the USGS. This data is presented on a 5-year basis. Monthly precipitation data for the Corn Belt is procured from the PRISM Climate Group, featuring a 4km resolution. I aggregate the data to the upstream watershed level for analysis. Water quality metrics—including dissolved oxygen deficit (DOD), nitrate and nitrite nitrogen, phosphorus, total suspended solids (TSS), Escherichia coli (E. coli), and total coliform—are sourced from the Water Quality Portal (WQP).

[6] A flowline represents a segment of a stream. It is the basic unit of analysis in the RSEI water Microdata.
[7] https://www.epa.gov/system/files/documents/2022-07/rsei-documentation-geographic-microdata-july-2022.pdf

2.2.3. Descriptive Statistics

Table 2.1 provides descriptive statistics for 1126 counties in the Corn Belt from 2001 to 2014. The data are stratified by lower-income and higher-income areas due to significantly different glyphosate health effects observed in counties with varying income levels.[8]

Lower-income and higher-income counties exhibit systematic differences across most birth outcomes, glyphosate use, and socioeconomic factors. Lower-income counties tend to have worse birth outcomes compared to their higher-income counterparts. Neonatal mortality rates, infant mortality rates, and preterm birth rates are all higher while birth weight is lower in lower-income areas. The mean of external neonatal mortality rates does not differ between the two regions.

Unlike most pollution, on average, glyphosate use is lower in lower-income areas than in higher-income areas. In contrast, industrial water pollution tends to be more concentrated in lower-income areas, a pattern consistently observed in many studies (Currie, 2011; Banzhaf et al., 2019), although the difference is not statistically significant. Lower-income counties exhibit higher poverty and unemployment rates, with a slightly lower share of the population working in agriculture. There are notable differences in mothers' characteristics. Mothers in lower-income areas tend to be younger, single, and less likely to have college degrees compared to those in higher-income areas. Higher-income areas have slightly more non-Hispanic blacks and fewer non-Hispanic white individuals, likely due to greater racial diversity in urban areas. Lower-income areas have a higher prevalence of mothers with hypertension, while the incidence of diabetes is slightly lower.

In terms of medical resources, lower-income areas have fewer hospital beds and health providers per thousand persons and lower spatial density. They also have a higher proportion of residents relying on private water sources and violation records for both MR and MCL.

Geographically, many lower-income counties are located in the southeastern Corn Belt, while higher-income counties are concentrated in the northwest (Appendix Figures 2A.2). Figures 2A.3 present maps of changes in glyphosate use by income group. Counties with high glyphosate use changes are generally centered in the middle of the region, but both lower- and higher-income areas include counties with varying levels of change. In terms of hydrological characteristics, rivers in

[8]Lower-income areas are counties with average incomes lower than the median average income in the Corn Belt, encompassing 13 states.

TABLE 2.1. Descriptive Statistics

	Lower-income		Higher-income		Diff
	mean	sd	mean	sd	
	(1)	(2)	(3)	(4)	(5)
Birth outcomes					
Number of newborns	434.70	1192.18	1090.38	3832.71	655.68*
Neonatal mortality rate	3.29	4.68	3.18	7.20	-0.11
External neonatal mortality rate	0.01	0.28	0.01	0.21	-0.00
Neonatal mortality rate (< 28 days)	4.16	5.23	3.80	7.56	-0.36*
Infant mortality rate (< 1 year)	6.24	6.58	5.36	9.07	-0.89*
Preterm birth rate	119.72	34.09	108.42	39.37	-11.30*
Birth weight	3379.71	67.48	3413.50	76.50	33.80*
Glyphosate					
Upstream glyphosate (tonne/km^2)	0.023	0.024	0.033	0.027	0.01*
Downstream glyphosate (tonne/km^2)	0.026	0.021	0.035	0.023	0.009*
Local glyphosate (tonne/km^2)	0.026	0.026	0.038	0.030	0.012*
Economic covariates					
Income per capita (thousand dollars)	32.82	4.38	43.41	8.96	10.59*
Unemployment rate	7.32	2.64	4.90	2.00	-2.42*
Poverty rate	16.14	6.12	10.78	3.04	-5.36*
% employment in agriculture	9.52	7.07	10.63	9.23	1.10
Demographic covariates					
% married	61.18	10.44	69.67	10.21	8.49*
% mothers born outside of the US	4.14	6.11	6.50	7.31	2.36*
% non-hispanic black	2.41	5.48	2.69	5.77	0.29
% non-hispanic white	89.28	15.97	87.76	12.05	-1.52
Mother's age	26.10	0.97	27.41	1.11	1.31*
% of mothers with a college degree	17.31	7.18	28.83	9.74	11.52*
Birth order	2.20	0.24	2.20	0.23	0.00
Number of plurality	1.032	0.02	1.035	0.03	0.003*
% diabetes	5.09	2.78	5.31	3.40	0.23*
% hypertension	7.11	3.10	6.40	3.32	-0.71*
Industrial water pollution					
Industrial pollution concentrations	13.22	175.59	6.37	103.34	-6.85
Medical resources					
Hospital beds per capita*1000	2.80	4.07	5.11	6.76	2.32*
Health providers per capita*1000	0.31	0.23	0.43	0.40	0.11*
Hospital beds density	0.08	0.22	0.21	0.64	0.13*
Health provider density	0.005	0.01	0.009	0.02	0.003*
Water quality					
% using private wells	31.98	24.11	26.28	17.11	-5.71*
MCL violation coverage (%)	8.26	18.30	6.86	17.33	-1.40*
MR violation coverage (%)	13.08	22.64	7.74	16.42	-5.34*
Other					
Monthly upstream precipitation in Apr-Sep	88.11	43.71	79.46	35.04	-8.64*
Monthly upstream precipitation in Oct-Mar	56.52	34.97	35.84	25.17	-20.68*
Flow rate (QA)	1263.47	5509.75	587.58	1835.87	-675.89*
Flow rate (QC)	1091.37	4978.60	468.41	1516.93	-622.96*
Flow rate (QE)	1431.59	6692.02	598.51	1924.74	-833.07*

Notes: Column (5) presents the differences in sample means between groups of counties by median income and test results of the null hypothesis of equality of means via regressions of each variable on a dummy variable representing higher-income areas. Standard errors are clustered at the watershed (HU8) level. * denotes significance at the 5 percent level. Approximately 9 percent of counties have missing data on mother's education. The statistics reported here pertain to the remaining data for the % of mothers with a college degree.

lower-income counties have higher average flow rates.[9] However, this difference is largely driven by a few counties through which the mainstem of the Mississippi River flows, resulting in extremely high flow values (Figures 2A.6–2A.8). Figures 2A.4–2A.5 show MCL and MR violation coverage by income group. While violations tend to be more common in lower-income areas on average, the spatial distribution of violations differs from income patterns and shows substantial variation within each group.

The high standard deviations of the birth outcomes are attributed to low population counts and newborn numbers in some counties, resulting in extreme values when only a few births occur and some have unfavorable birth outcomes. To address this issue, I exclude counties with fewer than 25 newborns in any year from the analysis. Different thresholds for extreme values are also explored, with results presented in Section 2.3.4.

2.3. Results

Table 2.2 presents the main estimates of upstream glyphosate on neonatal mortality rate (NMR). The results suggest that glyphosate has significant effects in lower-income areas, but not in higher-income areas. Column (1) demonstrates the estimates of glyphosate use upstream on local NMR for all counties in the Corn Belt. The estimate is small and insignificant, suggesting that glyphosate seems to not affect NMR. However, upon closer examination in Column (2), glyphosate actually exhibits heterogeneous effects on different income areas. The coefficients of interactions of upstream glyphosate with the first and second income quartiles are significantly positive. Columns (3) to (8) focus on lower-income areas, and upstream glyphosate estimates are consistently significant across various settings.

In more detail, the estimate in Column (3) comes from the model without any time-varying controls, while the estimates in Columns (4)-(7) are obtained from a model sequentially adding economic, demographic, industrial pollution, and medical resource covariates, excluding local glyphosate use. Column (8) further presents the results with local glyphosate added to the controls. The coefficient values in these six columns are similar. Column (8) reveals that a 1 tonne/km^2 increase

[9]Flow rate data are from EPA's NHDPlus Version 2 dataset, which provides three estimates: QA (mean annual flow from runoff), QC (reference-gage regression), and QE (gauge-adjusted flow). County-level measures are constructed as flowline-length-weighted averages.

TABLE 2.2. Glyphosate effects on neonatal mortality rate

	All counties		Lower-income areas					
	(1)	(2)	(3)	(4)	(5)	(6)	(7)	(8)
Upstream glyphosate	1.847	-2.315	15.08**	15.78**	15.65***	15.55***	15.95***	15.32***
	(3.815)	(4.119)	(6.502)	(6.091)	(5.738)	(5.728)	(5.763)	(5.869)
Upstream glyphosate × income quartile 1		15.51*						
		(8.044)						
Upstream glyphosate × income quartile 2		9.166*						
		(4.838)						
Upstream glyphosate × income quartile 3		3.502						
		(4.612)						
Local glyphosate	2.983	2.357						1.538
	(3.359)	(3.304)						(5.503)
Observations	14,630	14,630	7,770	7,770	7,770	7,770	7,770	7,770
R-squared	0.026	0.027	0.031	0.032	0.038	0.038	0.038	0.038
Number of counties	1,045	1,045	555	555	555	555	555	555
Economic covariates	Yes	Yes	No	Yes	Yes	Yes	Yes	Yes
Demographic covariates	Yes	Yes	No	No	Yes	Yes	Yes	Yes
Industrial pollution covariates	Yes	Yes	No	No	No	Yes	Yes	Yes
Medical resource covariates	Yes	Yes	No	No	No	No	Yes	Yes

Notes: The dependent variable is neonatal mortality rates. The first row shows the sample areas. See Table 2.1 for a full list of the economic, demographic, industrial, and medical resource control variables. The variable for mother's college education is excluded from the controls due to missing data. However, the results remain consistent when excluding these counties and including college education as a covariate in the regressions. All regressions incorporate county and state-year fixed effects, and within-R^2 values are reported. Robust standard errors clustered at the watershed (HU8) level are shown in parentheses: *** p<0.01, ** p<0.05, * p<0.1.

in upstream glyphosate use is associated with approximately a 15.32 increase in neonatal deaths per thousand newborns. This translates to a 0.153 increase in the neonatal mortality rate per 10 kg/km^2 of glyphosate, which represents a 4.6 percent increase, based on the average neonatal mortality rate of 3.295 in lower-income areas. Considering the average annual glyphosate use of 23.46 kg/km^2 and an average annual birth count of 243,645 in lower-income areas of the Corn Belt, glyphosate use during the study period is associated with 87.6 neonatal deaths annually (90% confidence interval [32.2, 142.9]).

The minimal impact of controls also suggests that the correlation between upstream glyphosate use and observed socioeconomic factors and mothers' original characteristics in a county is low, reducing the likelihood of omitted variable biases. Appendix Table 2A.13 presents regressions of local glyphosate and upstream glyphosate on covariates. The estimates indicate that local glyphosate use is correlated with various covariates, including income and unemployment rate, while the correlations between upstream glyphosate and covariates are low, providing additional evidence to support this identification strategy. It's important to note that the estimated glyphosate

contamination effect on birth outcomes could be considered a lower bound, as it only considers upstream glyphosate use, excluding local glyphosate use.

The estimate of local glyphosate use is positive but insignificant and small. Local glyphosate effects are likely confounded by the correlation between glyphosate adoption, agricultural development, and socioeconomic effects, as previous studies and the estimates in Table 2A.13 suggest. Regarding the choice of fixed effects, I also explore different fixed effects for the lower-income areas and report the results in Table 2A.14, with all estimates for control variables reported. The results suggest similarity across year fixed effects and state-year fixed effects. Standard errors are clustered at the HU8 level, which was used to determine glyphosate usage, though I also investigate broader watersheds to account for sufficient spatial correlation. Table 2A.15 replicates Table 2.2, except that standard errors are clustered at the HU4 level, yielding similar values. [10]

For the differing effects of upstream glyphosate use on lower-income and higher-income areas, table 2.1 reveals some potential reasons. Although glyphosate is used upstream, whether it reaches humans and whether people take avoidance actions could be some key factors in the differing outcomes. Lower-income areas have more people relying on private water sources, which are often less likely to regularly be tested or treated (Pieper et al., 2015; Malecki et al., 2017). Individuals with higher incomes or other characteristics might be more inclined to use filters, possess better filtration systems, or opt for bottled water (Triplett et al., 2019; Hadachek, 2024). Also, whether one can access or afford medical resources might contribute to this variance. Lower-income areas exhibit fewer hospital beds and health providers in terms of both the number per thousand population and spatial density. Section 2.3.5 and Appendix 2A.5 will discuss these potential mechanisms in detail and explore heterogeneity with regard to more dimensional factors. Hereafter, I focus on lower-income areas.

2.3.1. Internal Validity and other birth outcomes

The previous section reveals a correlation between glyphosate use and neonatal mortality rates (NMR). This section assesses the internal validity and explores biological mechanisms by examining glyphosate's effects on various birth outcomes. Table 2.3 provides estimates of glyphosate's impact

[10] In total, 72 HU4 cover the counties in the Corn Belt. HU2 is the largest hydrologic unit, with only eight of them covering the Corn Belt.

TABLE 2.3. Glyphosate on other birth outcomes

	External NMR	Internal NMR (<28 days)	Internal IMR (<1 year)	PTBR	LBWR	Birth weight
	(1)	(2)	(3)	(4)	(5)	(6)
Upstream glyphosate	0.111	17.68***	13.25	106.0**	-19.48	11.38
	(0.313)	(6.797)	(8.816)	(52.34)	(24.55)	(86.44)
Local glyphosate	-0.282	1.766	1.715	45.22	38.35**	29.56
	(0.269)	(5.871)	(7.104)	(40.32)	(19.00)	(75.18)
Observations	7,770	7,770	7,770	7,770	7,770	7,770
R-squared	0.018	0.041	0.048	0.230	0.068	0.176
Number of counties	555	555	555	555	555	555
Full controls	Yes	Yes	Yes	Yes	Yes	Yes

Notes: The regressions focus on the lower-income areas. The first row indicates the dependent variable of each regression. See the notes to Table 2.2 for the controls. All regressions incorporate county and state-year fixed effects, and within-R^2 values are reported. Robust standard errors clustered at the watershed (HU8) level are shown in parentheses: *** p<0.01, ** p<0.05, * p<0.1.

on other birth outcomes, utilizing full control, and county and state-year fixed effects, same as the specification in Table 2.2 Column (8).

Column (1) presents a placebo test for internal validity, using external NMR—deaths from external causes such as accidents-which should remain unaffected by upstream glyphosate use. The result is a small, insignificant estimate, aligning with expectations. Column (2) shows that a 1 kg/km^2 increase in glyphosate use upstream is associated with approximately a 0.177 neonatal death increase per thousand newborns when considering NMR with deaths less than 28 days old. Compared to the point estimates of glyphosate effects on NMR within one week, about 86 percent of the NMR less than 28 days happens in one week, suggesting glyphosate has relatively mild effects on infants who already survive for a period. The estimate for glyphosate effects on infant mortality rates (IMR), accounting for infant deaths up to one year old, is positive as shown in Column (3), but with a p-value of 0.13 and with a smaller magnitude. One reason for this could be that higher mobility after giving birth compared to during pregnancy leads to less accurate glyphosate exposure variables. Additionally, prenatal glyphosate exposure has moderate effects on infants who have already survived, and the deaths of other reasons may add noise when considering a longer period.

Preterm birth and low birth weight are some of the main causes of neonatal death.[11] I further examine glyphosate effects on preterm birth rate (PTBR), low birth weight rate (LBWR), and birth weight to identify the biological mechanisms. Column (4) shows a statistically significant association between increased glyphosate use and higher preterm birth rates, suggesting that preterm birth may be a pathway for increased mortality. However, in terms of LBWR and birth weight, the estimates appear inconsistent. For LBWR, the upstream glyphosate estimate is not significant, while a positively significant estimate appears for local glyphosate. As for birth weight, glyphosate seems to have no effect.

These findings suggest that birth weight may not be a primary pathway linking glyphosate water exposure to neonatal mortality. One explanation is that birth weight is not necessarily better when higher, as large for gestational age (LGA) is a risk factor for birth complications and long-term health issues (Weschenfelder et al., 2019). Additionally, birth weight is highly correlated with maternal pre-pregnancy weight and gestational weight gain (Zhao et al., 2018). Mothers may control weight gain not only for health reasons but also due to societal pressure (Keyser-Verreault, 2023). This pattern aligns with several studies that find glyphosate exposure is more strongly associated with preterm birth than with birth weight or low birth weight (Ling et al., 2018; Parvez et al., 2018; Savitz et al., 1997). It is broadly consistent with Reynier and Rubin (2025), who also find that glyphosate shortens gestation, though they report more robust negative effects on birth weight. This divergence may reflect differences in exposure pathways: their study focuses on local glyphosate use in rural areas, which may capture more direct or multiple routes of exposure, while mine isolates effects transmitted through water, for which birth weight potentially might not be a key mechanism. Differences in population characteristics could also contribute to the heterogeneity.

Overall, the results indicate a correlation between upstream glyphosate use and neonatal deaths short after birth in lower-income areas, but not with mortality due to external causes. To validate the robustness of these findings and demonstrate that the effects are causal and indeed attributable to water contamination from agricultural glyphosate use rather than other factors, I conducted several checks focusing on NMR in lower-income areas. These exercises provide additional supporting evidence for the observed correlations.

[11] https://www.who.int/news-room/fact-sheets/detail/preterm-birth; https://www.who.int/publications/i/item/WHO-NMH-NHD-19.21

TABLE 2.4. Placebo test: Downstream glyphosate effects on neonatal mortality rate

	(1)	(2)	(3)	(4)	(5)	(6)
Downstream glyphosate	-1.294	0.127	0.0916	-0.109	0.0166	-5.669
	(7.740)	(7.952)	(8.220)	(8.232)	(8.063)	(9.145)
Local glyphosate						7.739
						(6.196)
Observations	7,770	7,770	7,770	7,770	7,770	7,770
R-squared	0.030	0.031	0.037	0.037	0.037	0.038
Number of counties	555	555	555	555	555	555
Economic covariates	No	Yes	Yes	Yes	Yes	Yes
Demographic covariates	No	No	Yes	Yes	Yes	Yes
Industrial pollution covariates	No	No	No	Yes	Yes	Yes
Medical resource covariates	No	No	No	No	Yes	Yes

Notes: The regressions focus on the lower-income areas. The dependent variable is neonatal mortality rates. See the notes to Table 2.2 for the controls. All regressions incorporate county and state-year fixed effects, and within-R^2 values are reported. Robust standard errors clustered at the watershed (HU8) level are shown in parentheses: *** p<0.01, ** p<0.05, * p<0.1.

2.3.2. Water Contamination

In this section, I demonstrate that the observed effects stem from water contamination rather than other spatial correlations or alternative channels. I first use available glyphosate concentration data to examine correlations between measured concentrations and glyphosate applications to support the water-contamination mechanism. Concentrations are significantly correlated with upstream use within 200 km, but not beyond, and not with downstream use (Appendix 2A.1), suggesting that upstream glyphosate application flows to nearby downstream areas.

If birth outcome effects were driven by other spatial channels rather than water contamination, downstream glyphosate use would still have an impact. Table 2.4 challenges this alternative channel hypothesis by testing the effects of downstream glyphosate in lower-income areas using the same specifications as Table 2.2, Columns (3)–(8). The results show that downstream glyphosate effects are consistently small and insignificant across all models, reinforcing the argument that waterborne contamination is the primary mechanism. Similarly, regressions incorporating glyphosate use in nearby areas as an independent variable yield insignificant estimates (Table 2A.6).

I next examine glyphosate effects at greater upstream distances. The results indicate that effects are present within 200 km upstream but diminish beyond this distance, becoming small

TABLE 2.5. Glyphosate effects on neonatal mortality rate by distance

	Baseline: 0-200km	200-400km	400-600km	600-800km	All distances
	(1)	(2)	(3)	(4)	(6)
Upstream glyphosate	15.32***	7.678	0.557	3.652	
	(5.869)	(7.339)	(8.419)	(11.25)	
Upstream glyphosate (0-200km)					14.71**
					(6.255)
Upstream glyphosate (200-400km)					5.929
					(9.078)
Upstream glyphosate (400-600km)					-15.30
					(13.91)
Upstream glyphosate (600-800km)					12.12
					(17.01)
Observations	7,770	7,770	7,770	7,770	7,770
R-squared	0.038	0.038	0.038	0.038	0.039
Number of counties	555	555	555	555	555
Full controls	Yes	Yes	Yes	Yes	Yes

Notes: The regressions focus on the lower-income areas. The first row shows the upstream distance of glyphosate being considered. For details on the controls, refer to the notes in Table 2.2. All regressions include county and state-year fixed effects, and within-R^2 values are reported. Robust standard errors clustered at the watershed (HU8) level are shown in parentheses: *** p<0.01, ** p<0.05, * p<0.1.

and insignificant (Table 2.5). This pattern closely aligns with the relationship between upstream glyphosate application and measured concentrations: concentrations are strongly correlated with glyphosate use within 200 km but not beyond (Table 2A.3). This evidence suggests that the observed effects are not driven by broader agricultural conditions or methodological issues, but rather result from upstream contamination in nearby areas.

I also assess potential economic spillovers as an alternative pathway. Glyphosate use or the adoption of GM crops could impact local industries by boosting agricultural productivity, reducing labor demand for weed control, and reallocating labor to non-agricultural sectors or livestock production. Table 2A.13 already shows correlations between upstream glyphosate and various local conditions are low, which mitigates this concern. However, to fully assess this, I regress various economic indicators on glyphosate use, with results and a detailed discussion in Appendix Section 2A.2 and Table 2A.7. Most estimates suggest no significant spillover effects, though a few are borderline significant. Notably, the results suggest, if spillovers exist, they may actually be beneficial for birth outcomes, implying that the main estimates could be conservative.

Airborne glyphosate transport is another alternative channel, but this is unlikely. Glyphosate degrades rapidly in the air, and its concentrations are generally too low to travel significant distances

(Martins-Gomes et al., 2022). Camacho and Mejía (2017) found that aerial spraying negatively affects health, but these effects were observed from local applications. Since my regressions control for local glyphosate use, airborne exposure is already accounted for. Moreover, if air transport were a major factor, we would expect effects beyond downstream regions. The inclusion of nearby glyphosate use as a control further addresses this concern and again yields insignificant estimates, strengthening the case that the primary exposure pathway is through water.

2.3.3. Agricultural Glyphosate Use

In this section, I provide further evidence that the observed effects on birth outcomes are directly attributable to agricultural glyphosate use. While the previous section established that these effects stem from water contamination, it remains possible that other water contaminants could be responsible, such as co-occurring agricultural chemicals or industrial pollutants. I have included industrial water pollution as a control variable, which mitigates some of this concern. However, this does not fully account for other untracked pollutants.

To address this concern, I examine whether the effects align with glyphosate's unique application and transport patterns. Specifically, I analyze seasonal exposure variations, the role of rainfall in glyphosate runoff, and potential confounding by other agricultural chemicals.

Pesticide use exhibits seasonal variation, influencing environmental exposure and potential health effects (Calzada et al., 2023). Farmers in the U.S. Corn Belt apply glyphosate from April to September, and concentration data in Appendix 2A.1 and prior studies have documented peak glyphosate concentrations in water during the application period (Coupe et al., 2012). Researchers have also found that exposure during early pregnancy has stronger effects on birth outcomes (Ling et al., 2018; Gerona et al., 2022). If glyphosate drives the observed effects, its impact should follow a seasonal pattern.

To test this, I redefine birth measurement periods and examine how glyphosate's estimated effects change across different definitions. Table 2.6 presents the results. When considering infants born in the same calendar year as glyphosate application (Column 1: Birth year), the estimates are small and statistically insignificant. However, when shifting the period to include births from

TABLE 2.6. Glyphosate effects on neonatal mortality rate using different year definitions

	Birth year	Feb-Jan	Mar-Feb	Apr-Mar	May-Apr	Jun-May	Jul-Jun	Aug-Jul	Sep-Aug	Oct-Sep	Nov-Oct	Dec-Nov	One year lead
	(1)	(2)	(3)	(4)	(5)	(6)	(7)	(8)	(9)	(10)	(11)	(12)	(13)
Upstream glyphosate	7.634	7.746	7.912	9.914	10.55	11.20*	14.85**	15.51***	15.32***	11.12*	11.48*	11.52*	10.06
	(6.517)	(6.604)	(6.645)	(6.409)	(6.584)	(6.426)	(6.210)	(5.877)	(5.869)	(6.223)	(6.188)	(6.112)	(6.186)
Local glyphosate	-0.318	2.062	3.539	2.514	2.385	2.765	1.015	1.225	1.538	0.772	-0.582	-0.989	-1.097
	(5.718)	(5.602)	(5.532)	(5.560)	(5.557)	(5.712)	(6.089)	(5.797)	(5.503)	(5.563)	(5.772)	(6.001)	(6.185)
Observations	7,770	7,770	7,770	7,770	7,770	7,770	7,770	7,770	7,770	7,770	7,770	7,770	7,770
R-squared	0.044	0.044	0.045	0.041	0.040	0.038	0.037	0.036	0.038	0.041	0.041	0.043	0.042
Number of counties	555	555	555	555	555	555	555	555	555	555	555	555	555
Full controls	Yes	Yes	Yes	Yes	Yes	Yes	Yes	Yes	Yes	Yes	Yes	Yes	Yes

Notes: The regressions focus on the lower-income areas. The first row reports the year definition of each regression. For example, Column (1) includes infants born in the same calendar year as glyphosate application, while Column (2) considers infants born from February to the following January. For details on the controls, see the notes in Table 2.2. All regressions include county and state-year fixed effects, and within-R^2 values are reported. Robust standard errors clustered at the watershed (HU8) level are shown in parentheses: *** p<0.01, ** p<0.05, * p<0.1.

later months (Columns 2 to 9), the effects become larger and more significant, revealing a clear seasonal trend.

This pattern supports the role of glyphosate exposure. Infants born early in the calendar year had no exposure to that year's glyphosate since they were born before the application period. Those born during the application season were primarily exposed in late pregnancy, when susceptibility is lower. The strongest effects emerge when considering birth cohorts from August to the following July or September to the following August—aligning with the conception year used in this study, when the cohorts match glyphosate exposure and exposure during early pregnancy is highest. Appendix Figure 2A.9 illustrates this alignment, showing how using conception year better matches birth cohorts to the relevant glyphosate application period than using birth year.[12]

Further, the estimated effects diminish as additional later months are considered. The statistical significance disappears after one year (Column 13) as many infants are not affected by glyphosate used in the previous year. This provides evidence that the observed effects stem from glyphosate exposure rather than confounding factors that do not follow the same seasonal pattern. The results also serve as a placebo check: the effects only appear when birth cohorts match glyphosate exposure timing, reinforcing internal validity and ruling out methodological coincidence.

Furthermore, glyphosate is transported into water systems primarily through runoff, making precipitation a key factor in determining exposure. If the observed health effects are driven by

[12]Table 2A.16 presents the results using the conception year computed by birth month and gestational length. The effects are similar to the main results with a slightly larger magnitude, likely because this method captures more direct glyphosate effects but at the cost of missing observations.

TABLE 2.7. Rainfall and seasonal heterogeneous effects on neonatal mortality rate

	Rainfalls	
	April-Sep	Oct-Mar
	(1)	(2)
Upstream glyphosate	5.032	1.031
	(8.945)	(10.50)
Rainfall quartile 2 × upstream glyphosate	7.480	15.45
	(6.757)	(9.837)
Rainfall quartile 3 × upstream glyphosate	10.32	15.42
	(6.859)	(11.34)
Rainfall quartile 4 × upstream glyphosate	18.74**	13.56
	(7.662)	(11.51)
Local glyphosate	2.152	2.291
	(5.469)	(5.440)
Observations	7,770	7,770
R-squared	0.040	0.040
Number of counties	555	555
Full controls	Yes	Yes

Notes: The regressions focus on the lower-income areas. Columns (1) and (2) show regression results with interactions between rainfall quartiles and glyphosate use. The regressions also control for unreported rainfall quartiles. The second row specifies the months of rainfall considered. For details on controls, see Table 2.2. All regressions include county and state-year fixed effects, and within-R^2 values are reported. Robust standard errors clustered at the watershed (HU8) level are shown in parentheses: *** p<0.01, ** p<0.05, * p<0.1.

glyphosate contamination rather than other pollutants, we should observe stronger effects when upstream rainfall is higher during the application season.

To examine this, I interact glyphosate use with quartiles of monthly upstream precipitation data, both within and outside the application season. The precipitation quartiles are defined across counties and years, following Dias et al. (2023). Column (1) of Table 2.7 shows that the interaction between glyphosate and the highest quartile of rainfall during the application season yields a significantly positive coefficient. The estimate for the third quartile is also positive but smaller and statistically insignificant, while effects for the second quartile are even weaker. This suggests that significant rainfall amplifies glyphosate's impact, consistent with runoff-driven water contamination. In contrast, Column (2) finds no significant interactions between glyphosate and rainfall quartiles from October to March, further confirming that glyphosate's effects depend on seasonal rainfall.

TABLE 2.8. Testing the effects of overall agricultural chemicals on neonatal mortality rates

	(1)	(2)
Corn and soybeans area	0.0341	0.0231
	(0.0273)	(0.0280)
Upstream glyphosate		14.31**
		(6.038)
Local glyphosate	5.531	1.678
	(5.465)	(5.506)
Observations	7,770	7,770
R-squared	0.038	0.039
Number of counties	555	555
Full controls	Yes	Yes

Notes: The regressions focus on the lower-income areas. For details on the controls, see the notes in Table 2.2. All regressions include county and state-year fixed effects, and within-R^2 values are reported. Robust standard errors clustered at the watershed (HU8) level are shown in parentheses: *** p<0.01, ** p<0.05, * p<0.1.

A remaining concern is whether other agricultural pollutants following seasonal patterns could be confounding the glyphosate estimates. However, this is unlikely. Glyphosate use surged during the study period due to GM crop adoption, while the use of other agricultural chemicals remained relatively stable. If other chemicals were driving the effects, we would expect NMR to correlate with overall agricultural activity, not just glyphosate use.

To test this, I analyze the relationship between NMR and upstream acreage of corn and soybeans—the primary crops treated with both glyphosate and other agricultural chemicals in the Corn Belt. Table 2.8 presents the results. Column (1) shows a weak, statistically insignificant correlation between NMR and upstream crop acreage ($p = 0.21$). In Column (2), when upstream glyphosate use is included, the coefficient for crop acreage becomes even less significant, while glyphosate use remains highly significant. This suggests that glyphosate, rather than other agricultural chemicals, is the primary driver of the observed health effects.

Further, I examine correlations between glyphosate use and various agricultural water quality measures (Hooda et al., 2000; Kato et al., 2009; Keiser and Shapiro, 2018; Liu et al., 2023). Regressions in Appendix Table 2A.8 show no significant correlations. The results support the notion that glyphosate use increased distinctly during the study period and does not significantly covary with these water quality measures. However, weak positive associations are found with phosphorus ($p = 0.20$) and nitrate/nitrite nitrogen ($p = 0.14$), which are linked to fertilizer use. To rule out confounding, I add nitrogen and phosphorus as controls in the NMR regressions. Table 2A.9, Columns (1)-(4), shows that glyphosate's estimated effects remain stable regardless of these controls. Columns (5)-(6) further test other widely used pesticides, yet glyphosate's estimate remains consistently significant. These findings reinforce that glyphosate, rather than other agricultural pollutants, is responsible for the observed neonatal health effects.

2.3.4. Other robustness checks

Previous sections demonstrate that glyphosate impacts birth outcomes in lower-income areas due to agricultural glyphosate water pollution. The next step is to ensure the robustness of the chosen thresholds for extreme values. I test various thresholds to examine their impact on the conclusion of glyphosate effects. Table 2.9 displays the estimates obtained from different outlier definitions. The baseline models in the analysis consider counties with 25 or more births annually, as some neonatal mortality rates may be extremely high due to the small number of births in certain counties. Columns (1) and (2) present estimates with stricter criteria: counties with 50 or more births and those with 100 or more births, respectively. These results are consistent with the baseline findings.

Columns (3) and (4) address the outlier definition based on industrial water pollution indicators (RSEI). Column (3) presents the estimate with industrial water pollution averaged across flowlines below the 99.95th percentile, while Column (4) reports the estimates without any exclusions, whereas the baseline considers flowlines below the 99.99th percentile. Notably, all estimates remain similar across different threshold choices, indicating the robustness of the results.

TABLE 2.9. Robustness checks on neonatal mortality rate by different outlier definitions

	Births ≥ 50	Births ≥ 100	W/O RSEI $>$ 99.95 percentile	W/ all RSEI
	(1)	(2)	(3)	(4)
Upstream glyphosate	14.60**	16.61***	15.60***	15.31***
	(6.020)	(5.859)	(5.870)	(5.882)
Local glyphosate	2.079	2.809	1.362	1.645
	(5.575)	(5.719)	(5.504)	(5.535)
Observations	7,336	6,230	7,770	7,770
R-squared	0.040	0.044	0.038	0.038
Number of counties	524	445	555	555
Full controls	Yes	Yes	Yes	Yes

Notes: The regressions focus on the lower-income areas. The first row shows the considered subsample. For control details, refer to Table 2.2. All regressions include county and state-year fixed effects, and within-R^2 values are reported. Robust standard errors clustered at the watershed (HU8) level are shown in parentheses: *** p<0.01, ** p<0.05, * p<0.1.

2.3.5. Potential Mechanisms

Previous sections demonstrate the robust and significant effects of glyphosate on neonatal mortality rates in lower-income areas. A further consideration is why these effects are primarily observed in lower-income areas rather than in higher-income ones, with a detailed discussion provided in Appendix 2A.5.

Evidence indicates that water consumption behaviors and water treatment may play important roles in shaping exposure risks and contribute to the observed heterogeneity. Stronger impacts are observed in areas with younger, less educated, and more non-Hispanic white mothers (Table 2A.11, Columns 1–3), populations that are more likely to rely on tap water directly (Park et al., 2022; Triplett et al., 2019; Yang and Faust, 2019). At the same time, higher-income individuals are more likely to use bottled water and filters (Pieper et al., 2015; Malecki et al., 2017). In addition, glyphosate's effects are stronger in areas that rely more heavily on private water sources (Table 2A.11, Column 4), which lack regulation and systematic treatment. Because lower-income areas have a higher share of private water users, these patterns suggest that differential water treatment may also be an important contributor to the heterogeneous effects.

2.4. Conclusion

This study provides robust evidence of the impacts of glyphosate, the most commonly used herbicide, on birth outcomes through water contamination. By employing a quasi-experimental framework that considers water contamination mechanisms and various robustness checks, the research establishes a causal relationship between glyphosate and adverse birth outcomes. The evidence suggests that a 10 kg/km^2 increase in glyphosate application in upstream watersheds within 200km leads to a 4.6 percent increase in neonatal deaths per thousand births in lower-income areas, with no significant effects observed in higher-income areas. The average glyphosate use in the upstream regions of lower-income areas in the Corn Belt is 23.46 kg/km^2 per year in the study period, which corresponds to an estimated 87.6 additional neonatal deaths annually. This finding adds new information to the ongoing controversy surrounding glyphosate.

The two potential mitigation strategies include the use of bottled or filtered water by consumers and the treatment of public water systems to remove glyphosate. Although using filters and bottled water would have individuals pay the social costs. Using bottled water for drinking and cooking could cost a family between $983 and $4,757 annually (Javidi and Pierce, 2018), and the spending often accounts for a higher proportion of income for minorities (Gorelick et al., 2011). Moreover, without adequate contamination information, individual efforts may be inefficient. Enhancing water quality monitoring and providing timely contamination information could improve individual decision-making.

On the other hand, A review of US drinking water regulations indicates that treatment requirements for water systems often provide greater benefits than costs (Keiser and Shapiro, 2019). Methods such as adsorption, advanced oxidation processes (AOPs), and filtration can reduce glyphosate in water supplies (Jönsson et al., 2013; Espinoza-Montero et al., 2020). Among these, filtration is the most widely used but offers moderate glyphosate removal (Jönsson et al., 2013). AOPs are promising but require further research for large-scale deployment (Feng et al., 2020). Adsorption, such as via activated carbon, is both effective and already in use—one study finds that activated carbon can remove over 99 percent of glyphosate (Grant et al., 2018).

Based on estimated costs of granular activated carbon (GAC) ranging from $0.10 to $0.36 per 1,000 gallons (Heberling et al., 2015, 2022) and an average daily per capita water use of

86 gallons from USGS, annual per-person treatment costs would range from approximately $3 to $10.80—substantially lower than bottled water.[13] A back-of-the-envelope calculation suggests that reducing one neonatal death through this strategy would cost between $0.67 million and $2.4 million.[14] GAC also removes other harmful contaminants such as PFAS and pesticides, offering additional public health benefits (Belkouteb et al., 2020; DiStefano et al., 2022).[15] While more research is needed for a full cost-benefit analysis, these estimates suggest that public water treatment could be a cost-effective mitigation strategy.

Another potential strategy is to reduce glyphosate use at the source. This study shows that upstream applications can harm downstream populations, highlighting a clear externality. These findings offer economic justification for stronger upstream regulations, such as buffer zones or application limits. That said, tighter controls must consider the costs and benefits. This study does not quantify the full social cost of glyphosate use, but it presents evidence that the associated health costs may be substantial and should be considered in future regulatory evaluations.

Overall, this research contributes to the growing body of literature on glyphosate's health impacts on indirectly exposed populations, specifically in relation to birth outcomes. Further investigation is needed to explore the effects of glyphosate exposure on human health across different demographics.

[13]GAC costs are reported in 2016 dollars. Average daily per capita water use is from the USGS (https://www.epa.gov/watersense/statistics-and-facts).

[14]This estimate is based on a population of 19.6 million in lower-income Corn Belt counties, 87.6 neonatal deaths annually, and the simplifying assumption that glyphosate removal averts all associated deaths. If one were to use the value of a statistical life as a benchmark for benefits, the implied benefit of preventing one neonatal death would be $9.9 million (2016$) in the US (https://www.transportation.gov/office-policy/transportation-policy/revised-departmental-guidance-on-valuation-of-a-statistical-life-in-economic-analysis), which is substantially larger than the estimated costs.

[15]https://www.epa.gov/sdwa/overview-drinking-water-treatment-technologies

2A. Appendix

2A.1. Glyphosate concentration

To examine the relationship between glyphosate application and water concentrations, I use data from the Water Quality Portal (WQP), which compiles publicly available glyphosate concentration measurements from the USGS, USDA ARS, and EPA. However, glyphosate concentration data suffer from sparse coverage: over 80% of counties in the Corn Belt lack any glyphosate monitoring, and among those with data, about 70% have observations from only a single year.

Due to the limited number of repeated observations per county, it is not feasible to include county fixed effects to capture within-county temporal variation. I pool the data across counties and years and include fixed effects and covariates to account for both temporal (monthly) and spatial (geography) confounders. I estimate the following pooled cross-sectional model:

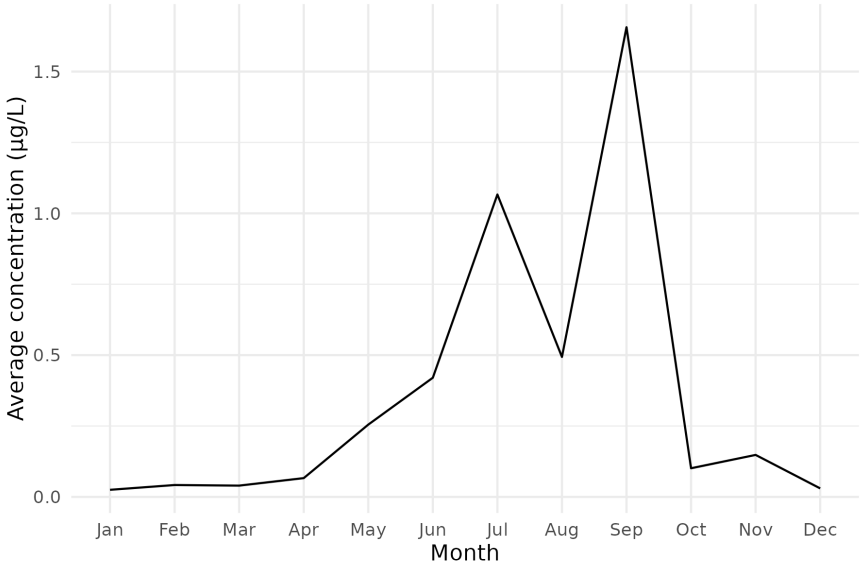
$$C_{ijtmh} = \alpha_0 + \alpha_1 \, up_gly_{it} + \alpha_h + \tau_m + \boldsymbol{X}_i'\gamma + fr_i + \varepsilon_{ijtmh}$$

where C_{itmh} denotes the glyphosate concentration record j in county i, year t, HU2 h, and month m, up_gly_{it} represents glyphosate application upstream of county i in year t, α_h captures HU2 fixed effects to account for shared hydrological conditions, and τ_m are month fixed effects to adjust for seasonal variation in glyphosate concentrations (see Figure 2A.1). The vector $\boldsymbol{X}_i'$ includes geographical controls such as average slope, soil erodibility, and stream level, and fr_i accounts for average flow rate.[16]

Table 2A.1 shows that glyphosate concentrations are significantly correlated with upstream glyphosate across all specifications. Interestingly, glyphosate concentration is not significantly correlated with local glyphosate use. Likely because local glyphosate captures the average glyphosate

[16]Slope and flow rate data are from the EPA's NHDPlus Version 2 dataset, which reports slope, stream level, and three types of flow rate estimates for each flowline. I construct county-level variables by averaging values across all flowlines within a county, weighted by flowline length. The flow metrics include: QA (mean annual flow from runoff), QC (mean annual flow estimated via reference-gage regression), and QE (mean annual flow from gage adjustment). These three estimates are highly correlated. Stream level identifies whether a segment is part of the mainstem (lower values) or a tributary (higher values). Soil erodibility is obtained from the Gridded Soil Survey Geographic (gSSURGO) Database and averaged across all 30-meter cells within each county. I use readings from all monitoring stations for dissolved glyphosate. To avoid the influence of outliers, I drop readings of glyphosate above the 99.5th percentile.

FIGURE 2A.1. Average glyphosate concentration by month, 2001-2014



Source: WQP

use in the county, but can't capture the application locations. Some applications may be downstream of monitoring stations, making the estimate noisy.

Table 2A.2 repeats the same specification to downstream glyphosate. As expected, downstream glyphosate shows no significant relationship with glyphosate concentrations, supporting the validity of the model specification. Table 2A.3 further includes upstream glyphosate use farther away and shows that glyphosate use beyond 200 km does not consistently correlate significantly to concentrations. This pattern closely aligns with the main finding that health effects are present within 200 km upstream but diminish beyond this distance.

To explore whether the heterogeneity in health effects is driven by geographic conditions differing by the income areas, I interact upstream glyphosate with income groups and flow rate. Table 2A.4 presents the results. I find that the relationship between upstream glyphosate and concentrations does not differ between income regions (Column 1), suggesting the natural geography in these two regions does not lead to different concentrations and is not sufficient to explain the stronger health impacts in lower-income areas. Also, I found glyphosate concentrations are more strongly associated with upstream use in counties with moderate flow rates (Columns 2-4), likely because high flow rates dilute contaminants. However, this heterogeneity in concentration by flow rate does

TABLE 2A.1. Relationship between glyphosate concentrations and upstream glyphosate applications

	(1)	(2)	(3)	(4)	(5)	(6)
Upstream glyphosate	3.386**	4.496***	4.503***	4.488***	4.478***	4.338***
	(1.413)	(1.584)	(1.582)	(1.580)	(1.580)	(1.371)
Local glyphosate	-1.267	-2.464	-2.530	-2.524	-2.506	-2.099
	(1.326)	(1.551)	(1.552)	(1.551)	(1.551)	(1.446)
Observations	3,099	3,099	3,099	3,099	3,099	3,099
R-squared	0.040	0.046	0.047	0.047	0.047	0.049
Month FE	Yes	Yes	Yes	Yes	Yes	Yes
Geogrophic covariates	No	Yes	Yes	Yes	Yes	Yes
Flow rate	No	No	QA	QC	QE	QA
HU2 FE	No	No	No	No	No	Yes

Notes: The dependent variable is glyphosate concentrations. Robust standard errors clustered at the watershed (HU8) level are shown in parentheses: *** p<0.01, ** p<0.05, * p<0.1.

TABLE 2A.2. Relationship between glyphosate concentrations and downstream glyphosate applications

	(1)	(2)	(3)	(4)	(5)	(6)
Downstream glyphosate	1.132	1.830	1.980	1.967	1.951	2.067
	(2.181)	(2.093)	(2.089)	(2.088)	(2.087)	(2.296)
Local glyphosate	0.114	-0.242	-0.387	-0.386	-0.367	-0.235
	(1.603)	(1.626)	(1.616)	(1.615)	(1.616)	(1.525)
Observations	3,099	3,099	3,099	3,099	3,099	3,099
R-squared	0.031	0.034	0.035	0.036	0.036	0.040
Month FE	Yes	Yes	Yes	Yes	Yes	Yes
Geogrophic covariates	No	Yes	Yes	Yes	Yes	Yes
Flow rate	No	No	QA	QC	QE	QA
HU2 FE	No	No	No	No	No	Yes

Notes: The dependent variable is glyphosate concentrations. Robust standard errors clustered at the watershed (HU8) level are shown in parentheses: *** p<0.01, ** p<0.05, * p<0.1.

not align with the pattern across income levels: more lower-income counties have higher flow rates, yet still show stronger health impacts.

Column (5) discusses whether glyphosate is easier to transport through surface water or groundwater and shows no statistical difference in the sample, either from upstream glyphosate or local glyphosate. One possible reason is that groundwater and surface water highly interact in the US (Winter et al., 1998) and can be the source of contamination for each other (Duncan et al., 1991; Squillace et al., 1993; Malaguerra et al., 2012; Van Stempvoort et al., 2016).[17]

[17]The interaction of groundwater and upstream glyphosate shows a big magnitude. This may be due to sample selection. Groundwater monitoring data contains more extreme high values.

TABLE 2A.3. Relationship between glyphosate concentrations and upstream glyphosate applications by distances

	(1)	(2)	(3)	(4)	(5)	(6)
Upstream glyphosate (0-200km)	2.253*	3.280**	3.330**	3.316**	3.312**	3.193**
	(1.360)	(1.521)	(1.513)	(1.514)	(1.515)	(1.473)
Upstream glyphosate (200-400km)	1.921	1.943	1.934	1.938	1.938	2.106*
	(1.512)	(1.290)	(1.285)	(1.281)	(1.283)	(1.257)
Upstream glyphosate (400-600km)	-0.109	2.392	2.032	2.038	1.975	0.375
	(3.680)	(3.358)	(3.440)	(3.409)	(3.435)	(3.374)
Upstream glyphosate (600-800km)	-3.107	-4.353	-3.095	-3.101	-3.014	-1.378
	(3.570)	(3.280)	(3.665)	(3.580)	(3.650)	(3.604)
Local glyphosate	-1.127	-2.273	-2.337	-2.333	-2.320	-1.903
	(1.308)	(1.496)	(1.492)	(1.492)	(1.493)	(1.447)
Observations	3,099	3,099	3,099	3,099	3,099	3,099
R-squared	0.045	0.051	0.052	0.052	0.052	0.054
Month FE	Yes	Yes	Yes	Yes	Yes	Yes
Geogrophic covariates	No	Yes	Yes	Yes	Yes	Yes
Flow rate	No	No	QA	QC	QE	QA
HU2 FE	No	No	No	No	No	Yes

Notes: The dependent variable is glyphosate concentrations. Robust standard errors clustered at the watershed (HU8) level are shown in parentheses: *** p<0.01, ** p<0.05, * p<0.1.

Table 2A.5 presents the correlations between concentrations and upstream glyphosate by rainfall quartile within and outside the application season, using the same quartile definitions applied in the health impact specifications. The results show that within-season precipitation increases the correlation between upstream glyphosate use and downstream concentrations, while outside-season rainfall has no significant effect. While the point estimate of the correlation in the highest rainfall quartile (Q4) is slightly lower than in Quartile 2, the difference is not statistically significant. This pattern suggests that dilution due to excessive rainfall is not a major concern in the study region. One possible reason is that precipitation levels in the Corn Belt, while variable, are generally moderate and do not reach levels that would overwhelm dilution thresholds.

TABLE 2A.4. Heterogeneity in glyphosate concentrations and upstream glyphosate applications

	Income	Flow rate (QA)	Flow rate (QC)	Flow rate (QE)	Water source
	(1)	(2)	(3)	(4)	(5)
Upstream glyphosate	3.912***	3.277*	3.335*	3.371*	3.669***
	(1.433)	(1.709)	(1.704)	(1.713)	(1.272)
Lower income × upstream glyphosate	1.323				
	(1.759)				
Quartile 1 × upstream glyphosate		-1.172	-0.727	-1.304	
		(1.260)	(1.228)	(1.646)	
Quartile 2 × upstream glyphosate		2.003**	1.853*	2.103**	
		(0.937)	(0.979)	(0.967)	
Quartile 3 × upstream glyphosate		2.336	2.599*	1.508	
		(1.564)	(1.556)	(1.411)	
Groundwater × upstream glyphosate					7.147
					(5.990)
Groundwater × local glyphosate					-2.863
					(4.931)
Local glyphosate	-2.144	-2.096	-2.114	-2.312	-2.449*
	(1.419)	(1.493)	(1.491)	(1.530)	(1.427)
Observations	3,099	3,087	3,087	3,087	2,988
R-squared	0.058	0.055	0.055	0.054	0.056
Controls	Yes	Yes	Yes	Yes	Yes

Notes: The dependent variable is glyphosate concentration. The first row indicates the variable used for interaction in each column. All regressions include month fixed effects, HU2 fixed effects, geographic covariates, and flow rate. Unless otherwise noted in the first row, the QA flow rate is used. The results are similar using different flow rate measures. Robust standard errors clustered at the watershed (HU8) level are shown in parentheses: *** p<0.01, ** p<0.05, * p<0.1.

TABLE 2A.5. Heterogeneity in glyphosate concentrations by precipitation

	Apr-Sep	Oct-Mar
	(1)	(2)
Upstream glyphosate	-0.316	-2.109
	(1.295)	(4.231)
Quartile 2 × upstream glyphosate	6.697***	0.530
	(2.296)	(2.726)
Quartile 3 × upstream glyphosate	6.291**	3.230
	(2.436)	(4.572)
Quartile 4 × upstream glyphosate	6.062***	
	(1.833)	
Observations	2,579	520
R-squared	0.051	0.040
Controls	Yes	Yes

Notes: The dependent variable is glyphosate concentrations. The first row displays the season considered. All regressions include month fixed effects, HU2 fixed effects, geographic covariates, and QA flow rate. The results are similar using different flow rate measures. There is no concentration data available from October to March in counties with a rainfall quartile of 4. Robust standard errors clustered at the watershed (HU8) level are shown in parentheses: *** p<0.01, ** p<0.05, * p<0.1.

2A.2. Economic Spillovers

To address economic spillovers, I run regressions adding glyphosate use in nearby areas as an independent variable, adapted from Dias et al. (2023), with results shown in Table 2A.6. If economic spillovers exist, they are expected to affect nearby areas in non-specific directions rather than following water flow. The nearby glyphosate use is the sum of glyphosate in upstream, downstream, and any watersheds within 200 km. This variable captures spatial spillovers based purely on geographic proximity, allowing the upstream glyphosate coefficient to reflect the difference between upstream and non-upstream nearby effects. The estimates suggest that nearby glyphosate use, if it has any effects, may lead to spillovers that are actually beneficial for birth outcomes. However, these estimates are statistically insignificant.

I further explore spillovers by regressing local economic indicators on glyphosate use (Table 2A.7). Local glyphosate use is negatively associated with agricultural employment and positively associated with manufacturing employment, suggesting a reallocation of labor potentially due to glyphosate or GM crop adoption. It is also positively correlated with agricultural GDP but shows no significant relationship with livestock sales. In contrast, upstream glyphosate use is generally statistically uncorrelated with these economic indicators, with two exceptions: small but borderline significant associations with total and manufacturing GDP. Given average upstream use of 0.023 tonne/km^2, these correlations translate to roughly 0.017% and 0.08% increases in total and manufacturing GDP, respectively, suggesting some economic spillovers. To assess whether these patterns reflect true spatial spillovers rather than upstream-specific effects, I include both upstream and nearby glyphosate use for the GDP equations. The results suggest some, but insignificant, spillover effects. There is no significant difference between upstream and non-upstream nearby effects—unlike the significant estimates observed for neonatal mortality.

Overall, while estimates suggest that economic spillovers from upstream glyphosate use are mostly insignificant, they cannot be fully ruled out. The identification strategy is designed to isolate waterborne transmission, but glyphosate use may still influence local economies through labor reallocation, productivity changes, or other indirect channels not fully captured in the empirical framework. Including nearby glyphosate use helps account for these possibilities and suggests that, if spillovers exist, the main health effect estimates may be conservative.

TABLE 2A.6. Nearby glyphosate effects on neonatal mortality rate

	(1)	(2)	(3)	(4)	(5)	(6)
Upstream glyphosate	25.14**	24.81**	24.65**	24.64**	24.73**	26.68**
	(10.33)	(10.50)	(10.31)	(10.26)	(10.13)	(10.67)
Sum of nearby glyphosate	-6.748	-6.092	-6.069	-6.128	-5.948	-8.762
	(6.101)	(6.337)	(6.457)	(6.452)	(6.351)	(7.265)
Local glyphosate						5.360
						(6.277)
Observations	7,770	7,770	7,770	7,770	7,770	7,770
R-squared	0.031	0.032	0.038	0.038	0.039	0.039
Number of counties	555	555	555	555	555	555
Economic covariates	No	Yes	Yes	Yes	Yes	Yes
Demographic covariates	No	No	Yes	Yes	Yes	Yes
Industrial pollution covariates	No	No	No	Yes	Yes	Yes
Medical resource covariates	No	No	No	No	Yes	Yes

Notes: For details on the controls, see the notes in Table 2. All regressions include county and state-year fixed effects. Robust standard errors clustered at the watershed (HU8) level are shown in parentheses: *** p<0.01, ** p<0.05, * p<0.1.

TABLE 2A.7. Correlations between glyphosate and farm/non-farm economic conditions

	Farm employment (1)	Non-farm employment (2)	Animal sales (3)	Log ag GDP (4)	Log total GDP (5)	Log manuf. GDP (6)	Log ag GDP (7)	Log total GDP (8)	Log manuf. GDP (9)
Local glyphosate	-0.650**	225.1*	102.9	10.25***	-0.152	-0.868	8.660***	-0.344	-1.231
	(0.284)	(135.3)	(124.1)	(2.960)	(0.301)	(0.926)	(3.217)	(0.332)	(1.086)
Upstream glyphosate	-0.373	-95.76	193.5	4.500	0.705*	3.558*	-1.110	0.116	2.442
	(0.452)	(79.68)	(180.3)	(3.654)	(0.410)	(1.808)	(6.055)	(0.457)	(1.752)
Glyphosate use nearby							4.079	0.450	0.868
							(3.828)	(0.333)	(1.289)
Observations	7,770	7,770	7,686	3,262	7,770	6,510	3,262	7,770	6,510
R-squared	0.625	0.540	0.239	0.326	0.535	0.307	0.327	0.535	0.307
Number of counties	555	555	549	233	555	465	233	555	465

Notes: The first row shows the dependent variable of each regression. The data on animal sales are from the census of agriculture, which is only available every five years. I used linear interpolation to generate values in the years between censuses. The GDP data for some counties in specific years are unavailable due to confidentiality. All regressions include county and state-year fixed effects and economic covariates. For details on the controls, see the notes in Table 2. Robust standard errors clustered at the watershed (HU8) level are shown in parentheses: *** p<0.01, ** p<0.05, * p<0.1.

2A.3. Other Agricultural Chemicals

To address other agricultural pollutants that could potentially confound the estimated effects of glyphosate, I examine the correlations between glyphosate use and various water quality measures associated with agricultural activity (Hooda et al., 2000; Kato et al., 2009; Keiser and Shapiro, 2018; Liu et al., 2023). These measures include dissolved oxygen deficit (DOD), nitrate and nitrite nitrogen, phosphorus, total suspended solids (TSS), Escherichia coli (E. coli), and total coliform. DOD is a widely used measure of water quality, as it reflects the amount of oxygen consumed by microorganisms breaking down pollutants. TSS captures solid particles in water and serves as an indicator of soil erosion. Nitrate and phosphorus represent nutrient pollution from sources such as fertilizers, livestock manure, and municipal sewage, with nitrate being the primary form of leached nitrogen from fertilizers in the Corn Belt (Bernhard, 2010). Coliform bacteria are indicators of harmful pathogens, often linked to human and animal fecal matter. Unfortunately, the water quality data is irregular in most regions and with limited spatial coverage.[18]

Table 2A.8 reports correlations between upstream glyphosate use and water quality, while Table 2A.9 controls for upstream phosphorus, nitrate/nitrite, and other pesticide use. Glyphosate's estimated effects on neonatal mortality remain robust after controlling for these substances, which themselves show no significant associations. Several factors may explain those insignificant estimates of other chemicals. First, many of the other chemicals (e.g., nitrate, atrazine, 2,4-D) are regulated under the Safe Drinking Water Act, and exceedances often prompt public notifications that trigger avoidance behaviors (Marcus, 2022; Hadachek, 2024). Second, MCLs vary substantially: glyphosate's is high (700 $\mu g/L$), whereas atrazine's is low (3 $\mu g/L$), making violations (and subsequent mitigation) more common for some substances than others (Warnemuende et al., 2007). Third, substances like phosphorus have little evidence of adverse effects in humans even at high doses.[19] Fourth, although other pesticides have been linked to adverse birth outcomes (e.g., atrazine with preterm birth and fetal growth restriction Chevrier et al., 2011; acetochlor with reduced birth

[18]For water quality measures in each county, I use readings from all monitoring stations testing unfiltered/total water for DOD, nitrate and nitrite nitrogen, phosphorus, TSS, and water for total coliform and E. coli. Data from non-water media, such as soil and sediment, are excluded. To avoid the influence of outliers, I drop readings above the 99.5th percentile or below the 0.5th percentile in each county, following Liu et al. (2023). The remaining readings are averaged to generate county-year level variables for each water measure.

[19]https://ods.od.nih.gov/factsheets/Phosphorus-HealthProfessional/

TABLE 2A.8. Correlations of water quality measures and glyphosate

	DOD	Phosphorus	Nitrate and nitrite	TSS	E. Coli	Coliform
	(1)	(2)	(3)	(4)	(5)	(6)
Upstream glyphosate	55.20	13.58	19.70	-23.28	-8,594	-224,952
	(76.87)	(10.57)	(13.42)	(109.5)	(6,718)	(211,669)
Observations	2,209	5,394	3,673	2,691	3,154	346
R-squared	0.192	0.061	0.174	0.205	0.033	0.386
Number of counties	392	531	401	382	447	150

Notes: The first row shows the dependent variable of each regression. All regressions include county and state-year fixed effects but control for no covariates. Robust standard errors clustered at the watershed (HU8) level are shown in parentheses: *** p<0.01, ** p<0.05, * p<0.1.

weight Wickerham et al., 2012), these effects may not be strong enough to affect neonatal mortality, especially via waterborne exposure. Finally, glyphosate use increased substantially during the study period, while most other chemical use remained stable. This sharp variation improves identification and may explain why glyphosate emerges as the most policy-relevant factor in our setting.

TABLE 2A.9. Glyphosate impacts on neonatal mortality with agricultural chemical controls

	Phosphorus		Nitrate and nitrite		Pesticides	
	(1)	(2)	(3)	(4)	(5)	(6)
Upstream glyphosate	15.47**	15.40**	22.48***	22.96***	15.32***	15.56**
	(7.276)	(7.282)	(8.089)	(8.046)	(5.869)	(6.861)
Phosphorus		0.00588				
		(0.0103)				
Nitrate and nitrite				-0.0287		
				(0.0333)		
Upstream atrazine						2.766
						(19.71)
Upstream acetochlor						11.41
						(22.14)
Upstream metolachlor-s						17.33
						(25.41)
Upstream 2,4-D						15.09
						(29.27)
Local glyphosate	0.298	0.252	-0.989	-0.826	1.538	1.097
	(5.844)	(5.840)	(7.182)	(7.196)	(5.503)	(5.462)
Observations	5,394	5,394	3,673	3,673	7,770	7,770
R-squared	0.048	0.048	0.059	0.059	0.038	0.039
Number of counties	531	531	401	401	555	555
Full controls	Yes	Yes	Yes	Yes	Yes	Yes

Notes: The first row indicates the agricultural chemical under consideration. The sample sizes for phosphorus and nitrate/nitrite are smaller due to data availability. For details on the controls, see the notes in Table 2. All regressions include county and state-year fixed effects. Robust standard errors clustered at the watershed (HU8) level are shown in parentheses: *** p<0.01, ** p<0.05, * p<0.1.

2A.4. Public water system violations

The EPA sets legally enforceable limits (Maximum Contaminant Levels, or MCLs) on about 90 contaminants in drinking water (Table 2A.10) and also prescribes water-testing schedules that public water systems must follow. Public water systems are required to monitor these contaminants based on EPA-specified schedules, though states may waive requirements. The frequency of monitoring depends on the type of contaminant, the water source, and the number of people served. For example, total coliforms must be monitored anywhere from once to 480 times per month, depending on population size. Nitrate must be tested annually in groundwater systems and quarterly in surface water systems. Some organic contaminants are monitored annually, while some are once or twice every three years.

A public water system is issued an MCL violation when contaminant levels exceed legal limits, and a Monitoring and Reporting (MR) violation if the system fails to conduct required testing or submit results to state or federal agencies on time.

To construct county-level violation exposure measures used in Section 3.5, I calculate the coverage of MCL and MR violations as the percentage of a county's population served by a public water system that had a given type of violation in a specific year. Since some systems serve multiple counties, I allocate their service populations across counties based on the proportion of each county's residents not already served by other systems. I exclude systems that were not operational during the study period, as well as transient non-community systems (e.g., campgrounds), which serve populations that are not necessarily the residents of that county.

TABLE 2A.10. EPA-Regulated Drinking Water Contaminants by Category

Contaminant Group	**Chemicals**
Inorganic Chemicals	Antimony, Arsenic, Asbestos (fiber 10 µm), Barium, Beryllium, Cadmium, Chromium (total), Copper, Cyanide (free), Fluoride, Lead, Mercury (inorganic), Nitrate (as Nitrogen), Nitrite (as Nitrogen), Selenium, Thallium
Organic Chemicals (excluding PFAS)	Acrylamide, Alachlor, Atrazine, Benzene, Benzo(a)pyrene (PAHs), Carbofuran, Carbon tetrachloride, Chlordane, Chlorobenzene, 2,4-D, Dalapon, 1,2-Dibromo-3-chloropropane (DBCP), o-Dichlorobenzene, p-Dichlorobenzene, 1,2-Dichloroethane, 1,1-Dichloroethylene, cis-1,2-Dichloroethylene, trans-1,2-Dichloroethylene, Dichloromethane, 1,2-Dichloropropane, Di(2-ethylhexyl) adipate, Di(2-ethylhexyl) phthalate, Dinoseb, Dioxin (2,3,7,8-TCDD), Diquat, Endothall, Endrin, Epichlorohydrin, Ethylbenzene, Ethylene dibromide, Glyphosate, Heptachlor, Heptachlor epoxide, Hexachlorobenzene, Hexachlorocyclopentadiene, Lindane, Methoxychlor, Oxamyl (Vydate), PCBs, Pentachlorophenol, Picloram, Simazine, Styrene, Tetrachloroethylene, Toluene, Toxaphene, 2,4,5-TP (Silvex), 1,2,4-Trichlorobenzene, 1,1,1-Trichloroethane, 1,1,2-Trichloroethane, Trichloroethylene, Vinyl chloride, Xylenes (total)
Radionuclides	Alpha particles, Beta particles and photon emitters, Radium 226/228 (combined), Uranium
Disinfection Byproducts	Bromate, Chlorite, Haloacetic acids (HAA5), Total Trihalomethanes (TTHMs)
Microorganisms	Total Coliforms (including fecal coliform and *E. coli*)
Selected PFAS	Hazard Index PFAS (HFPO-DA, PFBS, PFHxS, PFNA), HFPO-DA (GenX Chemicals), PFBS, PFHxS, PFNA, PFOA, PFOS

Notes: Sourced from EPA (https://www.epa.gov/ground-water-and-drinking-water/national-primary-drinking-water-regulations#one).

2A.5. Other Heterogeneous Effects and Potential Mechanisms

This section investigates potential reasons why the effects of glyphosate on neonatal mortality rates are primarily observed in lower-income areas and not in higher-income ones.

One explanation could be geographic variation. Many lower-income counties are clustered in specific parts of the Corn Belt, and it is possible that certain geographic conditions affect glyphosate transport and drive the observed heterogeneity. However, this seems not to be the case. Table 2A.4, Column (1), shows that upstream glyphosate use is positively associated with downstream concentrations in natural water systems, and this relationship does not differ significantly by income level. This suggests other mechanisms may be more relevant.

To explore further, I examine additional sources of heterogeneity. The suggestive results show avoidance behaviors may play a role. Even if glyphosate is present in drinking water, exposure can be mitigated through individual responses, such as using filters or bottled water. Roughly 20 percent of U.S. households rely exclusively on bottled water (Jaffee, 2024), reflecting persistent concerns over tap water quality (Keiser and Shapiro, 2019).

Studies show that higher-income, more educated, and older individuals are more likely to use water filters (Park et al., 2022; Triplett et al., 2019; Yang and Faust, 2019). Racial and ethnic differences also exist: non-Hispanic whites are more likely to trust tap water, whereas Hispanic and Black populations are more inclined to use bottled water for themselves and their children (Hobson et al., 2007; Viscusi et al., 2015; Javidi and Pierce, 2018; Rosinger et al., 2018).

The water consumption patterns align with observed heterogeneous effects across different demographic groups. Table 2A.11 Columns (1)-(3) show stronger glyphosate impacts in areas with a higher incidence of less-educated, younger, and non-Hispanic white mothers. Like higher income, it is consistent with findings in the health literature that more-educated people are less affected by adverse conditions, as they have more resources to mitigate these factors or are better able to take avoidance actions (Currie, 2011; Currie et al., 2013; Greve et al., 2017). For example, studies also find that better-educated people are less affected by air pollution (Bharadwaj et al., 2017). However, it is unusual for non-Hispanic whites to be more severely impacted by air pollution (Chay and Greenstone, 2003; Banzhaf et al., 2019). This different finding, where glyphosate has stronger effects in areas with a higher proportion of non-Hispanic white mothers, may be explained by water

TABLE 2A.11. Heterogeneous glyphosate effects on neonatal mortality rate by mother's demographics, private water sources, and flow rates

	Interacted variable						
	Age	Non-Hispanic whites	Education	Private Water sources	Flow rate (QA)	Flow rate (QC)	Flow rate (QE)
	(1)	(2)	(3)	(4)	(5)	(6)	(7)
Upstream glyphosate	0.124	8.852*	-3.967	9.008*	-5.037	-4.370	-4.260
	(3.918)	(5.021)	(4.117)	(5.167)	(5.082)	(4.757)	(4.920)
Quartile 1 × upstream glyphosate	8.489**	-9.009**	9.525**	-9.183	9.520*	8.931*	7.988
	(4.147)	(4.427)	(4.509)	(5.987)	(4.901)	(4.795)	(4.955)
Quartile 2 × upstream glyphosate	3.683	-4.854	5.090	-8.376	17.19**	17.20***	12.99**
	(3.006)	(4.192)	(3.640)	(6.025)	(6.701)	(6.478)	(6.254)
Quartile 3 × upstream glyphosate	0.714	-1.249	3.909	-7.774	7.860*	7.005	8.706*
	(2.410)	(3.403)	(3.298)	(5.884)	(4.658)	(4.755)	(4.815)
Observations	14,630	14,630	13,370	14,630	14,616	14,616	14,616
R-squared	0.027	0.027	0.029	0.027	0.027	0.027	0.027
Number of counties	1,045	1,045	955	1,045	1,044	1,044	1,044

Notes: Each column presents regression results with interactions between glyphosate use and quartiles of the variable indicated in the second row. For control details, refer to Table 2. All regressions include county and state-year fixed effects. The sample analyzed for regional heterogeneous effects includes all counties, consistent with Table 2 Column (1). Column (2) in this table has a smaller sample size due to missing data on mother's education, which is measured as the proportion of mothers with a college degree. Columns (5)-(7) have a slightly smaller sample size due to missing data on flow rate. Robust standard errors clustered at the watershed (HU8) level are shown in parentheses: *** p<0.01, ** p<0.05, * p<0.1.

usage behaviors, such as the decision to consume unfiltered tap water.[20] However, this is just correlation, not causation, as my data lacks random variation in interaction terms and cannot directly test this mechanism.

Water treatment may also play a role. Lower-income individuals are more likely to rely on private water sources, primarily wells, which are unregulated under the Safe Drinking Water Act. Private well users tend to test and treat their water less frequently than public water systems (Pieper et al., 2015; Malecki et al., 2017). Table 2A.11 Column (4) examines the interaction between glyphosate use and private water user quartiles, showing that glyphosate has a larger impact in areas with higher private water reliance. The magnitude and significance of the effect decline across private water use quartiles, although the first quartile remains marginally insignificant ($p = 0.12$). These results suggest that the lack of water treatment in private systems may amplify glyphosate's effects.

[20]The correlations between the non-Hispanic white share and income, age, and education are low, with correlation coefficients of -0.089, 0.061, and 0.072, respectively. These low correlations suggest that race and the associated water consumption patterns potentially contribute to the observed heterogeneous effects.

Columns (5)–(7) of Table 2A.11 examine heterogeneity by river characteristics.[21] The results show that glyphosate's impact is larger in areas with relatively lower river flow rates across all measurements—likely because higher flow dilutes contaminants. This pattern aligns with findings in Appendix 2A.1, where glyphosate concentrations are more strongly associated with upstream use in areas with moderate flow. Importantly, lower-income areas have more counties with those high flow rates, reinforcing that geographic conditions are insufficient to explain the observed heterogeneity across income.

Public water system violations offer further insight. On one hand, violations may signal poor water quality; the resulting exposure risk may increase if individuals do not respond to these signals. On the other hand, violations can trigger mandatory public notices, prompting avoidance behaviors that mitigate health impacts. To disentangle these effects, I regress neonatal mortality on glyphosate use and an interaction between glyphosate and high violation coverage (defined as above-median share of the population served by systems with MCL or MR violations).[22] For MCL violations, notifications must be issued within 30 days or within 24 hours for certain chemicals. Whereas, MR violations only require notification within one year.

Table 2A.12 shows that MCL violations are associated with reduced glyphosate effects (Column 1), particularly in higher-income areas (Column 5). In contrast, the mitigating effect is small and statistically insignificant in lower-income areas (Column 3). MR violations show no significant interaction with glyphosate use (Columns 2, 4, and 6). These results align with prior research suggesting that timely public notification of MCL violations can prompt avoidance behaviors (Marcus, 2022), especially in higher-income areas with greater capacity to respond (Hadachek, 2024). In lower-income communities, financial constraints and limited access to media or timely notification may reduce the effectiveness of such warnings, leaving health risks elevated.[23] That said, these results should be interpreted with caution, as violations may correlate with unobserved confounders.

[21]Flow rate data are from EPA's NHDPlus Version 2 dataset, which provides the three estimates: QA, QC, and QE. See the footnote 16 for more details.

[22]See Appendix 2A.4 for detailed information on how the violation variable is constructed.

[23]Previous studies find that prompt violation notices lead to increased bottled water purchases and mitigate health impacts, particularly in areas with lower poverty rates. These behaviors may reduce exposure not only to the chemical causing the violation but also to others like glyphosate. Thus, violations unrelated to glyphosate may still inadvertently reduce its health impacts if they prompt broader avoidance behaviors.

TABLE 2A.12. Regression of neonatal mortality on violations

	All counties		Lower-income areas		Higher-income areas	
	MCL	MR	MCL	MR	MCL	MR
	(1)	(2)	(3)	(4)	(5)	(6)
Upstream glyphosate	3.342	1.566	15.45**	14.95**	-1.750	-4.207
	(3.878)	(3.806)	(6.159)	(6.353)	(4.564)	(4.587)
High violation x upstream glyphosate	-2.631*	0.498	-0.211	1.081	-2.900*	1.244
	(1.589)	(1.153)	(3.004)	(2.800)	(1.676)	(1.495)
Local glyphosate	2.857	3.009	1.530	1.770	2.792	3.189
	(3.348)	(3.353)	(5.510)	(5.510)	(4.013)	(4.033)
Observations	14,630	14,630	7,770	7,770	6,860	6,860
R-squared	0.027	0.026	0.038	0.039	0.048	0.048
Number of counties	1,045	1,045	555	555	490	490
Full controls	Yes	Yes	Yes	Yes	Yes	Yes

Notes: The first row shows the considered sample, and the second row indicates the type of violations considered. For details on the controls, see the notes in Table 2. All regressions include county and state-year fixed effects. Robust standard errors clustered at the watershed (HU8) level are shown in parentheses: *** p<0.01, ** p<0.05, * p<0.1.

More broadly, all heterogeneity analyses in this section are correlational, not causal, given the lack of random variation in interaction terms. Future research is needed to establish causality.

Finally, socioeconomic disparities in healthcare access may also contribute to differential glyphosate effects. Higher-income individuals have greater access to prenatal care and medical resources (Mocan et al., 2015), which can mitigate environmental health risks. Proximity to hospitals and healthcare providers improves birth outcomes (Blondel et al., 2011; Daysal et al., 2015). Descriptive statistics in Table 2.1 show that lower-income areas have fewer hospital beds and healthcare providers per capita, as well as lower spatial access to medical services. If glyphosate exposure affects both high- and low-income populations similarly, higher-income individuals may mitigate its effects through better healthcare access.

2A.6. Supplementary Tables

TABLE 2A.13. Regression of local glyphosate and upstream glyphosate on covariates

	(1) Local glyphosate	(2) Upstream glyphosate
Income per capita	-0.000436**	0.000223
	(0.000170)	(0.000192)
Unemployment rate	-0.00128***	-0.000241
	(0.000209)	(0.000355)
Poverty rate	-3.08e-05	0.000107
	(0.000138)	(0.000109)
% employment in agriculture	0.000344	-0.000265
	(0.000355)	(0.000407)
% married	-4.50e-05	8.09e-05
	(6.26e-05)	(6.35e-05)
% mothers born outside of the US	-0.000113	-8.39e-05
	(0.000212)	(0.000280)
% non-hispanic black	0.000294	0.000305
	(0.000298)	(0.000304)
% non-hispanic white	-7.55e-05	-0.000221
	(0.000156)	(0.000139)
Mother's age	0.00114**	0.000217
	(0.000530)	(0.000464)
Number of plurality	0.00282	-0.000301
	(0.00634)	(0.00549)
Birth order	-0.00157	-0.00127
	(0.00192)	(0.00185)
% diabetes	-9.47e-06	2.36e-05
	(0.000116)	(0.000110)
% hypertension	-0.000492***	5.43e-05
	(0.000104)	(9.25e-05)
Industrial water pollution	4.43e-05**	-2.37e-05
	(2.16e-05)	(2.00e-05)
Hospital beds per capita*1000	0.000435*	0.000260
	(0.000232)	(0.000208)
Health providers per capita*1000	-0.000524	-0.0115***
	(0.00471)	(0.00368)
Hospital beds density	-0.00248	0.00493
	(0.00627)	(0.00642)
Health provider density	-0.143***	0.0238
	(0.0295)	(0.0318)
Observations	7,770	7,770
R-squared	0.621	0.699
F stat	8.43	1.78
Number of counties	555	555
Fixed-Effects	County+State-Year FE	County+State-Year FE

Notes: F statistics report the results of the joint test of significance for all covariates, excluding fixed effects. Robust standard errors clustered at the watershed (HU8) level are shown in parentheses: *** p<0.01, ** p<0.05, * p<0.1.

TABLE 2A.14. Glyphosate effects on neonatal mortality rate using different FE and controls

	No FE		County FE		County+Year FE		County+State-Year FE	
	(1)	(2)	(3)	(4)	(5)	(6)	(7)	(8)
Upstream glyphosate	-3.599	1.010	-2.606	10.58**	14.35***	13.08***	15.08**	15.32***
	(4.975)	(2.007)	(4.002)	(4.943)	(4.947)	(4.913)	(6.502)	(5.869)
Income per capita		-0.0299*		-0.0367		-0.0234		-0.0327
		(0.0174)		(0.0238)		(0.0276)		(0.0294)
Unemployment rate		0.0253		0.0494**		0.109**		0.0876*
		(0.0203)		(0.0195)		(0.0427)		(0.0509)
Poverty rate		-0.00380		-0.0296		-0.00652		-0.0113
		(0.0101)		(0.0219)		(0.0256)		(0.0244)
% employment in agriculture		-0.0175		-0.121**		-0.181***		-0.164**
		(0.0115)		(0.0583)		(0.0627)		(0.0731)
% married		-0.00308		0.00708		-0.00918		-0.00466
		(0.0101)		(0.0116)		(0.0131)		(0.0137)
% mothers born outside of the US		-0.00393		-0.0218		-0.0165		-0.0220
		(0.00921)		(0.0332)		(0.0332)		(0.0337)
% non-hispanic black		0.0237***		-0.000936		-0.00863		0.0140
		(0.00897)		(0.0423)		(0.0431)		(0.0458)
% non-hispanic white		-0.00790		-0.00839		-0.0195		-0.0214
		(0.00659)		(0.0275)		(0.0285)		(0.0293)
Mother's age		-0.192**		-0.346***		-0.357**		-0.403***
		(0.0792)		(0.114)		(0.145)		(0.147)
Number of plurality		15.14***		14.53***		14.82***		14.94***
		(2.876)		(3.039)		(3.033)		(3.087)
Birth order		0.604***		0.458		0.308		0.321
		(0.213)		(0.342)		(0.570)		(0.539)
% diabetes		-0.0225		-0.00616		0.000999		0.0178
		(0.0224)		(0.0264)		(0.0270)		(0.0292)
% hypertension		-0.0106		-0.0225		-0.0239		-0.0205
		(0.0195)		(0.0254)		(0.0257)		(0.0260)
Industrial water pollution		0.00200		-0.000410		-0.00384		-0.00321
		(0.00448)		(0.00726)		(0.00532)		(0.00656)
Hospital beds per capita*1000		-0.0340*		-0.0939*		-0.0979*		-0.102*
		(0.0204)		(0.0499)		(0.0505)		(0.0531)
Health providers per capita*1000		0.213		-0.657		-0.526		-0.367
		(0.326)		(0.978)		(0.993)		(1.026)
Hospital beds density		0.461***		0.349		0.298		0.515
		(0.0936)		(0.511)		(0.570)		(0.660)
Health provider density		-7.241***		-6.211		-6.112		-0.210
		(1.910)		(3.870)		(3.778)		(4.110)
Local glyphosate		2.177		-1.026		1.998		1.538
		(1.910)		(5.032)		(5.228)		(5.503)
Observations	7,770	7,770	7,770	7,770	7,770	7,770	7,770	7,770
R-squared	0.001	0.077	0.000	0.012	0.006	0.015	0.031	0.038
Economic covariates	No	Yes	No	Yes	No	Yes	No	Yes
Demographic covariates	No	Yes	No	Yes	No	Yes	No	Yes
Industrial pollution covariates	No	Yes	No	Yes	No	Yes	No	Yes
Medical resource covariates	No	Yes	No	Yes	No	Yes	No	Yes

Notes: The regressions focus on lower-income areas. The dependent variable is neonatal mortality rates. The first row shows the fixed effect considered. Robust standard errors clustered at the watershed (HU8) level are shown in parentheses: *** p<0.01, ** p<0.05, * p<0.1.

TABLE 2A.15. Neonatal mortality effects of glyphosate: HUC4-clustered standard errors

	All counties		Lower-income areas					
	(1)	(2)	(3)	(4)	(5)	(6)	(7)	(8)
Upstream glyphosate	1.847	-2.315	15.08**	15.78***	15.65***	15.55***	15.95***	15.32***
	(3.619)	(3.757)	(6.343)	(5.815)	(5.626)	(5.574)	(5.681)	(5.486)
Upstream glyphosate × income quartile 1		15.51*						
		(8.018)						
Upstream glyphosate × income quartile 2		9.166*						
		(4.612)						
Upstream glyphosate × income quartile 3		3.502						
		(4.880)						
Local glyphosate	2.983	2.357						1.538
	(3.275)	(3.192)						(5.369)
Observations	14,630	14,630	7,770	7,770	7,770	7,770	7,770	7,770
R-squared	0.026	0.027	0.031	0.032	0.038	0.038	0.038	0.038
Number of counties	1,045	1,045	555	555	555	555	555	555
Economic covariates	Yes	Yes	No	Yes	Yes	Yes	Yes	Yes
Demographic covariates	Yes	Yes	No	No	Yes	Yes	Yes	Yes
Industrial pollution covariates	Yes	Yes	No	No	No	Yes	Yes	Yes
Medical resource covariates	Yes	Yes	No	No	No	No	Yes	Yes

Notes: This table replicates Table 1, but uses robust standard errors clustered at the HU4 watershed level. Standard errors are reported in parentheses: *** p<0.01, ** p<0.05, * p<0.1.

TABLE 2A.16. Upstream glyphosate effects on neonatal mortality: gestational length specifications

	(1)	(2)	(3)	(4)	(5)	(6)
Upstream glyphosate	20.78***	21.25***	20.96***	20.65***	22.04***	20.60***
	(5.771)	(5.674)	(5.535)	(5.517)	(5.619)	(5.945)
Local glyphosate						3.643
						(6.236)
Observations	6,018	6,018	6,018	6,018	6,018	6,018
R-squared	0.034	0.035	0.040	0.040	0.042	0.042
Number of counties	552	552	552	552	552	552
Economic covariates	No	Yes	Yes	Yes	Yes	Yes
Demographic covariates	No	No	Yes	Yes	Yes	Yes
Industrial pollution covariates	No	No	No	Yes	Yes	Yes
Medical resource covariates	No	No	No	No	Yes	Yes

Notes: This table replicates Table 1 columns (3) to (8), but uses a sample constructed by gestational length. Robust standard errors clustered at the watershed (HU8) level are shown in parentheses: *** p<0.01, ** p<0.05, * p<0.1.

2A.7. Supplementary Figures

FIGURE 2A.2. Average per capita income by income groups

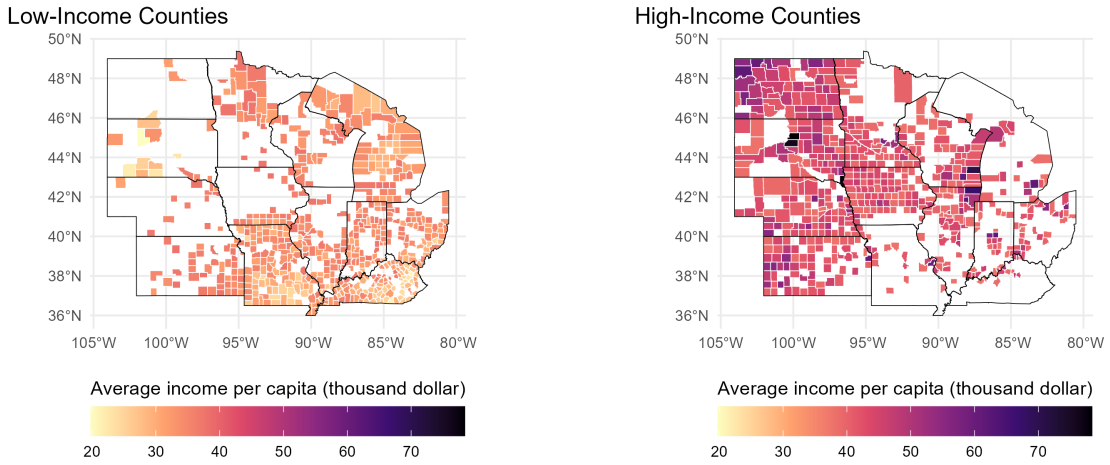
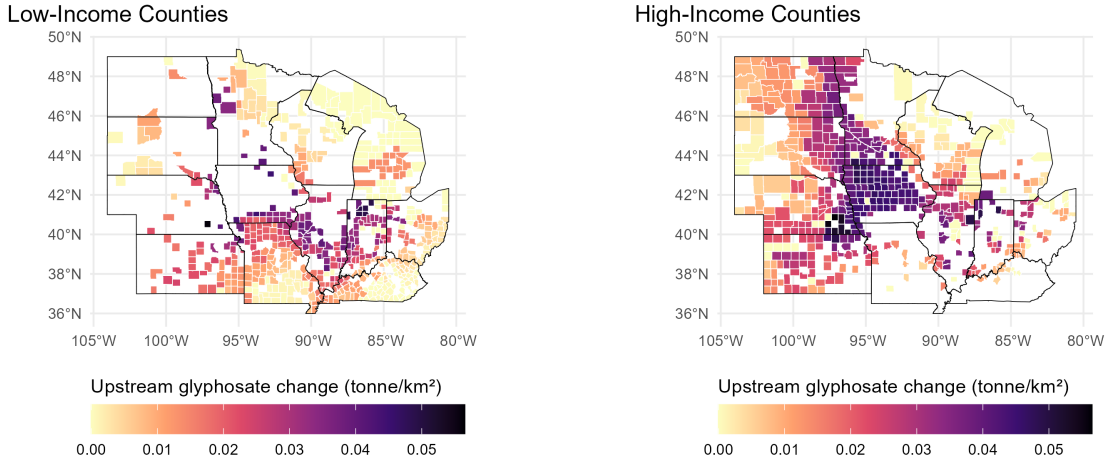


FIGURE 2A.3. Change in upstream glyphosate use by income groups



Notes: The figure shows the difference in average use between the first and second half of the study period.

FIGURE 2A.4. Average MCL violation coverage by income groups

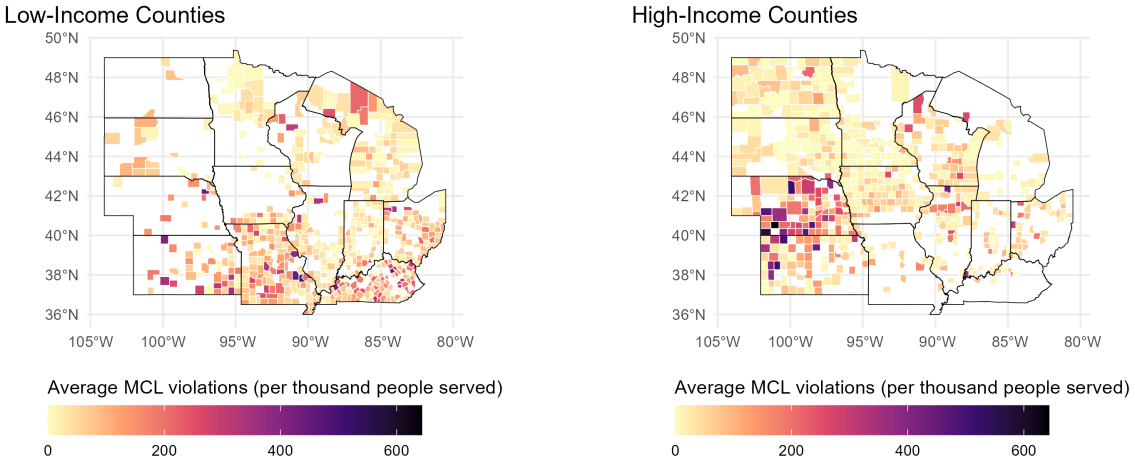


FIGURE 2A.5. Average MR violation coverage by income groups

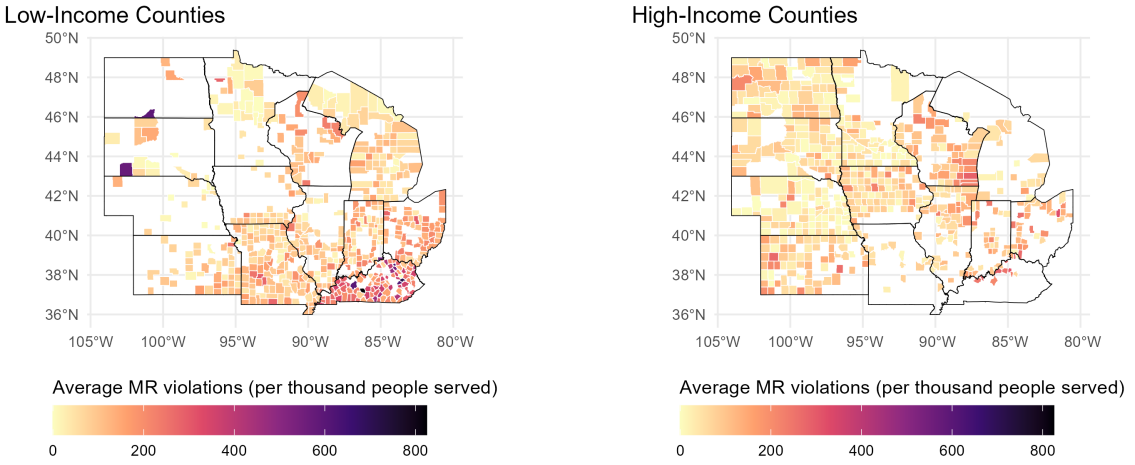
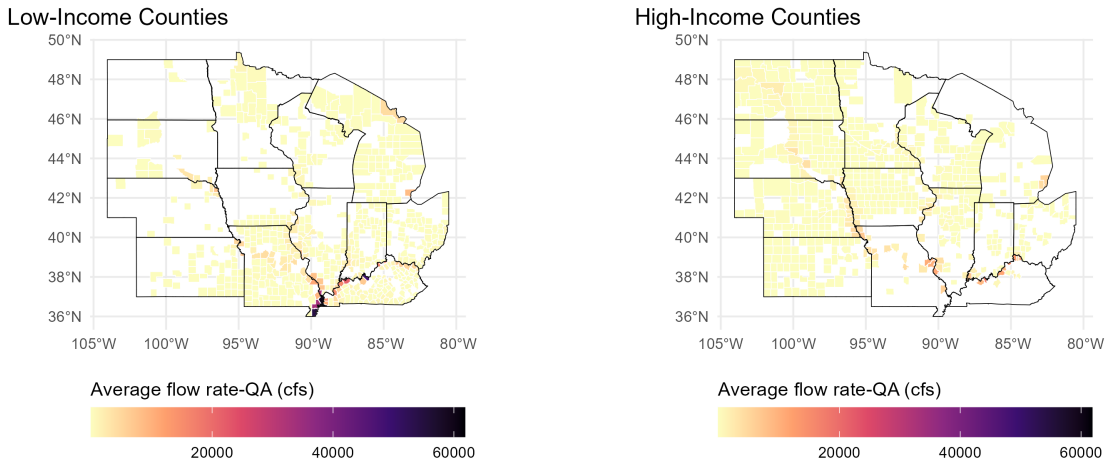
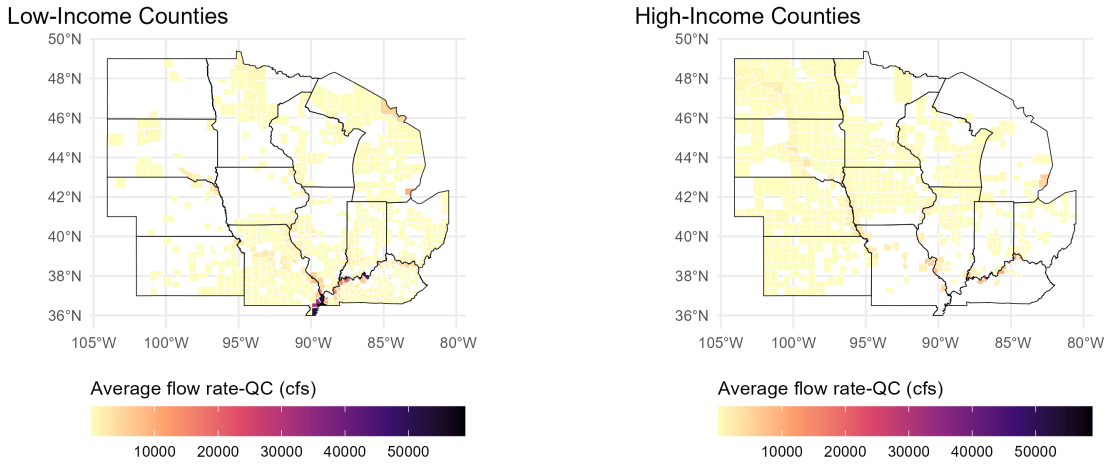


FIGURE 2A.6. Average annual flow rate (QA) by income groups



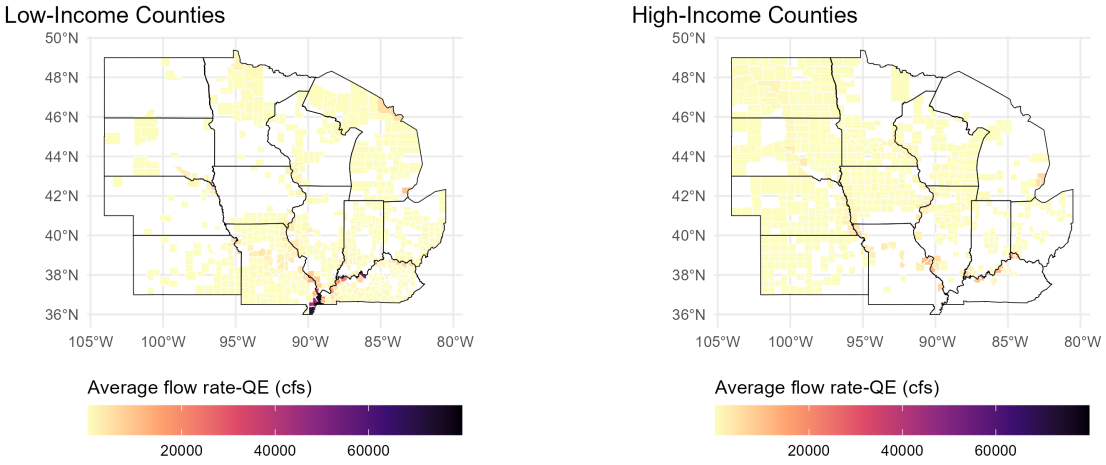
Notes: QA: mean annual flow from runoff. Source: EPA's NHDPlus Version 2 dataset, which reports QA, QC, and QE metrics. These estimates are highly correlated.

FIGURE 2A.7. Average annual flow rate (QC) by income groups



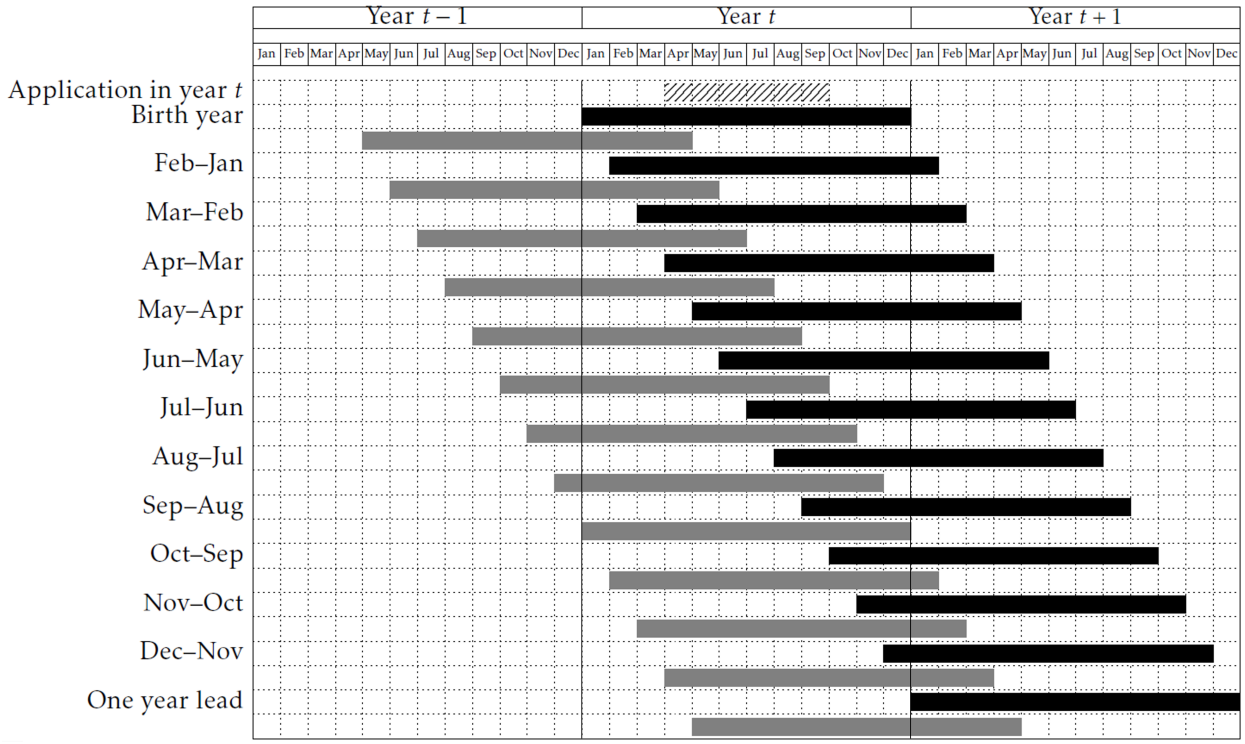
Notes: QC: mean annual flow estimated via reference-gage regression. Source: EPA's NHDPlus Version 2 dataset, which reports QA, QC, and QE metrics. These estimates are highly correlated.

FIGURE 2A.8. Average annual flow rate (QE) by income groups



Notes: QE: mean annual flow from gage adjustment. Source: EPA's NHDPlus Version 2 dataset, which reports QA, QC, and QE metrics. These estimates are highly correlated.

FIGURE 2A.9. Timeline of glyphosate exposure and birth months



Notes: Black bars indicate the birth months of the sample, while gray bars represent the corresponding conception months, assuming a 9-month gestational period. The diagonally hatched bar denotes the glyphosate application period in year t. Using birth year includes some neonates born before the glyphosate application in year t, as well as many who were conceived prior to the application and thus more exposed to glyphosate from the previous year. In contrast, using conception year (September–August) better aligns neonatal exposure with glyphosate applications in year t.

CHAPTER 3

Using vegetable oils for biofuel accelerates tropical deforestation and increases carbon emissions

Government policies in support of biofuels seek to cut carbon emissions, but they may also accelerate deforestation. Biomass-based diesel (BBD) made from vegetable oils has grown rapidly as a substitute for petroleum diesel, accounting for about 17% of global vegetable oil use in 2023. Yet, converting forests and other native vegetation to cropland produces roughly 10% of all human-induced carbon emissions (Searchinger et al., 2023), raising doubts about the climate benefits of BBD fuels. Understanding how biofuel expansion affects land-use conversion and emissions is therefore critical to assessing whether BBD truly advances, or undermines, climate goals (Lark et al., 2022; Lustgarten, 2018; Searchinger et al., 2008).

Palm oil is a primary BBD feedstock and a major driver of tropical deforestation, particularly in Indonesia and Malaysia, where forest loss has been extensive (Austin et al., 2019; Gaveau et al., 2022). For example, Borneo's forest cover declined 14% from 2001 to 2017 (Gaveau et al., 2019). Although several countries have restricted palm oil in biofuel policies because of deforestation concerns, increasing BBD demand for other vegetable oils can still raise palm oil prices because these oils are close substitutes for both cooking and BBD production. Higher prices, in turn, incentivize further forest conversion, a phenomenon known as indirect land-use change (ILUC).

Despite the policy relevance of ILUC, empirical evidence remains scarce (Lark et al., 2022), especially for the rapidly expanding BBD sector. Most existing studies on ILUC rely on ex-ante modeling approaches, such as computable general equilibrium (CGE) models, yielding mixed results

This chapter is a joint work with Richard J. Sexton and Aaron Smith, currently under review for publication. As the first author, T.-H. J. Chen, along with R. J. Sexton and A. Smith, developed the research methods jointly. T.-H. J. Chen collected the data and conducted the econometric analysis with input from R.J. Sexton and A. Smith. T.-H. J. Chen wrote the first draft of the manuscript. T.-H. J. Chen, R. J. Sexton and A. Smith edited the manuscript jointly.

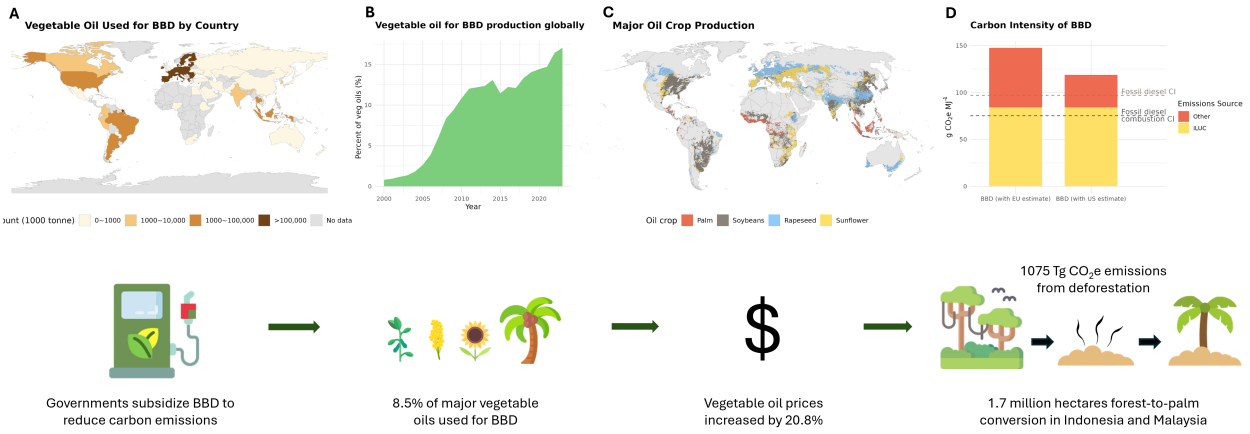
(Broch et al., 2013; Cui and Martin, 2017; Taheripour and Tyner, 2020; Warner et al., 2014). These broad discrepancies are largely due to divergent assumptions and choices of parameters, such as regarding consumer behaviors and the degree of yield response (intensification) to price incentives (Berry et al., 2024; Daioglou et al., 2020). Moreover, many models do not consider unmanaged land or predict accurately the location of land-use changes, leading to biased and uncertain estimates of emission factors (Berry et al., 2024; Warner et al., 2014).

We provide empirical evidence linking global BBD expansion to deforestation and associated carbon emissions. Our econometric approach reduces reliance on model assumptions and reveals causal relationships between global biofuel consumption, palm-oil prices, and observed land-use change. We use remote sensing data to detect the actual location and magnitudes of forest-to-palm conversion in Indonesia and Malaysia from 2002 to 2018. This not only lowers the uncertainty involved in carbon emission calculations but also enables analysis across land with varying environmental values and overcomes the limitation of tracing illegal deforestation activities in government data.

We integrate a series of econometric analyses, as illustrated in Figure 3.1. First, we quantify how global BBD policies affect palm oil prices by estimating econometric demand and supply models for oil palm and other major oil crops: soybeans, rapeseed (canola), and sunflower. Next, we estimate the effect of palm oil price fluctuations on deforestation using remote sensing data (Descals et al., 2024; Hansen et al., 2013; Xu et al., 2024) and panel econometric techniques. We generate 32,394 grid cells (9km $\times$ 9km resolution) covering the years 2002–2018. To estimate carbon emissions from forest-to-palm conversion, we integrate spatial data on biomass (Harris et al., 2021), peatland location (Global Forest Watch, 2023), palm plantations (Descals et al., 2024), forest cover (Hansen et al., 2013), and initial forest type (Xu et al., 2024). We then combine these estimates to quantify the overall impact of BBD policies on deforestation and associated carbon emissions.

Our analysis reveals that global BBD consumption from 2002 to 2018 has led to higher palm oil prices, contributing to the conversion of forests to oil palm plantations in Indonesia and Malaysia. Analysis of the regions where forest loss is linked to higher palm oil prices shows that expansion of oil palm plantations primarily leads to the conversion of natural forests, with little effect on planted forests or agroforestry. The carbon emissions from this deforestation likely exceed the emissions

FIGURE 3.1. Global use of vegetable oils for biomass-based diesel and resulting land use change and carbon emissions



A. Vegetable oils used for BBD by country, 2000-2023. Source: OECD (OECD/FAO, 2023). **B.** Global share of vegetable oils used for BBD production, showing that an average of 8.5% of vegetable oils were used for BBD between 2002 and 2018. Source: OECD (OECD/FAO, 2023). **C.** Major oil crop production regions in 2010. Source: (Yu et al., 2020). Our analysis estimates that BBD use from 2002–2018 increased vegetable oil prices by 21.2%. **D.** Estimated carbon intensity of BBD from ILUC, based on this study's analysis, compared to fossil diesel and other lifecycle emissions from US and EU government data (European Union, 2018; US Environmental Protection Agency, 2016). Our analysis further estimates that BBD use during this period led to 1.7 million hectares of forest-to-palm conversion in Indonesia and Malaysia, releasing approximately 1,086 Tg CO_2e.

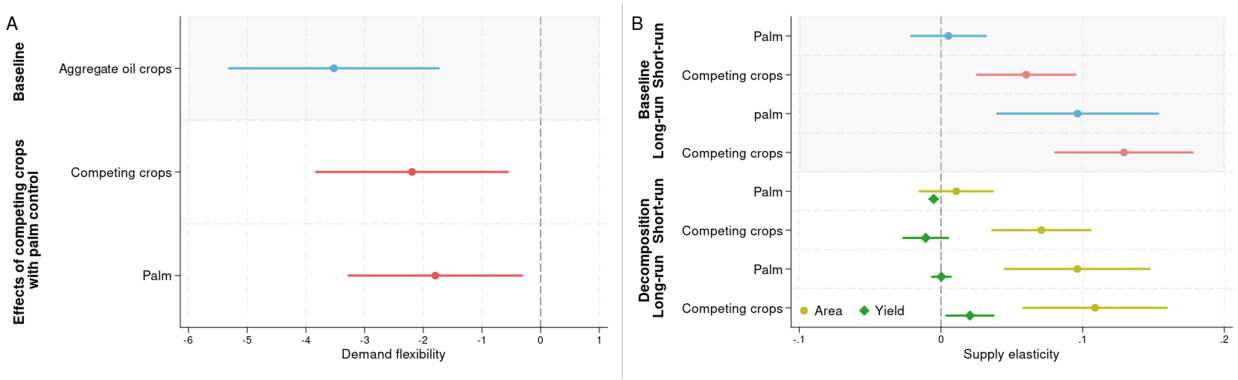
from petroleum diesel. Furthermore, the high substitutability among vegetable oils suggests that policies targeting only palm oil in BBD production are ineffective in reducing deforestation. These findings underscore the importance of accounting for ILUC effects in policy design and highlight the urgent need to shift future biofuel strategies away from crop-based feedstocks.

3.1. Results

3.1.1. Effects of BBD on palm oil prices

Government subsidies or mandates for BBD use boost demand for vegetable oils and increase prices for both palm oil and its substitutes, such as soybean, rapeseed, and sunflower oil. The magnitude of the price increase depends on the extent to which other users are willing to reduce consumption (demand elasticity) and the extent to which production expands (supply elasticity). From 2002 to 2018, BBD accounted for an average of 8.5% of annual global vegetable oil consumption. Using our

FIGURE 3.2. Estimated demand and supply responses to palm oil prices



A. Demand flexibility: Row 1 shows the baseline estimate of effects of aggregate oil crop production (oil palm fruit, soybeans, rapeseed, and sunflower) on palm oil prices, while rows 2–3 present the effects of competing oil crop production (soybeans, rapeseed, and sunflower) on palm oil prices, controlling for palm production. **B.** Baseline supply price elasticities with respect to palm oil prices: short-run palm (row 1), short-run competing crops (row 2), long-run palm (row 3), and long-run competing crops (row 4). Decomposition of supply elasticities into area and yield responses (rows 5-8). The estimates are from regressions with a flexible time trend of restricted cubic splines with 5 knots. Circles denote regression point estimates; lines represent 90% confidence intervals.

estimated demand and supply elasticities, we find that this BBD-driven demand shift raised palm oil prices by roughly 21.2% relative to business-as-usual (BAU) levels (90% confidence interval: [12.2%, 28.5%]).

Figure 3.2A row 1 demonstrates the estimated demand flexibility (inverse demand elasticity), indicating that, on average, a 1 percent decrease in the production of vegetable oils (palm oil, soybean oil, rapeseed oil, and sunflower oil) results in a 3.5% increase in palm oil prices (90% confidence interval: [1.7%, 5.3%]). Supplementary Text 3S.1 contains further details on these findings.

This price effect persists even when biofuel policies target non-palm vegetable oils. While some regions, like the US and EU, restrict palm oil in BBD production (Rum et al., 2022; US Energy Information Administration, 2025), we find that palm prices respond to production shocks in competing oil crops very similarly to shocks in palm production itself (Figure 3.2A). This result indicates that lower production of other oil crops raises palm oil prices even after controlling for palm production. The findings confirm that palm oil is highly substitutable with other major oil

crops, a finding consistent with prior studies (Declerck et al., 2023; Hashempour-Baltork et al., 2016; Hinrichsen, 2016) and with the cointegration results in the Supplementary Text 3S.2. These results indicate that diverting non-palm oil for BBD uses raises palm oil prices and does not allay concerns of forest-to-palm conversion.

If oil crop production were to expand easily in response to increased BBD demand, then palm oil prices would not increase sharply. However, we find the short-run supply elasticity of oil palm is small and insignificant (Figure 3.2B, row 1), indicating that palm production cannot expand immediately to mitigate price increases. This result is expected given that oil palm is a perennial crop that requires about four years from planting before fruiting (Feintrenie et al., 2010; Woittiez et al., 2017). Competing annual crops show a significant short-run supply response, but they only partially offset demand shocks (Figure 3.2B, row 2). In the long run (>6 years), palm production does respond to rising prices; a 1% price increase leads to a 0.1% production increase (90% confidence interval: [0.04%, 0.15%], Figure 3.2B, row 3). The long-run elasticity of the competing crops implies that a 1% price increase leads to a 0.13% production increase (90% confidence interval: [0.08%, 0.18%], Figure 3.2B, row 4), slightly larger than the short-run value, suggesting that some production adjustments take time. Further details on the long-run results are provided in the Supplementary Text 3S.3.

Critically, our decomposition of the supply response reveals that production increases are mainly driven by cropland expansion rather than yield response or intensification (Figure 3.2B). Although many CGE models assume a strong intensification response, which mitigates emissions due to ILUC, our empirical estimates show that yield improvements for oil palm in response to price changes are negligible. For the competing crops, approximately 84% of the supply response comes from area expansion, and yield improvements account for only 16%. Although the precise shares vary across model specifications (Supplementary Text 3S.3), the general pattern is clear: area responses dominate yield responses for both palm and the competing oil crops.

3.1.2. Effect of palm price on deforestation

Higher palm oil prices increase the attainable revenue from deforesting to produce palm. We find that an increase in attainable revenue of $1,000 (USD) per hectare corresponds to an additional 9.3

hectares of deforestation for palm plantations in the average cell in Indonesia and Malaysia (90% confidence interval: [7.2, 11.4]), amounting to approximately 300,000 hectares across the entire region (Figure 3.3A, row 1). For reference, between 2002 and 2018, the average annual attainable revenue was $1,933 per hectare, and the average annual deforestation for palm plantations was 15.44 hectares per cell.

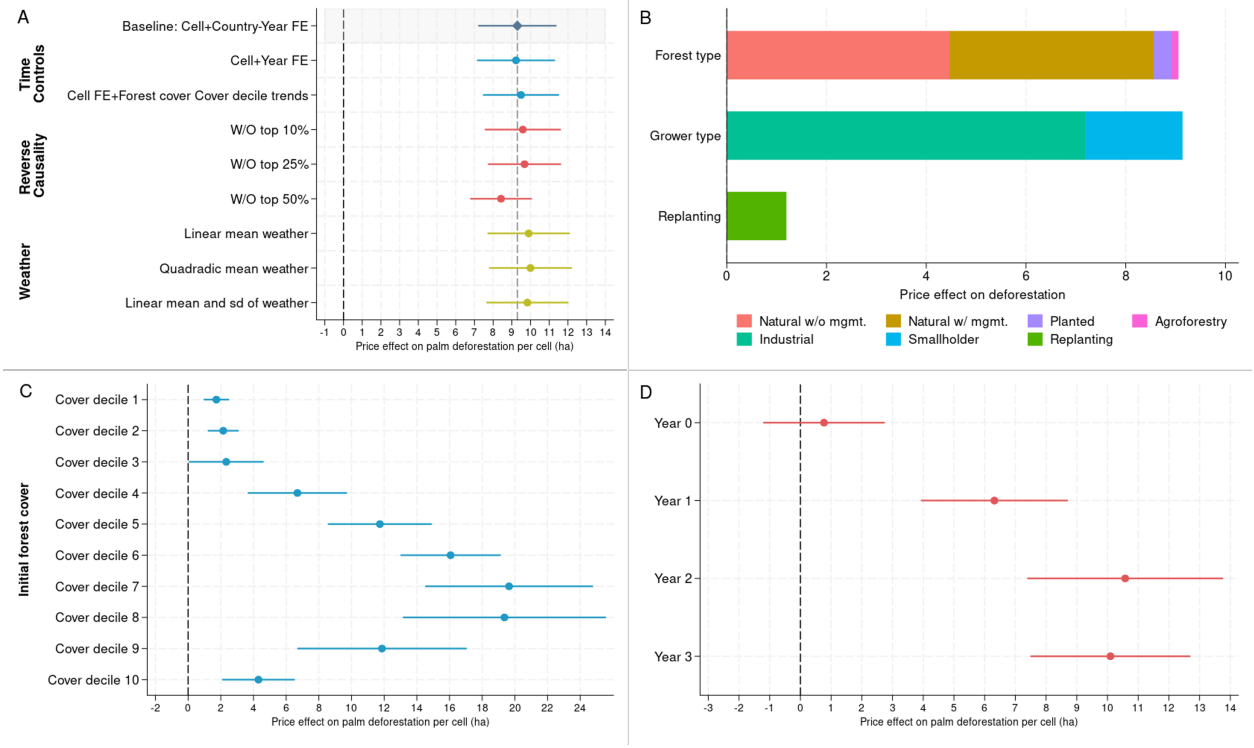
This estimate is similar across specifications and alternative channels, including different region and trend controls (Figure 3.3A, rows 2-3), reverse causality tests (Figure 3.3A, rows 4-6), weather controls (Figure 3.3A, rows 7-9), and different deforestation pressure due to attainable yields (See detailed discussion in Supplementary Text 3S.4).

The environmental impact is exacerbated by the type of land targeted. Decomposing the response by forest type reveals that revenue increases drive the most significant deforestation in unmanaged natural forests, followed by managed natural forests, with minimal effects on planted forests or agroforestry (Figure 3.3B). These results imply that palm growers preferentially expand into natural forests rather than replacing existing planted areas (Feintrenie et al., 2010). We exclude existing palm plantations from forest classifications because replanting does not alter long-term land-use carbon stocks. Separately, we find that high attainable revenues significantly increase replanting rates (Figure 3.3B), likely as growers anticipate sustained price strength and replace aging trees with higher-yielding palms.

We also explore heterogeneity by grower type and initial forest cover. Our results show that industrial growers are substantially more responsive to palm oil prices, contributing significantly more to deforestation than smallholders (Figure 3.3B, rows 2). For initial forest cover, deforestation responds most strongly to palm oil prices in cells with moderate initial cover (Figure 3.3C). Cells with low forest cover show limited response, as little land remains available for expansion. Conversely, cells with high forest cover—typically in remote and harder-to-access regions—also exhibit smaller responses, likely due to higher clearing costs. This pattern implies that, while palm expansion during the study period occurred predominantly in natural forests, it had not yet fully penetrated the most densely forested areas.

Because oil palm is a perennial crop, we also tested for lagged and persistent price effects. Producers appear to prioritize recent price changes in their clearing decisions, as cumulative multi-year

FIGURE 3.3. Effects of attainable revenue on deforestation area



The figures report the estimated effects of a $1,000/ha increase in attainable revenue on deforestation area (ha) per cell. Circles indicate regression point estimates; lines show 90% confidence intervals. **A.** Baseline estimate (row 1) and robustness to alternative specifications: different time controls (rows 2–3), reverse causality, i.e., whether expectations of future palm expansion affect prices (rows 4–6), and weather controls (rows 7–9). **B.** Decomposition of baseline effects by forest and grower types. Row 1 separates forest types: natural forests without management, natural forests with management (e.g., selective logging, logging, or other human activities), planted forests, and agroforestry. Row 2 distinguishes industrial plantations vs. smallholders, classified by plantation size, geometric patterns, tree structure, and stand age uniformity (Descals et al., 2024). Row 3 shows the price effects on replanting. **C.** Heterogeneous effects by initial forest cover deciles. **D.** Cumulative deforestation responses over ensuing years to revenues.

models yield results similar to our baseline one-year lag specification (Figure 3.3D and Supplementary Text 3S.4).

Finally, to test the robustness of our causal framework, we implement an alternative approach in which we estimate the annual palm oil price that would have existed in the absence of BBD use (Figure 3.3A). We then estimate annual deforestation implied by these price changes (Figure 3.3B). This alternative approach uses the supply elasticity implied by this estimates in Figure 3.3A

in place of the elasticity in Figure 3.2B. This method also more explicitly accounts for cumulative supply effects from past expansions, recognizing that oil palm is a perennial crop. The alternative estimate—an average 21.1% price increase—closely aligns with the baseline estimate of 21.2%. The estimated total deforestation area is 1.8 Mha, close to the baseline estimate of 1.73 Mha, reinforcing the robustness of our findings. (See the Supplementary Text 3S.5 for details).

3.1.3. Effects of BBD use on carbon emissions

Palm oil price increases driven by global BBD use from 2002 to 2018 led to an additional 1.7 Mha of forest-to-palm conversion in Indonesia and Malaysia (90% confidence interval: [1 Mha, 2.3 Mha]) compared to the BAU scenario, based on the estimated impact of palm oil prices on deforestation. This accounts for roughly 20% of the total forest-to-palm conversion in Indonesia and Malaysia over this period, and it released approximately 1086.4 Tg CO_2e (Table 1 column 1).

Dividing induced emissions by the total fuel energy produced in 2002-2018 by vegetable-oil BBD yields an ILUC carbon intensity (CI) of 84.1g CO_2e per megajoule (MJ) of BBD (90% confidence interval: [48.7 g CO2e/MJ, 113.5 g CO2e/MJ], Table 1 column 4). The ILUC CI alone is almost as large as the approximately 97 g CO_2e/MJ emitted by petroleum diesel across its entire life cycle (US Environmental Protection Agency, 2016). Because our estimates exclude ILUC from other vegetable oils and palm production outside our study region, they represent a conservative lower bound for ILUC emissions. Our estimates also omit the welfare losses borne by consumers from higher vegetable oil prices.

To obtain the total CI of vegetable-oil BBD, we add emissions from cultivation, processing, and transport (34.6-63.5 g CO_2e/MJ) (European Union, 2018; US Environmental Protection Agency, 2016) to our ILUC estimate and obtain 118.7-147.6 g CO_2e/MJ. Thus, even without considering emissions from other land use change, the CI of vegetable-oil BBD exceeds that of petroleum diesel by 22-52%. These results imply that when land-use change is considered, vegetable-oil BBD use increased, rather than reduced, emissions relative to petroleum diesel fuel during the period 2002-2018.

For forest-to-palm conversions, the ratio of carbon emissions to the BBD energy generated on the converted land equals 230.6 g CO_2e/MJ (Table 1 column 3). One possibility would be to

TABLE 3.1. Carbon emissions from land-use change due to oil palm expansion

	(1)			(2)	(3)	(4)		
	Total emissions (Tg CO_2e)			**Per ha per year** (Mg CO_2e/ha/yr)	**Direct CI** (g CO_2e/MJ)	**ILUC CI** (g CO_2e/MJ)		
	Estimate	90% Interval		Estimate	Estimate	Estimate	90% Interval	
		upper	lower				upper	lower
Biomass carbon (AGB+BGB)	757.7	439.0	1022.8	17.5	160.8	58.7	34.0	79.2
Non-peat soil organic carbon	94.8	54.9	128.0	2.2	20.1	7.3	4.3	9.9
Peat decomposition	614.0	355.7	828.7	14.2	130.3	47.5	27.5	64.2
Carbon sequestered by oil palm	-380.2	-220.3	-513.1	-8.8	-80.7	-29.4	-17.1	-39.7
Net carbon emissions from ILUC	1086.4	629.5	1466.4	25.1	230.6	84.1	48.7	113.5

Notes: Total emissions are amortized over 25 years to calculate emissions per hectare per year and carbon intensity (CI), consistent with the typical oil palm replanting cycle. This amortization period aligns with international policy conventions, falling between the U.S. EPA's 30-year standard and the EU's 20-year standard. Per hectare numbers calculated using the estimated 1.73Mha increase in deforestation. Direct CI is calculated as the ratio of net carbon emissions to the palm-based BBD volume that could be produced from the converted area, while ILUC CI is the ratio of net carbon emissions to the amount of BBD energy produced from vegetable oils in 2002-2018.

assign a "palm deforestation CI" of 230.6 to palm-based BBD and zero to other vegetable oils. However, because palm oil is traded on global markets along with other vegetable oils, and it is highly substitutable with those oils, the relevant policy metric is the indirect emissions from land use change due to increases in the use of any vegetable oil for BBD. This is the ILUC CI of 84.1g CO_2e/MJ that we report in Table 1 (column 4).

To understand where these emissions come from, we decompose total land-use change emissions into their underlying carbon sources. Land ecosystems store large amounts of carbon both above and below ground. Clearing land for palm production releases this carbon. We estimate that biomass loss, including above-ground biomass (AGB) and below-ground biomass (BGB), from BBD-induced conversion released approximately 757.7 Tg CO_2e (Table 3.1 column 1).

Peatland degradation constitutes another major source of emissions. Tropical peat swamp forests form massive carbon sinks, with an estimated deposit of 69 Gt of carbon in Southeast Asia (Miettinen et al., 2016). Indonesia and Malaysia together hold the world's largest share of tropical peat carbon, contributing about 74% and 60% of the total forest soil carbon pool in each country, respectively (Page et al., 2011). Plantation development on peatland leads to decomposition and continuous carbon release. Using palm plantation maps (Descals et al., 2024), initial forest type data (Xu et al., 2024), and peatland maps (Global Forest Watch, 2023), we estimate that between 2002 and 2018, about 8% of palm plantations expanded into intact peatland forests and 15% into peatlands already subject to human activity. BBD-driven expansion in these areas contributed about 614 Tg CO_2e over a 25-year palm lifecycle.

Palm expansion on non-peat soils also releases soil organic carbon (SOC). Accounting for the extent of non-peat expansion induced by BBD, the associated SOC emissions are estimated at 94.8 Tg CO_2e. At the same time, oil palm trees sequester carbon over their lifecycle. We estimate that plantations established due to BBD expansion will sequester about 380.2 Tg CO_2e over a 25-year lifespan. Combining these factors, the total net BBD-driven carbon emissions from land-use change is 1086.4 Tg CO_2e, which corresponds to an average of 25.1 Mg CO_2e per hectare per year (Table 3.1 column 2).

Supplementary Text 3S.6 compares our estimates of forest-to-palm conversion emissions with deforestation emissions from other studies. Our estimates are close to studies that explicitly account for emissions at the exact deforestation locations, while they diverge somewhat from studies that apply uniform biomass values across broad forest categories without considering variation by initial forest type or geography. This reinforces the importance of identifying the locations of forest-to-palm conversion and accounting for heterogeneity, as the environmental impacts and carbon emissions of converting different forest types and regions into feedstock plantations vary substantially.

3.2. Conclusion and discussion

Biofuels have become an important tool in the world's attempts to decarbonize transportation, and biomass-based diesel fuels play an increasing role in the fuel supplies in many countries. However, after taking land use change into account, some biofuels may have higher carbon emissions than the fossil fuels they replace. Most work on biofuel-driven land-use change to date has focused on the use of corn as a feedstock for the production of ethanol (Lark et al., 2022; Lustgarten, 2018; Searchinger et al., 2008). This study focuses on land use changes related to the production of biomass-based diesel (BBD) and, specifically, from the conversion of forest lands into palm plantations in Indonesia and Malaysia.

Our findings imply that BBD use, rather than delivering climate benefits, likely increases net carbon emissions. These calculations do not consider biodiversity losses, which are particularly severe in tropical forests (Barlow et al., 2016; Tudge et al., 2021), suggesting the true environmental costs are likely greater than those related to emissions. Moreover, during our study period, palm

expansion had not yet penetrated the most remote and densely forested areas, which generally hold higher carbon stocks. Continued expansion into such areas would further amplify carbon emissions. Such expansion appears likely as governments continue to expand BBD requirements and incentivize use of sustainable aviation fuel, which are currently produced using similar processes to BBD.

Policies in some countries, such as the US and those in the EU, recognize the harms associated with the use of palm oil in bio-based diesel fuel production and seek to curtail its use. However, such policies are unlikely to effectively mitigate deforestation in Indonesia and Malaysia. Because of the high substitution across vegetable oils, restrictions on palm oil simply shift BBD demand to other oils, which then raises palm prices indirectly as it substitutes for the displaced oils in cooking. More effective mitigation may come from expanding the role of alternative feedstocks, such as tallow and used cooking oil, in BBD production because these feedstocks likely do not cause significant adverse land use change effects.

3.3. Materials and Methods

We estimate the impacts of global BBD use on deforestation in Indonesia and Malaysia and the corresponding carbon emissions by linking a series of empirical models. First, we assess the impact of BBD use on palm oil prices by modeling global supply and demand for palm and cooking oils more generally. Second, we estimate the effect of palm oil prices on deforestation, leveraging observed remote sensing data and panel econometric techniques. Lastly, we combine these estimates to quantify the effect of BBD consumption on deforestation outcomes and carbon emissions.

This empirical strategy offers several advantages and contributions. First, it provides direct evidence on the environmental impacts of biofuel policies based on observed prices and land-use outcomes, minimizing assumptions and reliance on prescribed parameters. Second, it allows us to examine heterogeneity in price effects across regions in Indonesia and Malaysia with different environmental values. Third, by using high-resolution remote sensing data to detect the actual location of forest-to-palm conversion, we avoid reliance on assumptions about land types and enable the inclusion of unmanaged land, which is typically excluded from CGE models investigating ILUC (Berry et al., 2024). Remote sensing data also help overcome the limitations of government statistics

that often under report deforestation (Burgess et al., 2012; Cisneros et al., 2021). Fourth, we empirically model supply and demand for palm and cooking oils, offering evidence on both the high substitutability among cooking oils and the limited role of intensive-margin responses (yield increases) in offsetting demand shocks. The following subsections describe the methodologies and data used in each step.

3.3.1. Effects of BBD on palm oil prices

To evaluate the effects of BBD consumption on palm oil prices, we construct exogenous yield shocks (Roberts and Schlenker, 2013) using production data from the FAO (FAO, 2024) from 1961 to 2022 to estimate aggregated demand flexibilities for the four major oil crops and supply elasticities for the three oil crops besides oil palm. For oil palm supply, we rely on data from 1976 to 2019 from the USDA Foreign Agricultural Service (FAS) (United States Department of Agriculture, Foreign Agricultural Service, 2025) due to inconsistencies in FAO's reporting of harvested versus planted area for perennial crops. We obtain price data from the World Bank (World Bank, 2025), and nominal prices are deflated using the GDP deflator sourced from BEA (U.S. Bureau of Economic Analysis, 2024).

For the demand side, we estimate an inverse demand function for palm oil using two-stage least squares (Roberts and Schlenker, 2013) as follows:
First stage:

$$q_t = \xi_0 + \xi_1 \omega_t + h_1(t) + v_t. \tag{3.1}$$

Second stage:

$$P_t^{po} = \beta_0 + \beta_1 q_t + h_2(t) + \epsilon_t, \tag{3.2}$$

Here P^{po} is the log price of palm oil and q represents the log production of various oil crops. Depending on the model specification, q represents log of palm fruit production, log of the aggregate of production of the three major annual oil crops (soybeans, rapeseed, and sunflower), or log of the aggregate of production of all four crops (the three plus palm fruit). We use the December price because the production during the year affects the price at the end of the year. The parameter

β_1 equals the price flexibility of demand, which is the reciprocal of demand elasticity ($\epsilon^D = \frac{1}{\beta_1}$). The regressions include flexible time trends, $h_1(t)$ and $h_2(t)$ to allow intercepts to evolve over time. The baseline model specifies these trends using restricted cubic splines with five knots. Given that production and price are mutually determined, we follow previous studies and use yield shocks (ω) as an instrumental variable for production to address the endogeneity of q to demand shocks (Hendricks et al., 2015; Roberts and Schlenker, 2013).

Yield shocks are the log average deviations of yields from crop- and country-specific yield trends across production countries, weighted by predicted yield and growing area (Hendricks et al., 2015). The underlying yield trends are estimated using restricted cubic splines with five knots. The yield shocks are primarily caused by random weather events. Supplementary Text 3S.7, provides more details on the construction of yield shocks and their validity as an instrument, and Supplementary Text 3S.8 presents sensitivity checks on the derivation of yield shocks.

We estimate the oil supply elasticity separately for oil palm, which is a perennial crop, and the other three major oil crops, which are annuals. The supply equation is:

$$q_t = \alpha_0 + \sum_{s=1}^{k} \alpha_s P_{t-s}^{po} + \delta\omega_t + g(t) + \varepsilon_t, \tag{3.3}$$

where q_t is the log production of palm fruit or the three major annual oil crops (soybeans, rapeseed, and sunflower), depending on the model specification. The term, $g(t)$, is a flexible time trend. The estimate α_s represents the price elasticity of supply at lag s. Following previous literature (Hendricks et al., 2015), the model controls for realized yield shocks (ω) as a proxy for expected shocks. Since markets for storable goods incorporate production expectations, prices can become endogenous to supply. Controlling for yield shocks helps address this endogeneity by accounting for partially predictable production variations. Consistent with empirical evidence that farmers form price expectations based on recent prices (Chavas, 2000), we use the lagged annual average palm oil prices for P.

For the short-run supply, we include only one lag ($k = 1$). For the long run, we allow multiple lags and evaluate the cumulative elasticity because producers may respond to price changes gradually over time, especially for oil palm (Supplementary Text 3S.3 provides more details about lag

length selection). The aggregated supply elasticity is then calculated as a weighted average of the two elasticities, given by $\epsilon^S = \epsilon^{Sp} s^p + \epsilon^{So} s^o$, where ϵ^{Sp} and ϵ^{So} are the supply elasticities of palm oil and the other three oil crops, respectively; s^p is the market share of palm oil among the main vegetable oils, and s^o is the combined share of the other three oils.

Finally, to link these elasticity estimates to the effects of BBD on palm oil prices, we use OECD data on vegetable oil used for BBD. From 2002 to 2018, global BBD use accounted for approximately 8.5% of the combined global production of palm, soybean, canola, and sunflower oils. Using the demand and supply elasticities estimated above, we calculate the effect of BBD consumption on palm oil prices. A demand shift of percentage $\Delta\%Q$ changes the equilibrium price by $\Delta\%price = \frac{\Delta\%quantity}{\epsilon^S - \epsilon^D}$. We use this relationship to calculate the business-as-usual price in the absence of BBD demand.

We further consider two potential sources of bias in our estimates. First, our analysis focuses on the effects of BBD between 2002 and 2018, but the demand and supply elasticities are estimated using a longer time series extending further back. A potential concern is that market behavior in earlier decades may differ from recent years—particularly as BBD demand became more persistent—so elasticities estimated from older data may not fully reflect current responsiveness. To address this concern, we included a post-2000 dummy in both the demand and supply models. The results show no significant differences in elasticities before and after 2000 (Supplementary Text 3S.1), suggesting that our elasticity estimates are stable over time and not biased by the inclusion of earlier years.

Second, the OECD reports global BBD feedstock use only at the aggregate vegetable oil level—including the four major oils analyzed here (palm, soybean, rapeseed, and sunflower) as well as smaller contributors such as coconut, cottonseed, and groundnut oils. These major oils account for roughly 90% of global vegetable oil production, while the remainder contribute negligibly to BBD output. Therefore, our assumption that 8.5% of total vegetable oil use was devoted to BBD during 2002–2018 is conservative, and the true share is likely higher.

3.3.2. Effect of palm price on deforestation

To estimate the impact of palm oil prices on deforestation in Indonesia and Malaysia, we constructed a panel dataset covering 32,394 grid cells (9 km × 9 km) from 2002 to 2018. The main outcome of interest is the deforestation area converted to oil palm. We combine the Global Forest Change (GFC) dataset (Hansen et al., 2013), oil palm planting-year maps (Descals et al., 2024), and a pre-clearing vegetation map (Xu et al., 2024) to identify this variable. GFC is one of the most widely used datasets on forest loss (Pendrill et al., 2022), providing a 2000 baseline forest map at 30-meter resolution. Following Indonesia's official definition, we classify as forest any area with canopy cover greater than 30%. By merging GFC with planting-year maps (10 m resolution), we identify annual forest-to-palm conversion.

A challenge is that GFC defines all vegetation taller than 5 meters as forest, including planted forests, agroforests, and oil palm plantations. Since these land types differ substantially in ecological value (Tropek et al., 2014), and replanting palm does not constitute deforestation, we use the 2001 pre-clearing vegetation map (100 m resolution) to distinguish natural forest from planted forest and exclude palm-to-palm replanting from our deforestation measure. The palm planting-year map provides establishment dates until 2021, but very young plantations established in the final years are under detected, as they are not yet visible in the satellite imagery. To address this, we exclude the last three years of data. Our analysis thus focuses on 2002–2018.

To construct annual, cell-specific attainable revenue from palm production, we incorporated oil palm attainable yields from UN FAO's GAEZ dataset [1] and World Bank price data (World Bank, 2025), following (Busch et al., 2015) and (Berman et al., 2023). The resolution of the GAEZ dataset is 5 arc minutes (about 9 km at the equator). We also used ERA-Interim weather data (Muñoz Sabater, 2019) to control for confounding factors.

We estimated the following empirical model to investigate the price effects on deforestation in Indonesia and Malaysia:

$$df_{ct} = \alpha_0 + \theta R_{c,t-1} + \alpha_c + \tau_{st} + \epsilon_{ct}, \tag{3.4}$$

[1] Global Agro Ecological Zones version 4 (GAEZ v4).

where df_{ct} represents the area of deforestation for palm plantations in cell c year t and R_{ct} is the attainable revenue from palm oil production. This revenue is calculated as the product of the international price P_t and attainable yields (a_c) for each cell, expressed as $R_{ct} = P_t \times a_c$. Regressions include cell fixed effects α_c to account for all time-invariant characteristics of each cell. The preferred specifications incorporate country-year fixed effects (τ_{st}) to capture national policy changes or other country-specific shocks that could promote or hinder deforestation in the country s year t. We also examine different time controls, including year fixed effects and a time trend that varies by initial cover to capture heterogeneous deforestation pressures. Standard errors are clustered at the second-level administrative unit, reflecting the role of local governments in granting permits for palm expansion and logging (Cisneros et al., 2021; McCarthy et al., 2012).

In the baseline, we regress deforestation on attainable revenue lagged one year, capturing responses to recent price changes. Since oil palm is a perennial crop with long investment horizons, we also test alternative revenue specifications, including longer lags, multi-year averages, and deviations from long-term price trends. To assess robustness, we examine reverse causality (i.e., whether expectations of future palm expansion affect current prices), additional weather controls, and sensitivity to attainable yield definitions (Supplementary Information, Section 3S.4).

3.3.3. Effects of BBD use on carbon emissions

We calculate carbon emissions by quantifying changes in carbon stocks resulting from forest-to-oil palm conversion between 2002 and 2018. The accounting includes emissions from above-ground biomass (AGB), below-ground biomass (BGB), soil organic carbon (SOC) in non-peatland, and peatland decomposition, net of the carbon sequestered by oil palm trees. In Supplementary Text 3S.6, we assess the robustness of our carbon emission estimates from land-use change by comparing them with findings from previous studies conducted in similar regions.

For biomass-related emissions, we estimate the biomass of deforested areas using the Above-ground Live Woody Biomass Density Map (Harris et al., 2021) and apply a below-to-above-ground biomass ratio of 0.24 (Busch et al., 2015). AGB and BGB are then converted to carbon stocks using a biomass-to-carbon ratio of 0.47 (Harris et al., 2021).

To capture emissions from peatlands, we combine the peatland map (Global Forest Watch, 2023), the palm plantation map (Descals et al., 2021), and the pre-clearing vegetation map (Xu et al., 2024) to identify palm expansion into peatland across different initial forest types. For conversion of disturbed peatland forests (natural forests with management, planted forests, and agroforestry), we adopt the IPCC estimate of 40.3 Mg CO_2e ha^{-1} yr^{-1} for long-term drained organic peat soils (Hiraishi et al., 2014), which excludes the initial emission peak. For conversion of intact peatland forests, we use an average of 100 Mg CO_2e ha^{-1} yr^{-1} over 25 years (Hooijer et al., 2012).

Emissions from SOC in non-peat areas and carbon sequestration by oil palm trees are based on (Pendrill et al., 2019). All biomass and non-peat soil emissions are amortized over 25 years, consistent with the typical oil palm replanting cycle. This amortization period is aligned with international policy conventions, falling between the U.S. EPA's 30-year and the EU's 20-year standards. We estimate that about 20% of the total forest-to-palm conversion during 2002-2018 is due to BBD demand, and proportionally assign the corresponding land-use change emissions to BBD.

To derive the carbon intensity of BBD per unit of energy, we use the biodiesel conversion rate of crude palm oil and energy content data from USDA (USDA, 2024). Since BBD includes both biodiesel (BD) and renewable diesel (RD), we rely on BD's conversion rates, as BD has dominated global BBD production (S&P Global, 2024). Because RD conversion rates are lower (Uusitalo et al., 2014), our CI estimates are likely conservative, meaning the true carbon intensity per MJ may be larger than our estimate. We compute confidence intervals using the bootstrap procedure detailed in Supplementary Text 3S.9.

3S. Supplementary Materials

3S.1. Further details on demand and supply elasticity estimates

Table 3S.1 reports estimates of demand flexibility for aggregate oil crops with respect to palm oil prices. The baseline model (Column 3) adopts the most flexible specification, a restricted cubic spline with five knots, while Columns 1 and 2 use spline trends with three and four knots,

respectively. The estimated coefficients are similar across specifications. Asterisks in all regression tables are based on two-sided p-values unless otherwise noted.

The estimated demand elasticity from the baseline model is -0.28, indicating an inelastic response of vegetable oil demand to price changes. This finding is consistent with the common finding that the elasticity of derived demand for an input is small when its share in production is small (Bronfenbrenner, 1961). Because vegetable oil represents a relatively small share of total input in food production, its demand tends to be inelastic. Our global demand elasticity estimate is also consistent with (James Seale et al., 2003), who report unconditional own-price demand elasticities for oils and fats across 114 countries: -0.158 for high-income, -0.325 for middle-income, and -0.442 for low-income countries.

Table 3S.2 presents the demand flexibility estimates when oil palm fruit is separated from the three competing oil crops, under alternative time-trend specifications. The results remain stable across specifications.

Table 3S.3 examines whether market behavior differed between earlier decades and more recent years, particularly after BBD demand became more persistent in the 2000s. The interaction terms between the post-2000 dummy and the estimated supply elasticities and demand flexibility are both economically small and statistically insignificant. This suggests that the elasticities are stable over time and not biased by the inclusion of earlier years in the estimation sample.

3S.2. Vegetable oil prices are cointegrated

We test whether palm oil and other vegetable oil prices are cointegrated using the Engle–Granger method (Engle and Granger, 1987). The results indicate that these oil prices move together in the long run, consistent with the view that the major vegetable oils are close substitutes.

Theoretically, if products A and B are perfect substitutes, the marginal rate of substitution (MRS) between them is constant:

$$MRS_{A,B} = \frac{P_A}{P_B} = C,$$

where C is a constant and P_A and P_B denote the prices of goods A and B, respectively. In this case, prices move proportionally. In practice, when the price of one oil rises, consumers substitute

perfectly towards other oils, increasing their demand and driving up their prices (CME Group, 2017).

Figure 3S.1 plots monthly prices for the four major vegetable oils from 1960 to 2024 (World Bank data), showing they track each other closely. Using global price data from 1960 to 2024 from the World Bank, Augmented Dickey–Fuller (ADF) tests indicate that all log price series are nonstationary (I(1)) for the four major oil crops, with the null of a unit root rejected only for their first differences (Table 3S.4).[2] Residuals from regressions of palm oil prices on each competing oil's prices are stationary (Table 3S.5), confirming cointegration. The estimates in Table 3S.5 suggest strong long-run co-movement between palm oil and other major oils. The coefficients are close to unity for soybean and canola oil (about 1.04 and 1.01, respectively), and slightly below unity for sunflower oil (about 0.86). These near one-to-one relationships reinforce the view that the oils are close substitutes in consumption and trade, with price shocks in one market transmitting strongly to others.

3S.3. Further details on long-run supply response estimates

A long-run supply model considers multiple lags and evaluates the cumulative elasticity, as specified in Eq. (3.3):

$$q_t = \alpha_0 + \sum_{s=1}^{k} \alpha_s P_{t-s}^{po} + \delta\omega_t + g(t) + \varepsilon_t,$$

which can be re-parameterized as:

(S1)

$$\begin{aligned} q_t &= \alpha_0 + \sum_{s=1}^{k-1} \zeta_s \Delta P_{t-s}^{po} + \zeta_k P_{t-k}^{po} + \delta\omega_t + g(t) + \varepsilon_t \\ &= \alpha_0 + \alpha_1 \Delta P_{t-1}^{po} + (\alpha_1 + \alpha_2)\Delta P_{t-2}^{po} + \cdots + (\alpha_1 + \cdots + \alpha_{k-1})\Delta P_{t-k+1}^{po} + (\alpha_1 + \cdots + \alpha_k) P_{t-k}^{po} \\ &\quad + \delta\omega_t + g(t) + \varepsilon_t, \end{aligned}$$

where the cumulative effects of lagged prices become more transparent. This formulation facilitates identifying the long-run response pattern. Tables 3S.6 and 3S.7 report the detailed estimates of long-run supply elasticities using Eq. (S1). Based on the Akaike Information Criterion (AIC) and

[2]Canola oil prices are only available from February 2002 onward, and sunflower oil prices are not available before 2002 and are incomplete for that year.

Bayesian Information Criterion (BIC), the long-run analysis includes 6 lags for the three annual oil crops and 7 lags for oil palm.

The results highlight distinct response dynamics between palm and the other oil crops, reflecting their biological and agronomic differences. For soybeans, rapeseed, and sunflower—annual crops—the production response occurs quickly within one year (Table 3S.6, Columns 1–3). The main adjustment comes from area expansion (Columns 4–6). Under the specification with 5 knots, yield even shows a small negative response in the first two years (Column 9), possibly because expansion pushes cultivation into marginal land with lower productivity. Over longer horizons, yields increase slightly, possibly from investment in productivity improvements, but the dominant adjustment channel remains area expansion.

In contrast, oil palm exhibits a markedly delayed response. Prices have no significant effects on either harvested area or production until three to five years later, which aligns with the biological lag of oil palm maturation (Table 3S.7). As with the other crops, the main driver of expansion is cropland area (Columns 4–6). Yield responses are even smaller and more sensitive to alternative time-trend specifications (Columns 7–9). This pattern underscores that palm oil supply adjustment is slow, persistent, and heavily dependent on land conversion, rather than yield intensification.

3S.4. Price effects on deforestation are robust to alternate specifications

We performed multiple checks to ascertain the robustness of our deforestation results. We first verified that the main findings are not sensitive to alternative FE or time trend specifications, as shown in Table 3S.8. The baseline estimate with country–year FE in Column 1 is very similar to the estimates in Columns 2–3, which instead control for year FE and initial forest-cover–decile trends. The decile-specific trends capture differences in deforestation likelihood or pressure associated with initial forest cover, which may potentially covary with attainable revenue.

Another potential concern is that the relationship between prices and deforestation might also reflect reverse causality—i.e., traders might anticipate increased palm production, and this drives down prices. This effect is less likely for a perennial like palm fruits, which take 3-5 years to harvest after planting. To further address this potential concern, we excluded the top 10%, 25%, and 50% of production cells to focus on smaller production areas. The results in Figure 3.3A rows

4-6 and Table 3S.9 show that the estimates remain consistent, suggesting reverse causality is not a significant issue.

Weather conditions can be another confounder. Weather influences fire risks, impacts palm production (Noojipady et al., 2017), and potentially co-varies with palm oil prices. To mitigate this concern, we controlled for temperature and precipitation in the model, specifying deforestation area as a quadratic function of each.[3] Results, as shown in Table 3S.10 and Figure 3.3A rows 7-9, indicate a convex relationship between deforestation area and both temperature and precipitation, although the coefficients on the quadratic terms are not statistically significant. Importantly, the estimates for palm revenue remain robust after accounting for weather effects.

Moreover, since the revenue variable is constructed using attainable yields (AY), it is possible that the estimates are biased by variations that co-vary with yield potential, as yield potential may correlate with other factors influencing deforestation pressure. To address this concern, we included interaction terms between deciles of attainable yields and linear time trends to allow for different deforestation trends by the yields. Additionally, we tested the sensitivity of the results by dropping extreme values. Table 3S.11 demonstrates that the estimates remain stable across these robustness tests.

Finally, we test whether growers primarily respond to recent prices, as assumed in the baseline model, or to alternative measures of price dynamics. Table 3S.12 Columns (1)–(5) and Figure 3.3D show that one-year-lagged prices account for most of the effect. Columns (5)–(8) of Table 3S.12 use moving averages of prices over different horizons (from $t-1$ to t, $t-3$, and $t-5$), with results indicating that longer averaging windows attenuate the estimated effect. Following the previous study (Cisneros et al., 2021), we also construct a variable capturing the deviation of current prices from multi-year historical averages. The hypothesis is that growers adjust deforestation when current profitability diverges sharply from past norms. Table 3S.13 reports the results, showing significant estimates for the deviation of last year's price from 5-, 7-, and 10-year averages. These estimates reinforce the conclusion that farmers place greater weight on recent price changes.

[3]Temperature and precipitation are demeaned.

3S.5. Using supply elasticity implied by the deforestation model does not change estimate of price effect

To assess the robustness of the deforestation estimates and compare results from the long-run palm supply elasticity model with those from the deforestation-response model using remote sensing data, we implement an alternative approach in which BAU prices are estimated from deforestation-response coefficients rather than from the palm long-run supply elasticity. This method also explicitly accounts for the cumulative supply effect of past palm expansion, recognizing that oil palm is a perennial crop and that a one-time expansion generates fruit for many years. Accordingly, we compute net BBD demand shocks by subtracting the palm oil production resulting from earlier expansions.

We begin by estimating BAU prices for the first four years of the study period using only the supply elasticities of competing oil crops, assuming no immediate supply response from palm due to its biological lag. These BAU prices are then combined with the estimated deforestation response to palm oil prices to infer the associated palm-driven deforestation area. This area is converted into palm oil production using adjustments for: (i) the share of production from Indonesia and Malaysia, (ii) the proportion of palm expansion occurring in forests, (iii) palm fruit yields of each year, and (iv) average oil content of palm fruits.

From the fifth year onward, we subtract the additional palm oil production from four years earlier (when the corresponding deforestation occurred) from the BBD-induced demand shock to obtain a net demand shock. The BAU price and associated deforestation for that year are then re-estimated. This iterative process continues for all subsequent years, incorporating the cumulative production effects of earlier expansions.

Figure 3S.2 (A) plots observed and BAU palm oil prices. The average price increase over the study period is 21.1%—similar to the baseline estimate using the long-run palm supply elasticity (21.2%). Figure 3S.2 (B) shows observed and BAU forest–palm conversion. The difference between the two lines is the estimated deforestation area driven by BBD in Indonesia and Malaysia, with an estimated total deforestation area of 1.8 Mha, close to the baseline estimate of 1.73 Mha, supporting the robustness of our findings.

3S.6. Comparison to other estimates of carbon emissions from land-use change in Indonesia

To assess the robustness of our carbon emission estimates from land-use change, we compare them with findings from previous studies conducted in similar regions. Table 3S.14 presents both our estimates and those from the literature. Our results are broadly consistent with studies that explicitly calculate emissions at the exact deforestation locations (Busch et al., 2015; Groom et al., 2022). For example, we estimate carbon emissions from biomass at 438.2 Mg CO_2e/ha, while Groom et al. (2022) (Groom et al., 2022) report a higher estimate of 570.1 Mg CO_2e/ha. Their higher figure likely reflects their focus on deforestation in primary and peatland forests, which generally store more carbon.

When summing emissions from biomass, SOC, and peatland, our estimate of 848.1 Mg CO_2e/ha is close to the 749.9 Mg CO_2e/ha reported by Busch et al. (2015) (Busch et al., 2015). The remaining discrepancy may arise because their scope includes deforestation for logging and timber extraction, in addition to palm expansion, and the study period and area.

By contrast, our estimates differ more from studies that apply uniform biomass values across broad forest categories or locations (Carlson et al., 2013; Guillaume et al., 2018). These studies tend to report higher biomass values than ours, likely because their baseline forests are denser than many of the forests in the actual study area.

Taken together, these comparisons reinforce the importance of identifying the locations of forest-to-palm conversion and accounting for heterogeneity. The environmental impacts and carbon emissions from converting forests into feedstock plantations vary considerably depending on forest type and regional conditions.

3S.7. Further details on construction of yield shocks as instrumental variables

We adapt the method from previous studies (Hendricks et al., 2015; Roberts and Schlenker, 2013) to model demand and supply. The aggregate oil crop quantity in year t is constructed using the oil production share s_c of each crop c:

$$Q_t = \sum_c s_c Q_{ct}.$$

The oil production share s_c is an oil conversion factor; it is the proportion of crop c that is oil by weight. Aggregate oil production can be decomposed as:

$$Q_t = A_t \, Y_t \, \Psi_t,$$

where A_t is the total growing area, Y_t is the average yield trend (weighted by oil share), and Ψ_t is the average yield shock, primarily driven by weather as shown in the latter part of this section.

Total growing area is measured as the sum of country i and crop c areas across all oil crops in the dataset. This variable reflects the extensive margin of production. Mathematically:

$$A_t = \sum_i \sum_c A_{cit}.$$

The yield trend (Y_t) represents the intensive margin, the technological and agronomic improvements in productivity, net of short-run shocks. For each crop c in country i and year t, we fit a restricted cubic spline trend with five knots to the yield series. We construct the annual yield trend as the weighted average of country–crop-specific yield trends, using weights based on area (A_{cit}) and the oil production share of each crop (s_c):

$$Y_t = \frac{\sum_i \sum_c s_c \times A_{cit} \times Y_{cit}}{\sum_i \sum_c A_{cit}}.$$

Yield shocks (Ψ_{cit}) represent deviations from the estimated yield trend, primarily reflecting short-run weather conditions. The shock is computed as the proportional deviation of observed yield from its estimated trend value, i.e., $\Psi_{cit} = Y_{cit}^{obs}/Y_{cit}$, where Y_{cit}^{obs} denotes observed yield. To obtain the annual aggregate yield shock, we average these deviations across all countries and crops, weighting by each crop's oil production share (s_c), its growing area (A_{cit}), and its trend yield (Y_{cit}):

$$\Psi_t = \frac{\sum_i \sum_c s_c \times \Psi_{cit} \times A_{cit} \times Y_{cit}}{\sum_i \sum_c s_c \times A_{cit} \times Y_{cit}},$$

We denote the log quantity, log area, log yield trend, and log yield shocks as $q_t = ln(Q_t)$, $a_t = ln(A_t)$, $y_t = ln(Y_t)$, and $\omega_t = ln(\Psi_t)$. Demand flexibilities for the four major oil crops and supply elasticities for the three annual oil crops are estimated using FAO data from 1961 to 2022 across all producing countries. For oil palm supply, we rely on USDA FAS data from 1976–2019 for

Indonesia, Malaysia, Thailand, and the Philippines, which together account for over 82% of global palm oil production. FAS data are preferred due to inconsistencies in FAO's reporting of harvested versus planted area for perennial crops. The underlying assumption is that producer behavior in these four countries reflects global oil palm supply dynamics.

The log yield shock serves as an instrumental variable and must satisfy both relevance and exogeneity conditions. Relevance follows directly from the production identity: yield shocks are deviations from yield trend, a key determinant of production. Empirically, relevance is confirmed by highly significant first-stage regressions with strong F-statistics (Table 3S.1).

Exogeneity is a more substantive concern. One potential issue is that yield shocks could be endogenous if they are driven by prices. However, several pieces of evidence suggest this is unlikely. First, yield shocks vary substantially across countries even though all countries are exposed to the same global prices, indicating that they are not mechanically determined by price movements. Figure 3S.3 shows the correlations between yield shocks of the top two exporters for each crop. The correlations are uniformly low across crops, suggesting that shocks are largely idiosyncratic to country-specific conditions, such as weather, rather than global price dynamics.[4] Second, while palm oil prices exhibit strong autocorrelation, aggregate yield shocks show little to no persistence over time, which is consistent with shocks being driven by weather-related events rather than market forces. This distinction is further supported by formal tests: Breusch–Godfrey test statistics for the aggregated yield shocks are very low (0.004–0.015 for all four oil crops, 0.132–0.351 for the three competing crops, and 1.42–1.48 for palm oil), all of which fail to reject the null hypothesis of no autocorrelation. By contrast, test statistics for palm oil prices range from 10.7–20.1, exceeding the 1% critical value in all cases, indicating strong autocorrelation. Taken together, this evidence supports the validity of yield shocks as an exogenous instrument.

[4]The correlation coefficients for the top two exporters are −0.118 for soybeans, 0.074 for rapeseed, 0.208 for sunflower seed, and 0.086 for palm based on FAO data, 1961–2022). For palm based on FAS data (1976–2019), the correlation coefficient is 0.291.

3S.8. Demand and supply elasticities not sensitive to assumptions in yield shock construction

The baseline model constructs yield shocks using a flexible yield trend based on restricted cubic splines with five knots. To test the sensitivity of the results to the choice of yield shock construction, we re-estimate the demand and supply models using trends with three and four knots. Table 3S.15 presents results for the demand model, while Tables 3S.16, 3S.17, 3S.18, and 3S.19 report results for the short-run palm supply model, the short-run supply of the other oil crops, the long-run palm supply model, and the long-run supply of the other crops, respectively.

For each specification of yield shocks derived from a different trend (Row 1), we also vary the flexible time trends that allow intercepts to evolve over time. The baseline includes restricted cubic splines with five knots, while we additionally test specifications with three and four knots, as indicated in the last row of each table. The estimates are robust across all specifications.

3S.9. Bootstrap method for computing confidence interval of BBD-induced deforestation

To construct the confidence interval for the deforestation area attributable to BBD policies, we use a bootstrap approach designed to account for potential correlation between elasticity estimates and the nonlinear transformation used in the calculation. The procedure is as follows:

(1) We first detrend the dependent and independent variables in the demand and supply equations (Eq. (3.2) and (3.3)). To address autocorrelation, we apply a block bootstrap. The detrended observations are divided into the ceiling of n/m blocks of length m, with $m = 2$ as the baseline choice.[5]

(2) Because the sample length n differs across the palm supply, other crop supply, and demand models (and in lagged specifications), we oversample blocks and then retain the first n observations. In cases where n/m is not an integer, the position of a year within a block affects its sampling probability (earlier positions are more likely to be selected). To correct for this, we randomly select observations from the last (possibly truncated) block.

[5]We also test $m = 3$ and obtain similar estimates. Choosing $m > 1$ helps preserve temporal autocorrelation.

(3) We then add the original trend back to the detrended bootstrap sample and re-estimate the elasticities or flexibilities. This process is repeated 10,000 times.

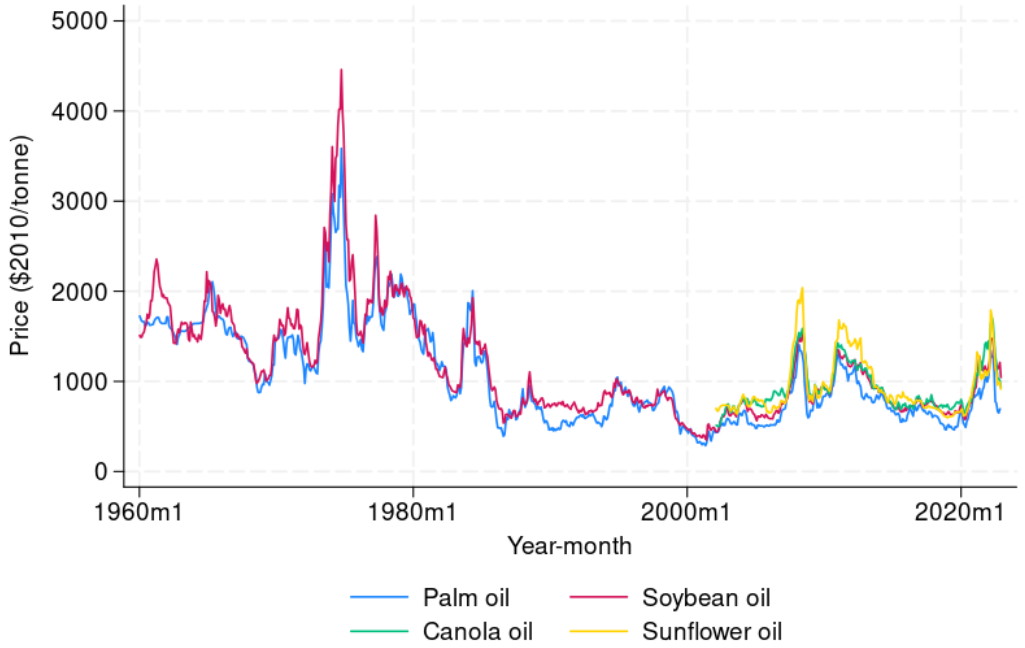
(4) Separately, we draw 10,000 random values of the estimated price effect on deforestation in Eq. (3.4), θ, from a normal distribution with the mean and variance obtained from the OLS regression. Given the large sample size in this regression, the normal approximation from asymptotic theory is appropriate. We assume zero covariance between θ and the elasticity estimates.

(5) For each draw, we compute the deforestation effect using Eq. (3.4). We then obtain a confidence interval by applying the percentile interval method; we use the 5th and 95th percentiles of the distribution to form a 90% confidence interval.[6]

[6]The percentile method is appropriate given that the bootstrap distributions are approximately symmetric. We do not use the percentile-t method because the standard error of the deforestation estimate is not available, given the unclear correlation structure between the elasticity estimates and the nonlinear transformation.

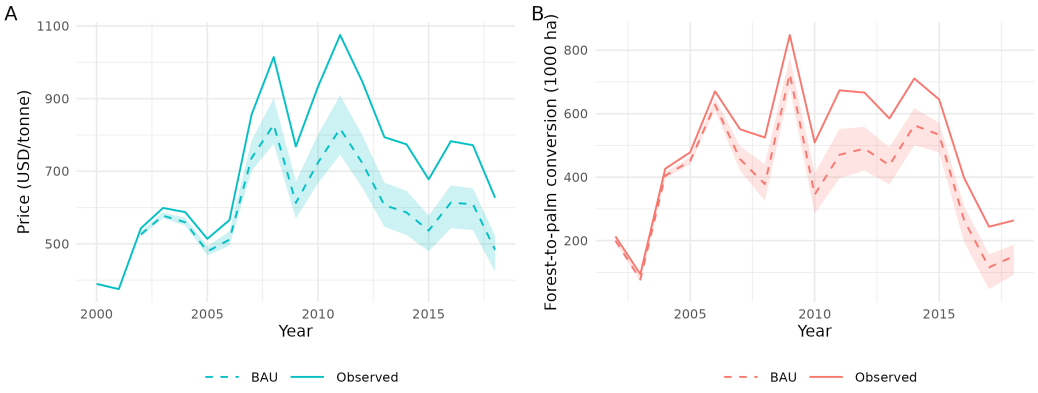
3S.10. Supplementary Figures

FIGURE 3S.1. Real prices of major vegetable oils (2010 USD), 1960–2022



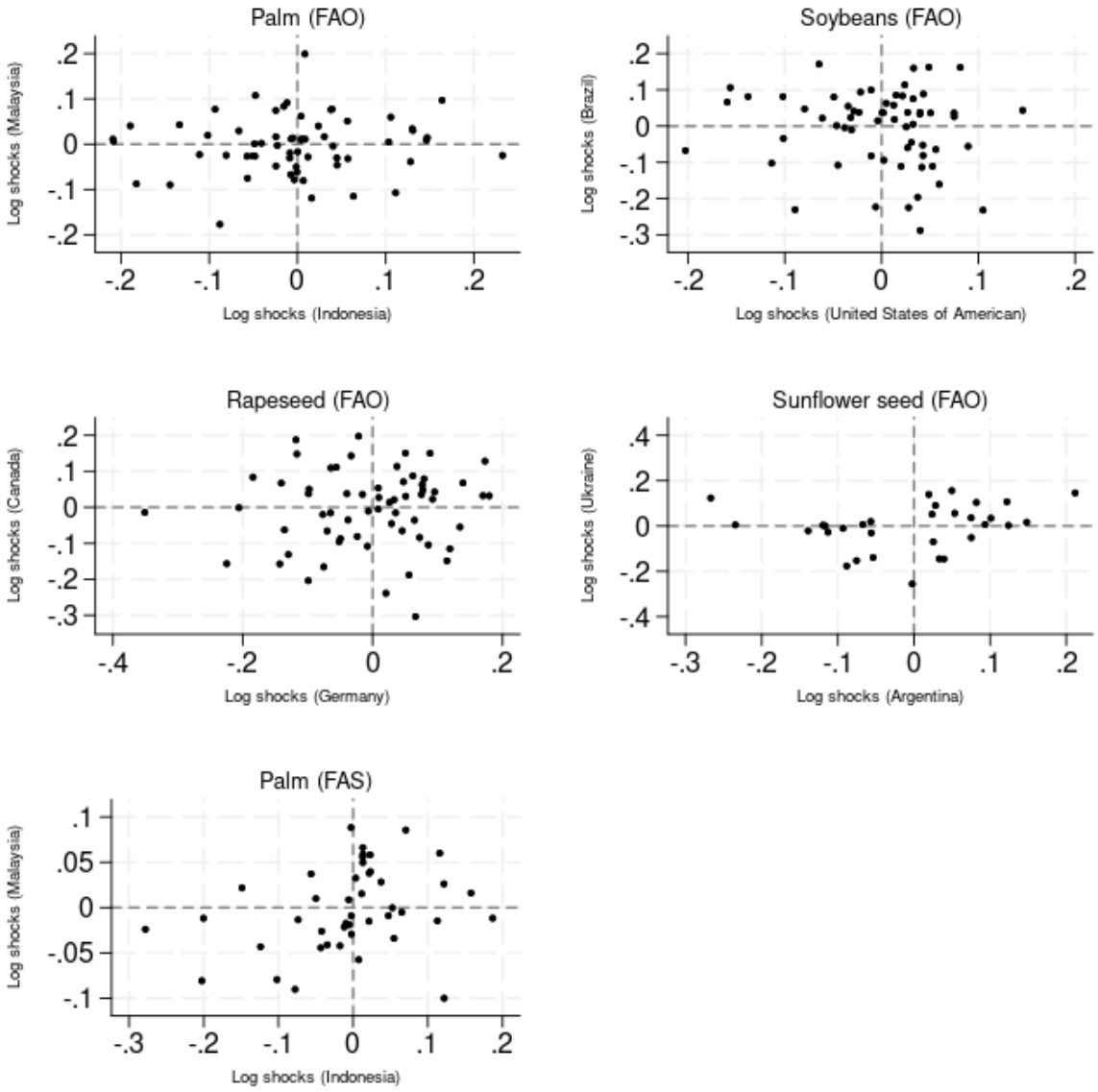
Notes: Canola oil prices are only available from February 2002 onward, and sunflower oil prices are not available before 2002 and are incomplete for that year. Source: World Bank.

FIGURE 3S.2. Observed and BAU palm oil prices and land-use changes



A. Observed and BAU palm oil prices. **B.** Observed and BAU forest-to-palm conversion in Indonesia and Malaysia. Shaded areas denote 90% confidence intervals.

FIGURE 3S.3. Correlations of yield shocks for the top two exporters of each oil crop



Notes: The correlation coefficients are −0.118 for soybeans, 0.074 for rapeseed, 0.208 for sunflower seed, and 0.086 for palm (based on FAO data, 1961–2022). For palm based on FAS data (1976–2019), the correlation coefficient is 0.291.

3S.11. Supplementary Tables

TABLE 3S.1. Inverse palm oil demand: alternative flexible time trend specifications

	(1)	(2)	(3)
Log oil crops q	-2.368*	-2.832**	-3.523***
	(1.293)	(1.181)	(1.085)
First stage			
Shocks ω_t	1.170***	1.198***	1.204***
	(0.187)	(0.199)	(0.209)
Observations	62	62	62
R-squared	0.504	0.530	0.580
Knots	3	4	5
Effective F	39.30	36.15	33.03

Notes: The baseline model (Column 3) uses the most flexible specification, a restricted cubic spline with five knots, while Columns 1 and 2 use spline trends with three and four knots, respectively. Robust standard errors are shown in parentheses: *** p<0.01, ** p<0.05, * p<0.1.

TABLE 3S.2. Inverse palm oil demand: separating oil crops with alternative flexible time trend specifications

	(1)	(2)	(3)
Log palm q	-1.700	-1.721*	-1.794**
	(1.184)	(0.972)	(0.899)
Log three oil crops q	-1.862**	-1.893*	-2.191**
	(0.858)	(1.037)	(0.994)
First stage: Log palm fruit q			
Shock of palm fruit	0.801***	1.058***	1.024***
	(0.275)	(0.219)	(0.144)
Shock of three oil crops	-0.563	-0.293	-0.168
	(0.502)	(0.298)	(0.293)
First stage: Log three oil crops q			
Shock of palm fruit	0.308**	0.256**	0.268**
	(0.124)	(0.113)	(0.119)
Shock of three oil crops	1.211***	1.154***	1.138***
	(0.173)	(0.148)	(0.153)
Observations	62	62	62
R-squared	0.511	0.506	0.533
Knots	3	4	5

Notes: The baseline model (Column 3) uses the most flexible specification, a restricted cubic spline with five knots, while Columns 1 and 2 use spline trends with three and four knots, respectively. Robust standard errors are shown in parentheses: *** p<0.01, ** p<0.05, * p<0.1.

TABLE 3S.3. Comparison of supply elasticities and demand flexibility across time periods

	Palm supply		Other supply		Demand flexibility	
	Baseline	Cut at 2000	Baseline	Cut at 2000	Baseline	Cut at 2000
	(1)	(2)	(3)	(4)	(5)	(6)
ΔP_{t-1}	0.00516	0.0435	0.0814***	0.0590**		
	(0.0213)	(0.0627)	(0.0240)	(0.0233)		
ΔP_{t-2}	0.0118	0.0480	0.0383	0.00418		
	(0.0158)	(0.0537)	(0.0290)	(0.0288)		
ΔP_{t-3}	0.0315	0.0776	0.0616*	0.0286		
	(0.0220)	(0.0974)	(0.0328)	(0.0375)		
ΔP_{t-4}	0.0150	-0.0515	0.0752***	0.0483		
	(0.0223)	(0.0955)	(0.0227)	(0.0288)		
ΔP_{t-5}	0.0629**	0.0414	0.0805**	0.0787*		
	(0.0275)	(0.0993)	(0.0323)	(0.0392)		
ΔP_{t-6}	0.0485*	0.0232				
	(0.0257)	(0.0820)				
Log palm oil price P_{t-6}			0.129***	0.127***		
			(0.0288)	(0.0314)		
Log palm oil price P_{t-7}	0.0965***	0.0800				
	(0.0335)	(0.0672)				
$\Delta P_{t-1} \times 1\{Year \geq 2000\}$		-0.0143		0.0558		
		(0.0917)		(0.0440)		
$\Delta P_{t-2} \times 1\{Year \geq 2000\}$		0.00625		0.101**		
		(0.0825)		(0.0412)		
$\Delta P_{t-3} \times 1\{Year \geq 2000\}$		0.00282		0.0580		
		(0.132)		(0.0446)		
$\Delta P_{t-4} \times 1\{Year \geq 2000\}$		0.0992		0.0764		
		(0.127)		(0.0456)		
$\Delta P_{t-5} \times 1\{Year \geq 2000\}$		-0.00506		-0.0260		
		(0.0969)		(0.0410)		
$\Delta P_{t-6} \times 1\{Year \geq 2000\}$		-0.00872				
		(0.0839)				
Log palm oil price $P_{t-6} \times 1\{Year \geq 2000\}$				0.00380		
				(0.00450)		
Log palm oil price $P_{t-7} \times 1\{Year \geq 2000\}$		0.00123				
		(0.00611)				
Log oil crops q					-3.523***	-3.451***
					(1.085)	(1.009)
Log oil crops $q \times 1\{Year \geq 2000\}$						-0.0598
						(0.0643)
Observations	44	44	57	57	62	62

Notes: Columns 1, 3, and 5 present the baseline estimates. Columns 2, 4, and 6 include a post-2000 dummy to test for changes in elasticities over time. The results show no statistically significant difference in the long-run elasticities before and after 2000 and only one statistically significant difference among the short-run responses. These findings indicate stable supply and demand responses. Newey-West standard errors with one lag in parentheses are shown in Columns (1)-(4) and Robust standard errors are in parentheses in Columns (5)-(6): *** p<0.01, ** p<0.05, * p<0.1.

TABLE 3S.4. ADF test statistics for the log price series of major vegetable oils

	Palm oil	Soybean oil	Canola oil	Sunflower oil
Level	-2.109	-1.918	-2.345	-1.834
First difference	-19.906***	-20.258***	-11.363***	-10.782***
Observations	756	756	251	228

Notes: The null hypothesis of a unit root is rejected for all first differences of the log price series, indicating stationarity. The ADF test is a one-sided test. Results are similar when using the level price series. The sunflower series begins in 2003 due to gaps in 2002. *** p<0.01, ** p<0.05, * p<0.1.

TABLE 3S.5. Long-run relationships: log palm oil and vegetable oil prices

	Soybean oil (1)	Canola oil (2)	Sunflower oil (3)
Log price of a competing oil	1.038***	1.014***	0.862***
	(0.0101)	(0.0317)	(0.0256)
Observations	756	251	228
R-squared	0.933	0.804	0.834
ADF stat. of residuals	-5.991***	-3.482**	-3.530**

Notes: The left-hand-side variable is the log price of palm oil. The first row indicates the competing oil considered in the regression. Standard errors in parentheses. The ADF test is a one-sided test. *** p<0.01, ** p<0.05, * p<0.1.

TABLE 3S.6. Long-run supply elasticity: competing oil crops

	Log quantity (q)			Log area (a)			Log yield (y)		
	(1)	(2)	(3)	(4)	(5)	(6)	(7)	(8)	(9)
ΔP_{t-1}	0.0786***	0.0773***	0.0814***	0.0898***	0.0926***	0.0811***	-0.0111	-0.0153	0.000262
	(0.0202)	(0.0194)	(0.0240)	(0.0184)	(0.0184)	(0.0224)	(0.00981)	(0.00924)	(0.00665)
ΔP_{t-2}	0.0367	0.0348	0.0383	0.0510**	0.0517**	0.0401	-0.0143	-0.0169	-0.00186
	(0.0286)	(0.0275)	(0.0290)	(0.0249)	(0.0237)	(0.0254)	(0.0121)	(0.0115)	(0.00952)
ΔP_{t-3}	0.0590*	0.0554*	0.0616*	0.0797***	0.0803***	0.0596*	-0.0207	-0.0249**	0.00200
	(0.0339)	(0.0321)	(0.0328)	(0.0294)	(0.0275)	(0.0314)	(0.0136)	(0.0123)	(0.0104)
ΔP_{t-4}	0.0709***	0.0683***	0.0752***	0.0789***	0.0833***	0.0642***	-0.00807	-0.0150	0.0110
	(0.0188)	(0.0170)	(0.0227)	(0.0197)	(0.0172)	(0.0228)	(0.0137)	(0.0129)	(0.0117)
ΔP_{t-5}	0.0765**	0.0735**	0.0805**	0.0894**	0.0929***	0.0734**	-0.0129	-0.0194	0.00711
	(0.0301)	(0.0281)	(0.0323)	(0.0350)	(0.0323)	(0.0340)	(0.0175)	(0.0170)	(0.0127)
Log palm oil price P_{t-6}	0.120***	0.120***	0.129***	0.115***	0.128***	0.109***	0.00530	-0.00814	0.0204**
	(0.0206)	(0.0217)	(0.0288)	(0.0258)	(0.0256)	(0.0302)	(0.0102)	(0.0115)	(0.00994)
Shocks ω_t	1.304***	1.305***	1.293***	0.249*	0.240*	0.263*	0.0545	0.0646	0.0308
	(0.128)	(0.131)	(0.132)	(0.140)	(0.139)	(0.138)	(0.0631)	(0.0622)	(0.0521)
Observations	57	57	57	57	57	57	57	57	57
Knots	3	4	5	3	4	5	3	4	5

Notes: Long-run supply elasticity of the three competing oil crops (soybeans, rapeseed, and sunflower) with respect to palm oil prices. Model selection criteria for the 6-lag specification of the quantity regression with 5 spline knots are AIC = -212.424 and BIC = -188.336. For comparison, the 7-lag model yields AIC = -210.981 and BIC = -184.886, and the 5-lag model yields AIC = -210.037 and BIC = -187.957. Based on these values, the 6-lag specification is preferred. Production data are from FAO, 1961–2022. Newey-West standard errors with one lag are shown in parentheses. *** p<0.01, ** p<0.05, * p<0.1.

TABLE 3S.7. Long-run supply elasticity of oil palm

	Log quantity (q)			Log area (a)			Log yield (y)		
	(1)	(2)	(3)	(4)	(5)	(6)	(7)	(8)	(9)
ΔP_{t-1}	0.0512	0.0380	0.00516	0.0302	0.0227	0.00729	0.0202	0.0146	-0.00267
	(0.0428)	(0.0411)	(0.0213)	(0.0271)	(0.0249)	(0.0205)	(0.0187)	(0.0201)	(0.00245)
ΔP_{t-2}	0.0432	0.0295	0.0118	0.0319	0.0254	0.0167	0.0118	0.00453	-0.00432**
	(0.0416)	(0.0398)	(0.0158)	(0.0236)	(0.0217)	(0.0153)	(0.0202)	(0.0209)	(0.00189)
ΔP_{t-3}	0.0798	0.0626	0.0315	0.0601**	0.0518**	0.0365*	0.0193	0.0105	-0.00517*
	(0.0522)	(0.0458)	(0.0220)	(0.0284)	(0.0244)	(0.0208)	(0.0267)	(0.0255)	(0.00289)
ΔP_{t-4}	0.0588	0.0411	0.0150	0.0457	0.0373	0.0242	0.0135	0.00411	-0.00869***
	(0.0546)	(0.0493)	(0.0223)	(0.0333)	(0.0318)	(0.0221)	(0.0251)	(0.0205)	(0.00269)
ΔP_{t-5}	0.104	0.108**	0.0629**	0.0896**	0.0898***	0.0678**	0.0148	0.0190	-0.00398
	(0.0616)	(0.0490)	(0.0275)	(0.0373)	(0.0311)	(0.0255)	(0.0276)	(0.0220)	(0.00332)
ΔP_{t-6}	0.0884	0.0882*	0.0485*	0.0762*	0.0746**	0.0551**	0.0126	0.0141	-0.00597*
	(0.0685)	(0.0514)	(0.0257)	(0.0401)	(0.0317)	(0.0234)	(0.0306)	(0.0229)	(0.00340)
Log palm oil price P_{t-7}	0.144*	0.174***	0.0965***	0.124**	0.133***	0.0962***	0.0201	0.0408*	0.000279
	(0.0744)	(0.0567)	(0.0335)	(0.0470)	(0.0373)	(0.0301)	(0.0301)	(0.0237)	(0.00390)
Shocks ω_t	0.827***	0.889***	0.809***	-0.192	-0.171*	-0.207***	0.0146	0.0552	0.0111
	(0.243)	(0.190)	(0.0603)	(0.134)	(0.0980)	(0.0554)	(0.113)	(0.0985)	(0.0105)
Observations	44	44	44	44	44	44	44	44	44
Knots	3	4	5	3	4	5	3	4	5

Notes: Long-run supply elasticity of oil palm with respect to palm oil prices. Model selection criteria for the 7-lag specification of the quantity regression with 5 spline knots are AIC = -200.387 and BIC = -177.192. For comparison, the 8-lag model yields AIC = -199.725 and BIC = -174.746, while the 6-lag model yields AIC = -193.808 and BIC = -172.398. Based on these criteria, the 7-lag specification is preferred. Production data are from FAS, 1976–2019. Newey-West standard errors with one lag are shown in parentheses. *** p<0.01, ** p<0.05, * p<0.1.

TABLE 3S.8. Price effects on deforestation area for palm

	(1)	(2)	(3)
Palm revenue (t-1)	9.295***	9.225***	9.490***
	(1.248)	(1.243)	(1.211)
Observations	550,698	550,698	550,698
Cells	32,394	32,394	32,394
Time control	Country-year FE	Year FE	Forest cover trends

Robust standard errors clustered at the second administrative level
*** p<0.01, ** p<0.05, * p<0.1

TABLE 3S.9. Reverse causality check: excluding high palm-share cells

	W/O top 10% (1)	W/O top 25% (2)	W/O top 50% (3)
Palm revenue (t-1)	9.589***	9.680***	8.420***
	(1.212)	(1.162)	(0.981)
Observations	546,261	538,781	522,920
Number of id	32,133	31,693	30,760
FE	Cell+County-year	Cell+County-year	Cell+County-year

Robust standard errors clustered at the second administrative level
*** p<0.01, ** p<0.05, * p<0.1

TABLE 3S.10. Price effects on deforestation area for palm controlling for weather

	(1)	(2)	(3)
Palm revenue (t-1)	9.901***	9.995***	9.833***
	(1.316)	(1.323)	(1.310)
Precipitation	-0.0531	-2.132	-1.628
	(1.561)	(3.493)	(2.620)
Temperature	650.4***	279.2	579.1***
	(86.51)	(301.1)	(92.33)
Precipitation squared		0.480	
		(0.500)	
Temperature squared		176.4	
		(134.8)	
S.D. of precipitation			0.440
			(0.570)
S.D. of temperature			9.447***
			(3.095)
Observations	509,592	509,592	509,592
Cells	29,976	29,976	29,976
FE	Cell+County-year	Cell+County-year	Cell+County-year

Robust standard errors clustered at the second administrative level
*** p<0.01, ** p<0.05, * p<0.1

TABLE 3S.11. Attainable yield confounders: sensitivity analysis

	AY X time trend	W/O AY>90th quantile	W/O AY<10th quantile	W/O AY<10th | >90th quantile
	(1)	(2)	(3)	(4)
Palm revenue (t-1)	11.95***	8.903***	10.10***	9.749***
	(1.664)	(1.319)	(1.359)	(1.440)
Observations	550,698	495,635	495,618	440,555
Cells	32,394	29,155	29,154	25,915
FE	Cell+County-year	Cell+County-year	Cell+County-year	Cell+County-year

Robust standard errors clustered at the second administrative level
*** p<0.01, ** p<0.05, * p<0.1

TABLE 3S.12. Palm price effects on deforestation: alternative price periods

	(1)	(2)	(3)	(4)	(5)	(6)	(7)	(8)
Palm prices	7.174***		-0.0229	0.555	0.769			
	(1.312)		(1.007)	(1.022)	(1.188)			
Palm revenue (t-1)		9.295***	9.309***	5.794***	5.549***			
		(1.248)	(1.084)	(1.115)	(1.228)			
Palm revenue (t-2)				3.795***	4.260***			
				(0.894)	(1.374)			
Palm revenue (t-3)					-0.480			
					(1.408)			
Mean of revenue (t-1 to t)						9.937***		
						(1.493)		
Mean of revenue (t-3 to t)							10.55***	
							(1.497)	
Mean of revenue (t-5 to t)								7.360***
								(1.557)
Observations	550,698	550,698	550,698	550,698	550,698	550,698	550,698	550,698
Cells	32,394	32,394	32,394	32,394	32,394	32,394	32,394	32,394

Notes: All regressions control for cell and county-year fixed effects. Robust standard errors clustered at the second administrative level are shown in parentheses: *** p<0.01, ** p<0.05, * p<0.1.

TABLE 3S.13. Palm price deviation effects on deforestation area for palm

	(1)	(2)	(3)
Revenue deviation from past 5 years	9.348***		
	(1.517)		
Revenue deviation from past 7 years		9.347***	
		(1.406)	
Revenue deviation from past 10 years			10.41***
			(1.462)
Observations	550,698	550,698	550,698
Cells	32,394	32,394	32,394

Robust standard errors clustered at the second administrative level
*** p<0.01, ** p<0.05, * p<0.1

TABLE 3S.14. Comparison of carbon emission estimates (Mg CO_2e/ha) from land-use change across studies

Study	Biomass	SOC	Peatland	Palm sequestration	Total	Notes
Our estimate	438.19	54.84	355.04	-219.84	628.24	
Guillaume et al. (2018)	756.98	39.94	–	-160.85	636.07	The study was conducted in Jambi Province, central Sumatra, Indonesia, across 32 plots comparing carbon stocks under different land uses, from rainforest to plantations. Their estimated biomass is higher, likely because their baseline forest is restricted to rainforest. Biomass varies widely across regions and forest types, so studies focusing only on rainforest are expected to report higher values than our estimates, which are based on 30 m resolution biomass data. Emissions from peatland decomposition are not considered in their study.
Carlson et al. (2013)	749.45	–	131.17	-103.69	776.93	This study focuses on Kalimantan, Indonesia, from 1990 to 2010. Forest loss is classified by type (intact, logged, agroforest), but a single AGB value is applied to each category without accounting for local variation due to climate or geography. These methodological choices, along with differences in study period and coverage, likely explain the higher AGB estimate relative to ours. For peatland, they assume only ten years of drainage emissions; if extended to the full oil palm lifecycle, assuming the same emission per year, their implied peatland emissions (327.92 Mg CO_2e/ha) are close to ours. Remaining differences may reflect study scope and timing, which affect the extent of peatland conversion considered. They do not account for SOC from non-peat soils.
Busch et al. (2015)		749.93		–	749.93	This study examines deforestation in Indonesia from 2000 to 2010, covering palm expansion as well as other drivers such as logging. It does not report separate estimates for biomass, peatland, and SOC. Biomass and peat data are applied to the exact deforestation locations. Their estimate (749.93 Mg CO_2e/ha, including biomass, SOC, and peatland decomposition) is close to our estimate of 848.08 Mg CO_2e/ha, supporting our use of spatially explicit data on biomass and peatland transitions. Remaining differences likely reflect study period, geographic scope, and their inclusion of non-palm deforestation. They do not account for carbon sequestered by replanted trees.
Groom et al. (2022)	570.12	–	–	–	570.12	This estimate focuses on primary and peatland forests that avoided deforestation during Indonesia's moratorium on new forest concessions (2011–2017). Their biomass estimates are based on exact deforestation locations and are close to—but higher than—ours (438.19 Mg CO_2e/ha). The higher values likely reflect differences in forest types: our study also includes managed natural forests, planted forests, and agroforestry, which generally have lower biomass than primary forests. Differences in study period and geographic scope may also contribute. Emissions from SOC and peatland decomposition, and carbon sequestered by replanted trees are not considered in their study.

Notes: For studies reporting emissions in terms of carbon (C), we convert to CO_2 by multiplying the carbon mass by 3.664.

TABLE 3S.15. Demand flexibility: yield shock sensitivity checks

	Baseline: Yield trend with 5 knots			Yield trend with 3 knots			Yield trend with 4 knots		
	(1)	(2)	(3)	(4)	(5)	(6)	(7)	(8)	(9)
Log oil crops q	-2.368*	-2.832**	-3.523***	-2.948**	-3.772***	-3.558***	-3.255***	-3.160***	-3.208***
	(1.293)	(1.181)	(1.085)	(1.382)	(1.253)	(1.107)	(1.219)	(1.127)	(1.009)
First stage									
Shocks ω_t	1.170***	1.198***	1.204***	1.072***	1.151***	1.166***	1.289***	1.287***	1.280***
	(0.187)	(0.199)	(0.209)	(0.174)	(0.201)	(0.199)	(0.198)	(0.197)	(0.198)
Observations	62	62	62	62	62	62	62	62	62
R-squared	0.504	0.530	0.580	0.478	0.474	0.577	0.461	0.513	0.597
Knots	3	4	5	3	4	5	3	4	5
Effective F	39.30	36.15	33.03	37.83	32.71	34.30	42.48	42.53	41.76

Notes: Production data are from FAO, 1976–2022. Robust standard errors with one lag are shown in parentheses. *** p<0.01, ** p<0.05, * p<0.1.

TABLE 3S.16. Short-run supply elasticity (palm): yield shock sensitivity

	Baseline: Yield trend with 5 knots			Yield trend with 3 knots			Yield trend with 4 knots		
	(1)	(2)	(3)	(4)	(5)	(6)	(7)	(8)	(9)
Log palm oil price P_{t-1}	0.0300	0.0252	0.00526	0.00291	0.0109	0.00726	0.0177	0.00761	0.00620
	(0.0339)	(0.0347)	(0.0156)	(0.0208)	(0.0223)	(0.0149)	(0.0191)	(0.0188)	(0.0152)
Shocks ω_t	0.767***	0.772***	0.750***	0.976***	0.967***	0.772***	0.959***	0.946***	0.759***
	(0.229)	(0.218)	(0.0805)	(0.0706)	(0.0739)	(0.0745)	(0.0659)	(0.0543)	(0.0781)
Observations	44	44	44	44	44	44	44	44	44
Knots	3	4	5	3	4	5	3	4	5

Notes: Production data are from FAS, 1976–2019. Newey-West standard errors with one lag are shown in parentheses: *** p<0.01, ** p<0.05, * p<0.1.

TABLE 3S.17. Short-run supply elasticity (other oil crops): yield shock sensitivity

	Baseline: Yield trend with 5 knots			Yield trend with 3 knots			Yield trend with 4 knots		
	(1)	(2)	(3)	(4)	(5)	(6)	(7)	(8)	(9)
Log palm oil price P_{t-}	0.0680***	0.0521**	0.0602***	0.0785***	0.0648***	0.0616***	0.0828***	0.0630***	0.0560***
	(0.0222)	(0.0204)	(0.0207)	(0.0210)	(0.0193)	(0.0201)	(0.0207)	(0.0188)	(0.0196)
Shocks ω_t	1.278***	1.229***	1.251***	1.212***	1.173***	1.178***	1.288***	1.270***	1.285***
	(0.118)	(0.115)	(0.125)	(0.113)	(0.117)	(0.118)	(0.125)	(0.119)	(0.117)
Observations	62	62	62	62	62	62	62	62	62
Knots	3	4	5	3	4	5	3	4	5

Notes: Production data are from FAO, 1961–2022. Newey-West standard errors with one lag are shown in parentheses: *** p<0.01, ** p<0.05, * p<0.1.

TABLE 3S.18. Long-run supply elasticity (palm): yield shock sensitivity

	Baseline: Yield trend with 5 knots			Yield trend with 3 knots			Yield trend with 4 knots		
	(1)	(2)	(3)	(4)	(5)	(6)	(7)	(8)	(9)
ΔP_{t-1}	0.0512	0.0380	0.00516	0.0133	0.0129	0.00571	0.0193	0.00951	0.00578
	(0.0428)	(0.0411)	(0.0213)	(0.0285)	(0.0267)	(0.0209)	(0.0286)	(0.0233)	(0.0210)
ΔP_{t-2}	0.0432	0.0295	0.0118	0.0128	0.0139	0.0140	0.0224	0.0120	0.0128
	(0.0416)	(0.0398)	(0.0158)	(0.0263)	(0.0246)	(0.0157)	(0.0268)	(0.0199)	(0.0155)
ΔP_{t-3}	0.0798	0.0626	0.0315	0.0337	0.0361	0.0335	0.0471	0.0331	0.0327
	(0.0522)	(0.0458)	(0.0220)	(0.0299)	(0.0280)	(0.0213)	(0.0338)	(0.0247)	(0.0217)
ΔP_{t-4}	0.0588	0.0411	0.0150	0.0445	0.0388	0.0194	0.0546*	0.0315	0.0169
	(0.0546)	(0.0493)	(0.0223)	(0.0312)	(0.0310)	(0.0220)	(0.0311)	(0.0265)	(0.0220)
ΔP_{t-5}	0.104	0.108**	0.0629**	0.0840**	0.0851***	0.0630**	0.0786**	0.0761***	0.0632**
	(0.0616)	(0.0490)	(0.0275)	(0.0335)	(0.0301)	(0.0262)	(0.0375)	(0.0272)	(0.0269)
ΔP_{t-6}	0.0884	0.0882*	0.0485*	0.0724**	0.0713**	0.0488*	0.0700*	0.0624**	0.0487*
	(0.0685)	(0.0514)	(0.0257)	(0.0339)	(0.0302)	(0.0241)	(0.0400)	(0.0266)	(0.0250)
Log palm oil price P_{t-7}	0.144*	0.174***	0.0965***	0.124***	0.128***	0.0918***	0.0952*	0.114***	0.0949***
	(0.0744)	(0.0567)	(0.0335)	(0.0434)	(0.0376)	(0.0318)	(0.0485)	(0.0344)	(0.0327)
Shocks ω_t	0.827***	0.889***	0.809***	1.080***	1.018***	0.820***	0.993***	0.967***	0.813***
	(0.243)	(0.190)	(0.0603)	(0.0791)	(0.0716)	(0.0564)	(0.0821)	(0.0583)	(0.0589)
Observations	44	44	44	44	44	44	44	44	44
Knots	3	4	5	3	4	5	3	4	5

Notes: Production data are from FAS, 1976–2019. Newey-West standard errors with one lag are shown in parentheses: *** p<0.01, ** p<0.05, * p<0.1.

TABLE 3S.19. Long-run supply elasticity (other oil crops): yield shock sensitivity

	Baseline: Yield trend with 5 knots			Yield trend with 3 knots			Yield trend with 4 knots		
	(1)	(2)	(3)	(4)	(5)	(6)	(7)	(8)	(9)
ΔP_{t-1}	0.0786***	0.0773***	0.0814***	0.0867***	0.0886***	0.0798***	0.0862***	0.0859***	0.0789***
	(0.0202)	(0.0194)	(0.0240)	(0.0189)	(0.0191)	(0.0229)	(0.0192)	(0.0190)	(0.0232)
ΔP_{t-2}	0.0367	0.0348	0.0383	0.0450*	0.0452*	0.0363	0.0434	0.0422	0.0350
	(0.0286)	(0.0275)	(0.0290)	(0.0256)	(0.0248)	(0.0267)	(0.0267)	(0.0259)	(0.0282)
ΔP_{t-3}	0.0590*	0.0554*	0.0616*	0.0788**	0.0775***	0.0595*	0.0742**	0.0713**	0.0567*
	(0.0339)	(0.0321)	(0.0328)	(0.0294)	(0.0278)	(0.0310)	(0.0302)	(0.0289)	(0.0317)
ΔP_{t-4}	0.0709***	0.0683***	0.0752***	0.0842***	0.0865***	0.0712***	0.0810***	0.0798***	0.0677***
	(0.0188)	(0.0170)	(0.0227)	(0.0189)	(0.0176)	(0.0226)	(0.0186)	(0.0175)	(0.0230)
ΔP_{t-5}	0.0765**	0.0735**	0.0805**	0.0906***	0.0920***	0.0761**	0.0861***	0.0844***	0.0717**
	(0.0301)	(0.0281)	(0.0323)	(0.0326)	(0.0305)	(0.0327)	(0.0311)	(0.0295)	(0.0320)
Log palm oil price P_{t-6}	0.120***	0.120***	0.129***	0.130***	0.139***	0.124***	0.127***	0.129***	0.117***
	(0.0206)	(0.0217)	(0.0288)	(0.0233)	(0.0247)	(0.0294)	(0.0221)	(0.0240)	(0.0289)
Shocks ω_t	1.304***	1.305***	1.293***	1.193***	1.208***	1.271***	1.236***	1.247***	1.294***
	(0.128)	(0.131)	(0.132)	(0.125)	(0.125)	(0.129)	(0.128)	(0.130)	(0.132)
Observations	57	57	57	57	57	57	57	57	57
Knots	3	4	5	3	4	5	3	4	5

Notes: Production data are from FAO, 1966–2022. Newey-West standard errors with one lag are shown in parentheses: *** p<0.01, ** p<0.05, * p<0.1.

Bibliography

Ali, A. and Abdulai, A. (2010). The adoption of genetically modified cotton and poverty reduction in pakistan. *Journal of Agricultural Economics*, 61(1):175–192.

Allaire, M., Wu, H., and Lall, U. (2018). National trends in drinking water quality violations. *Proceedings of the National Academy of Sciences*, 115(9):2078–2083.

Angrist, J. D. and Pischke, J.-S. (2009). *Mostly Harmless Econometrics: An Empiricist's Companion*. Princeton University Press.

Aparicio, V. C., De Gerónimo, E., Marino, D., Primost, J., Carriquiriborde, P., and Costa, J. L. (2013). Environmental fate of glyphosate and aminomethylphosphonic acid in surface waters. *Chemosphere*, 93:1866–73.

Austin, K. G., Schwantes, A., Gu, Y., and Kasibhatla, P. S. (2019). What causes deforestation in Indonesia? *Environmental Research Letters*, 14(2):024007.

Banzhaf, S., Ma, L., and Timmins, C. (2019). Environmental justice: The economics of race, place, and pollution. *Journal of Economic Perspectives*, 33(1):185–208.

Barlow, J., Lennox, G. D., Ferreira, J., Berenguer, E., Lees, A. C., Nally, R. M., Thomson, J. R., de Barros Ferraz, S. F., Louzada, J., Oliveira, V. H. F., Parry, L., de Castro Solar, R. R., Vieira, I. C. G., Aragão, L. E. O. C., Begotti, R. A., Braga, R. F., Cardoso, T. M., de Oliveira, R. C., Jr, C. M. S., Moura, N. G., Nunes, S. S., Siqueira, J. V., Pardini, R., Silveira, J. M., de Mello, F. Z. V., Veiga, R. C. S., Venturieri, A., and Gardner, T. A. (2016). Anthropogenic disturbance in tropical forests can double biodiversity loss from deforestation. *Nature*, 535(7610):144–147.

Battaglin, W., Meyer, M., Kuivila, K., and Dietze, J. (2014). Glyphosate and its degradation product AMPA occur frequently and widely in U.S. soils, surface water, groundwater, and precipitation. *Journal of the American Water Resources Association*, 50(2):275–290.

Bayer Crop Science (2020). Determining corn growth stages. `https://www.cropscience.bayer.us/articles/bayer/corn-growth-stages-and-gdu-requirements`. Accessed at 01/31/2024.

Bayer Crop Science (2024). Corn growth stage and herbicide application postemergence. https://www.cropscience.bayer.us/articles/bayer/corn-growth-stage-herbicide-application-postemergence. Accessed at 01/31/2024.

Belkouteb, N., Franke, V., McCleaf, P., Köhler, S., and Ahrens, L. (2020). Removal of per- and polyfluoroalkyl substances (pfass) in a full-scale drinking water treatment plant: Long-term performance of granular activated carbon (gac) and influence of flow-rate. *Water Research*, 182:115913.

Benachour, N., Sipahutar, H., Moslemi, S., Gasnier, C., Travert, C., and Séralini, G. E. (2007). Time- and dose-dependent effects of roundup on human embryonic and placental cells. *Archives of environmental contamination and toxicology*, 53(1):126–133.

Benachour, N. and Séralini, G.-E. (2009). Glyphosate formulations induce apoptosis and necrosis in human umbilical, embryonic, and placental cells. *Chemical Research in Toxicology*, 22(1):97–105.

Benbrook, C. M. (2016). Trends in glyphosate herbicide use in the united states and globally. *Environmental Sciences Europe*, 28(3).

Berman, N., Couttenier, M., Leblois, A., and Soubeyran, R. (2023). Crop prices and deforestation in the tropics. *Journal of Environmental Economics and Management*, 119:102819.

Bernhard, A. (2010). The nitrogen cycle: Processes, players, and human impact. *Nature Education Knowledge*, 3(10).

Berry, S., Searchinger, T., and Yang, A. (2024). Biofuels, deforestation, and the GTAP model. *Tobin Center Working Paper Series*.

Bharadwaj, P., Gibson, M., Zivin, J. G., and Neilson, C. (2017). Gray matters: Fetal pollution exposure and human capital formation. *Journal of the Association of Environmental and Resource Economists*, 4(2):505–542.

Blondel, B., Drewniak, N., Pilkington, H., and Zeitlin, J. (2011). Out-of-hospital births and the supply of maternity units in france. *Health & Place*, 17(5):1170–1173.

Broch, A., Hoekman, S. K., and Unnasch, S. (2013). A review of variability in indirect land use change assessment and modeling in biofuel policy. *Environmental Science & Policy*, 29:147–157.

Bronfenbrenner, M. (1961). Notes on the elasticity of derived demand. *Oxford Economic Papers*, 13(3):254–261.

Brown, A. K. and Farenhorst, A. (2024). Quantitation of glyphosate, glufosinate, and AMPA in drinking water and surface waters using direct injection and charged-surface ultra-high performance liquid chromatography-tandem mass spectrometry. *Chemosphere*, 349:140924.

Burgess, R., Hansen, M., Olken, B. A., Potapov, P., and Sieber, S. (2012). The political economy of deforestation in the tropics. *The Quarterly Journal of Economics*, 127(4):1707–1754.

Busch, J., Ferretti-Gallon, K., Engelmann, J., Wright, M., Austin, K. G., Stolle, F., Turubanova, S., Potapov, P. V., Margono, B., Hansen, M. C., and Baccini, A. (2015). Reductions in emissions from deforestation from Indonesia's moratorium on new oil palm, timber, and logging concessions. *Proceedings of the National Academy of Sciences*, 112(5):1328–1333.

Calzada, J., Gisbert, M., and Moscoso, B. (2023). The hidden cost of bananas: The effects of pesticides on newborns' health. *Journal of the Association of Environmental and Resource Economists*, 10(6):1623–1663.

Camacho, A. and Mejía, D. (2017). The health consequences of aerial spraying illicit crops: The case of colombia. *Journal of Health Economics*, 54:147–160.

Carlson, K. M., Curran, L. M., Asner, G. P., Pittman, A. M., Trigg, S. N., and Adeney, J. M. (2013). Carbon emissions from forest conversion by kalimantan oil palm plantations. *Nature Climate Change*, 3(3):283–287.

Chavas, J.-P. (2000). On information and market dynamics: The case of the u.s. beef market. *Journal of Economic Dynamics and Control*, 24(5):833–853.

Chay, K. Y. and Greenstone, M. (2003). The Impact of Air Pollution on Infant Mortality: Evidence from Geographic Variation in Pollution Shocks Induced by a Recession. *The Quarterly Journal of Economics*, 118(3):1121–1167.

Chay, K. Y. and Greenstone, M. (2005). Does air quality matter? evidence from the housing market. *Journal of Political Economy*, 113(2):376–424.

Chen, T.-H. J. (2026). Glyphosate use, water contamination, and neonatal health in the united states. *Journal of the Association of Environmental and Resource Economists*, 13(3):755–790.

Chevrier, C., Limon, G., Monfort, C., Rouget, F., Garlantézec, R., Petit, C., Durand, G., and Cordier, S. (2011). Urinary biomarkers of prenatal atrazine exposure and adverse birth outcomes in the pelagie birth cohort. *Environmental Health Perspectives*, 119(7):1034–1041.

Cisneros, E., Kis-Katos, K., and Nuryartono, N. (2021). Palm oil and the politics of deforestation in Indonesia. *Journal of Environmental Economics and Management*, 108:102453.

CME Group (2017). Spread trading in CBOT soybean oil and bmd crude palm oil. Accessed at 08/05/2025.

Connolly, A., Koch, H. M., Bury, D., Koslitz, S., Kolossa-Gehring, M., Conrad, A., Murawski, A., McGrath, J. A., Leahy, M., Brüning, T., and Coggins, M. A. (2022). A human biomonitoring study assessing glyphosate and aminomethylphosphonic acid (AMPA) exposures among farm and non-farm families. *Toxics*, 10(11).

Coupe, R. H., Kalkhoff, S. J., Capel, P. D., and Gregoire, C. (2012). Fate and transport of glyphosate and aminomethylphosphonic acid in surface waters of agricultural basins. *Pest Management Science*, 68(1):16–30.

Cui, J. and Martin, J. I. (2017). Impacts of US biodiesel mandates on world vegetable oil markets. *Energy Economics*, 65:148–160.

Currie, J. (2011). Inequality at birth: Some causes and consequences. *American Economic Review*, 101(3):1–22.

Currie, J., Graff Zivin, J., Meckel, K., Neidell, M., and Schlenker, W. (2013). Something in the water: contaminated drinking water and infant health. *Canadian Journal of Economics/Revue canadienne d'économique*, 46(3):791–810.

Curwin, B. D., Hein, M. J., Sanderson, W. T., Striley, C., Heederik, D., Kromhout, H., and Alavanja, M. C. (2006). Urinary Pesticide Concentrations Among Children, Mothers and Fathers Living in Farm and Non-Farm Households in Iowa. *The Annals of Occupational Hygiene*, 51(1):53–65.

Daioglou, V., Woltjer, G., Strengers, B., Elbersen, B., Barberena Ibañez, G., Sánchez Gonzalez, D., Gil Barno, J., and van Vuuren, D. P. (2020). Progress and barriers in understanding and preventing indirect land-use change. *Biofuels, Bioproducts and Biorefining*, 14(5):924–934.

Daysal, N. M., Trandafir, M., and van Ewijk, R. (2015). Saving lives at birth: The impact of home births on infant outcomes. *American Economic Journal: Applied Economics*, 7(3):28–50.

Declerck, F., Hikouatcha, P., Tchoffo, G., and Tédongap, R. (2023). Biofuel policies and their ripple effects: An analysis of vegetable oil price dynamics and global consumer responses. *Energy*

Economics, 128:107127.

Descals, A., Gaveau, D. L. A., Wich, S., Szantoi, Z., and Meijaard, E. (2024). Global mapping of oil palm planting year from 1990 to 2021. *Earth System Science Data*, 16(11):5111–5129.

Descals, A., Wich, S., Meijaard, E., Gaveau, D. L. A., Peedell, S., and Szantoi, Z. (2021). High-resolution global map of smallholder and industrial closed-canopy oil palm plantations. *Earth System Science Data*, 13(3):1211–1231.

Dias, M., Rocha, R., and Soares, R. R. (2023). Down the River: Glyphosate Use in Agriculture and Birth Outcomes of Surrounding Populations. *The Review of Economic Studies*, 90(6):2943–2981.

DiStefano, R., Feliciano, T., Mimna, R. A., Redding, A. M., and Matthis, J. (2022). Thermal destruction of pfas during full-scale reactivation of pfas-laden granular activated carbon. *Remediation Journal*, 32(4):231–238.

Duke, S. O. and Powles, S. B. (2008). Glyphosate: a once-in-a-century herbicide. *Pest Management Science*, 64(4):319–325.

Duncan, D., Pederson, D. T., Shepherd, T. R., and Can, J. D. (1991). Atrazine used as a tracer of induced recharge. *Groundwater Monitoring & Remediation*, 11(4):144–150.

Elrod, A. A., Karadas, S., and Theyson, K. C. (2019). The effect of gubernatorial political parties on monitoring and enforcement of federal environmental regulation: evidence from the clean water act. *Environmental Economics and Policy Studies*, 21:171–202.

Endres, G. and Kandel, H. (2021). Soybean growth and management quick guide. `https://www.ndsu.edu/agriculture/ag-hub/publications/soybean-growth-and-management-quick-guide`. Accessed at 01/31/2024.

Engle, R. F. and Granger, C. W. J. (1987). Co-integration and error correction: Representation, estimation, and testing. *Econometrica*, 55(2):251–276.

EPA (2009). Community water system survey volume I: Overview. `https://nepis.epa.gov/Exe/ZyPDF.cgi?Dockey=P1009JJI.txt`. Accessed at 07/15/2024.

EPA (2014). Providing safe drinking water in America: 2014 national public water systems compliance report. `https://www.epa.gov/compliance/providing-safe-drinking-water-america-2014-national-public-water-systems-compliance`. Accessed at 01/31/2024.

Espinoza-Montero, P. J., Vega-Verduga, C., Alulema-Pullupaxi, P., Fernández, L., and Paz, J. L. (2020). Technologies employed in the treatment of water contaminated with glyphosate: A review. *Molecules*, 25(23).

European Union (2018). Directive (EU) 2018/2001 of the European Parliament and of the Council of 11 December 2018 on the promotion of the use of energy from renewable sources. `https://eur-lex.europa.eu/eli/dir/2018/2001/oj/eng`. Accessed at 7/5/2025.

FAO (2024). FAOSTAT statistical database. Accessed 2024/11/22.

Feintrenie, L., Chong, W. K., and Levang, P. (2010). Why do farmers prefer oil palm? lessons learnt from Bungo District, Indonesia. *Small-scale Forestry*, 9:379–396.

Feng, D., Soric, A., and Boutin, O. (2020). Treatment technologies and degradation pathways of glyphosate: A critical review. *Science of The Total Environment*, 742:140559.

Flanagan, S. V., Marvinney, R. G., and Zheng, Y. (2015). Influences on domestic well water testing behavior in a central maine area with frequent groundwater arsenic occurrence. *Science of The Total Environment*, 505:1274–1281.

Gaveau, D. L., Locatelli, B., Salim, M. A., Yaen, H., Pacheco, P., and Sheil, D. (2019). Rise and fall of forest loss and industrial plantations in Borneo (2000–2017). *Conservation Letters*, 12(3):e12622.

Gaveau, D. L. A., Locatelli, B., Salim, M. A., Husnayaen, Manurung, T., Descals, A., Angelsen, A., Meijaard, E., and Sheil, D. (2022). Slowing deforestation in Indonesia follows declining oil palm expansion and lower oil prices. *PLOS ONE*, 17(3):e0266178.

Gerona, R. R., Reiter, J. L., Zakharevich, I., Proctor, C., Ying, J., Mesnage, R., Antoniou, M., and Winchester, P. D. (2022). Glyphosate exposure in early pregnancy and reduced fetal growth: a prospective observational study of high-risk pregnancies. *Environmental Health*, 21.

Gillezeau, C., van Gerwen, M., Shaffer, R. M., Rana, I., Zhang, L., Sheppard, L., and Taioli, E. (2019). The evidence of human exposure to glyphosate: a review. *Environmental Health*, 18:663–702.

Global Forest Watch (2023). Global peatlands. Accessed at 03/31/2025.

Gorelick, M. H., Gould, L., Nimmer, M., Wagner, D., Heath, M., Bashir, H., and Brousseau, D. C. (2011). Perceptions About Water and Increased Use of Bottled Water in Minority Children.

Archives of Pediatrics & Adolescent Medicine, 165(10):928–932.

Grant, G. A., Fisher, P. R., Barrett, J. E., and Wilson, P. C. (2018). Removal of agrichemicals from water using granular activated carbon filtration. *Water, Air, & Soil Pollution*, 230(1):7.

Grant, L. E. and Grooms, K. K. (2017). Do nonprofits encourage environmental compliance? *Journal of the Association of Environmental and Resource Economists*, 4(S1):171–202.

Grau, D., Grau, N., Gascuel, Q., Paroissin, C., Stratonovitch, C., Lairon, D., Devault, D. A., and Cristofaro, J. D. (2022). Quantifiable urine glyphosate levels detected in 99% of the french population, with higher values in men, in younger people, and in farmers. *Environmental Science and Pollution Research*, 29.

Greve, J., Schultz-Nielsen, M. L., and Tekin, E. (2017). Fetal malnutrition and academic success: Evidence from muslim immigrants in denmark. *Economics of Education Review*, 60:20–35.

Griffith, K. N., Feyman, Y., Auty, S. G., Crable, E. L., and Levengood, T. W. (2021). County-level data on U.S. opioid distributions, demographics, healthcare supply, and healthcare access. *Data in Brief*, 35:106779.

Groom, B., Palmer, C., and Sileci, L. (2022). Carbon emissions reductions from Indonesia's moratorium on forest concessions are cost-effective yet contribute little to Paris pledges. *Proceedings of the National Academy of Sciences*, 119(5):e2102613119.

Guillaume, T., Kotowska, M. M., Hertel, D., Knohl, A., Krashevska, V., Murtilaksono, K., Scheu, S., and Kuzyakov, Y. (2018). Carbon costs and benefits of Indonesian rainforest conversion to plantations. *Nature Communications*, 9(1):2388.

Hadachek, J. (2024). Benefits of avoiding nitrates in drinking water. *Working paper*.

Hansen, M. C., Potapov, P. V., Moore, R., Hancher, M., Turubanova, S. A., Tyukavina, A., Thau, D., Stehman, S. V., Goetz, S. J., Loveland, T. R., Kommareddy, A., Egorov, A., Chini, L., Justice, C. O., and Townshend, J. R. G. (2013). High-resolution global maps of 21st-century forest cover change. *Science*, 342(6160):850–853.

Harris, N. L., Gibbs, D. A., Baccini, A., Birdsey, R. A., de Bruin, S., Farina, M., Fatoyinbo, L., Hansen, M. C., Herold, M., Houghton, R. A., Potapov, P. V., Suarez, D. R., Roman-Cuesta, R. M., Saatchi, S. S., Slay, C. M., Turubanova, S. A., and Tyukavina, A. (2021). Global maps of twenty-first century forest carbon fluxes. *Nature Climate Change*, 11(3):234–240.

Hashempour-Baltork, F., Torbati, M., Azadmard-Damirchi, S., and Savage, G. P. (2016). Vegetable oil blending: A review of physicochemical, nutritional and health effects. *Trends in Food Science & Technology*, 57:52–58.

Heberling, M. T., Nietch, C. T., Thurston, H. W., Elovitz, M., Birkenhauer, K. H., Panguluri, S., Ramakrishnan, B., Heiser, E., and Neyer, T. (2015). Comparing drinking water treatment costs to source water protection costs using time series analysis. *Water Resources Research*, 51(11):8741–8756.

Heberling, M. T., Price, J. I., Nietch, C. T., Elovitz, M., Smucker, N. J., Schupp, D. A., Safwat, A., and Neyer, T. (2022). Linking water quality to drinking water treatment costs using time series analysis: Examining the effect of a treatment plant upgrade in ohio. *Water Resources Research*, 58(5):e2021WR031257. e2021WR031257 2021WR031257.

Hendricks, N. P., Janzen, J. P., and Smith, A. (2015). Futures prices in supply analysis: Are instrumental variables necessary? *American Journal of Agricultural Economics*, 97(1):22–39.

Hinrichsen, N. (2016). Commercially available alternatives to palm oil. *Lipid Technology*, 28(3-4):65–67.

Hiraishi, T., Krug, T., Tanabe, K., Srivastava, N., Jamsranjav, B., Fukuda, M., and Troxler, T. (2014). *2013 Supplement to the 2006 IPCC Guidelines for National Greenhouse Gas Inventories: Wetlands*. IPCC.

Hobson, W. L., Knochel, M. L., Byington, C. L., Young, P. C., Hoff, C. J., and Buchi, K. F. (2007). Bottled, Filtered, and Tap Water Use in Latino and Non-Latino Children. *Archives of Pediatrics & Adolescent Medicine*, 161(5):457–461.

Hooda, P., Edwards, A., Anderson, H., and Miller, A. (2000). A review of water quality concerns in livestock farming areas. *Science of The Total Environment*, 250(1):143–167.

Hooijer, A., Page, S., Jauhiainen, J., Lee, W. A., Lu, X. X., Idris, A., and Anshari, G. (2012). Subsidence and carbon loss in drained tropical peatlands. *Biogeosciences*, 9(3):1053–1071.

Jaffee, D. (2024). Unequal trust: Bottled water consumption, distrust in tap water, and economic and racial inequality in the united states. *WIREs Water*, 11(2):e1700.

James Seale, J., Regmi, A., and Bernstein, J. (2003). International evidence on food consumption patterns. Technical Bulletin 1904, U.S. Department of Agriculture, Economic Research Service.

Accessed 10/24/2025.

Javidi, A. and Pierce, G. (2018). U.S. households' perception of drinking water as unsafe and its consequences: Examining alternative choices to the tap. *Water Resources Research*, 54(9):6100–6113.

Jhala, A. (2017). Consider application restrictions of postemergence herbicides based on soybean growth stage. `https://cropwatch.unl.edu/2017/consider-application-restrictions-postemergence-herbicides-based-soybean-growth-stage`. Accessed at 01/31/2024.

Jönsson, J., Camm, R., and Hall, T. (2013). Removal and degradation of glyphosate in water treatment: a review. *Journal of Water Supply: Research and Technology-Aqua*, 62(7):395–408.

Kato, T., Kuroda, H., and Nakasone, H. (2009). Runoff characteristics of nutrients from an agricultural watershed with intensive livestock production. *Journal of Hydrology*, 368(1):79–87.

Keiser, D. A. and Shapiro, J. S. (2018). Consequences of the clean water act and the demand for water quality. *The Quarterly Journal of Economics*, 134(1):349–396.

Keiser, D. A. and Shapiro, J. S. (2019). US water pollution regulation over the past half century: Burning waters to crystal springs? *Journal of Economic Perspectives*, 33(4):51–75.

Keyser-Verreault, A. (2023). The continuum of regaining one's body: Childbirth and reproductive choice under beauty pressure in Taiwan. *European Journal of Cultural Studies*, 26(2):167–188.

Kim, K.-H., Kabir, E., and Jahan, S. A. (2017). Exposure to pesticides and the associated human health effects. *Science of The Total Environment*, 575:525–535.

Kongtip, P., Nankongnab, N., Phupancharoensuk, R., Palarach, C., Sujirarat, D., Sangprasert, S., Sermsuk, M., Sawattrakool, N., and Woskie, S. R. (2017). Glyphosate and paraquat in maternal and fetal serums in Thai women. *Journal of Agromedicine*, 22(3):282–289.

Lacroix, R. and Kurrasch, D. M. (2023). Glyphosate toxicity: in vivo, in vitro, and epidemiological evidence. *Toxicological Sciences*, 192(2):131–140.

Lark, T. J., Hendricks, N. P., Smith, A., Pates, N., Spawn-Lee, S. A., Matthew Bougie, E. G. B., Kucharik, C. J., and Gibbs, H. K. (2022). Environmental outcomes of the us renewable fuel standard. *PNAS*, 119(9).

Lesseur, C., Pathak, K. V., Pirrotte, P., Martinez, M. N., Ferguson, K. K., Barrett, E. S., Nguyen, R. H., Sathyanarayana, S., Mandrioli, D., Swan, S. H., and Chen, J. (2022). Urinary glyphosate concentration in pregnant women in relation to length of gestation. *Environmental Research*, 203:111811.

Lima, I. B., Boëchat, I. G., Fernandes, M. D., Monteiro, J. A. F., Rivaroli, L., and Gucker, B. (2022). Glyphosate pollution of surface runoff, stream water, and drinking water resources in southeast Brazil. *Environmental Science and Pollution Research*, 30(10).

Ling, C., Liew, Z., Von Ehrenstein, O. S., Heck, J. E., Park, A. S., Cui, X., Cockburn, M., Wu, J., and Ritz, B. (2018). Prenatal exposure to ambient pesticides and preterm birth and term low birthweight in agricultural regions of California. *Toxics*, 6(3).

Liu, P., Wang, Y., and Zhang, W. (2023). The influence of the environmental quality incentives program on local water quality. *American Journal of Agricultural Economics*, 105(1):27–51.

Lustgarten, A. (2018). Palm Oil Was Supposed to Help Save the Planet. Instead It Unleashed a Catastrophe. *The New York Times*.

Malaguerra, F., Albrechtsen, H.-J., Thorling, L., and Binning, P. J. (2012). Pesticides in water supply wells in zealand, denmark: A statistical analysis. *Science of The Total Environment*, 414:433–444.

Malecki, K. M., Schultz, A. A., Severtson, D. J., Anderson, H. A., and VanDerslice, J. A. (2017). Private-well stewardship among a general population based sample of private well-owners. *Science of The Total Environment*, 601-602:1533–1543.

Mallat, E. and Barcelo, D. (1998). Analysis and degradation study of glyphosate and of aminomethylphosphonic acid in natural waters by means of polymeric and ion-exchange solid-phase extraction columns followed by ion chromatography-post-column derivatization with fluorescence detection. *Journal of Chromatography A*, 823(1):129–136.

Marcus, M. (2022). Testing the water: Drinking water quality, public notification, and child outcomes. *The Review of Economics and Statistics*, 104(6):1289–1303.

Martins-Gomes, C., Silva, T. L., Andreani, T., and Silva, A. M. (2022). Glyphosate vs. glyphosate-based herbicides exposure: A review on their toxicity. *Journal of Xenobiotics*, 12(1):21–40.

McCarthy, J. F., Gillespie, P., and Zen, Z. (2012). Swimming upstream: Local Indonesian production networks in "globalized" palm oil production. *World Development*, 40(3):555–569.

Medalie, L., Baker, N. T., Shoda, M. E., Stone, W. W., Meyer, M. T., Stets, E. G., and Wilson, M. (2020). Influence of land use and region on glyphosate and aminomethylphosphonic acid in streams in the usa. *Science of The Total Environment*, 707:136008.

Mendez, F., Ordoñez-Betancourth, J., and Abrahams, N. (2022). Effects of glyphosate exposure on reproductive health: A systematic review of human, animal and in-vitro studies. *Exposure and Health*, 14:635–669.

Miettinen, J., Shi, C., and Liew, S. C. (2016). Land cover distribution in the peatlands of Peninsular Malaysia, umatra and Borneo in 2015 with changes since 1990. *Global Ecology and Conservation*, 6:67–78.

Mills, P. J., Kania-Korwel, I., Fagan, J., McEvoy, L. K., Laughlin, G. A., and Barrett-Connor, E. (2017). Excretion of the Herbicide Glyphosate in Older Adults Between 1993 and 2016. *JAMA*, 318(16):1610–1611.

Mocan, N., Raschke, C., and Unel, B. (2015). The impact of mothers' earnings on health inputs and infant health. *Economics & Human Biology*, 19:204–223.

Mose, T., Kjaerstad, M. B., Mathiesen, L., Nielsen, J. B., Edelfors, S., and Knudsen, L. E. (2008). Placental passage of benzoic acid, caffeine, and glyphosate in an ex vivo human perfusion system. *Journal of Toxicology and Environmental Health, Part A*, 71(15):984–991.

Mueller, J. T. and Gasteyer, S. (2021). The widespread and unjust drinking water and clean water crisis in the United States. *Nature Communications*, 12(3544).

Muñoz Sabater, J. (2019). ERA5-land monthly averaged data from 1950 to present. Copernicus Climate Change Service (C3S) Climate Data Store (CDS). `DOI:10.24381/cds.68d2bb30`. Accessed at 10/31/2024.

Myers, J. P., Antoniou, M. N., Blumberg, B., Carroll, L., Colborn, T., Everett, L. G., Hansen, M., Landrigan, P. J., Lanphear, B. P., Mesnage, R., Vandenberg, L. N., vom Saal, F. S., Welshons, W. V., and Benbrook, C. M. (2016). Concerns over use of glyphosate-based herbicides and risks associated with exposures: a consensus statement. *Environmental Health*, 15(19).

Naeve, S. L. (2018). Soybean growth stages. https://extension.umn.edu/growing-soybean/soybean-growth-stages. Accessed at 01/31/2024.

Noojipady, P., Morton, D. C., Schroeder, W., Carlson, K. M., Huang, C., Gibbs, H. K., Burns, D., Walker, N. F., and Prince, S. D. (2017). Managing fire risk during drought: the influence of certification and El Niño on fire-driven forest conversion for oil palm in Southeast Asia. *Earth System Dynamics*, 8(3):749–771.

OECD/FAO (2023). Oecd-fao agricultural outlook 2023-2032. https://doi.org/10.1787/08801ab7-en. Accessed at 1/6/2025.

Osawa, T., Kohyama, K., and Mitsuhashi, H. (2016). Multiple factors drive regional agricultural abandonment. *Science of The Total Environment*, 542:478–483.

Ospina, M., Schütze, A., Morales-Agudelo, P., Vidal, M., Wong, L.-Y., and Calafat, A. M. (2022). Exposure to glyphosate in the united states: Data from the 2013–2014 national health and nutrition examination survey. *Environment International*, 170:107620.

Page, S. E., Rieley, J. O., and Banks, C. J. (2011). Global and regional importance of the tropical peatland carbon pool. *Global Change Biology*, 17(2):798–818.

Park, S., Onufrak, S. J., Cradock, A. L., Hecht, C., Patel, A., Chevinsky, J. R., and Blanck, H. M. (2022). Factors related to water filter use for drinking tap water at home and its association with consuming plain water and sugar-sweetened beverages among u.s. adults. *American Journal of Health Promotion*, 36(5):813–822.

Parvez, S., Gerona, R. R., Proctor, C., Friesen, M., Ashby, J. L., Reiter, J. L., Lui, Z., and Winchester, P. D. (2018). Glyphosate exposure in pregnancy and shortened gestational length: a prospective indiana birth cohort study. *Environmental Health*, 17.

Pendrill, F., Gardner, T. A., Meyfroidt, P., Persson, U. M., Adams, J., Azevedo, T., Lima, M. G. B., Baumann, M., Curtis, P. G., Sy, V. D., Garrett, R., Godar, J., Goldman, E. D., Hansen, M. C., Heilmayr, R., Herold, M., Kuemmerle, T., Lathuillière, M. J., Ribeiro, V., Tyukavina, A., Weisse, M. J., and West, C. (2022). Disentangling the numbers behind agriculture-driven tropical deforestation. *Science*, 377(6611):eabm9267.

Pendrill, F., Persson, U. M., Godar, J., Kastner, T., Moran, D., Schmidt, S., and Wood, R. (2019). Agricultural and forestry trade drives large share of tropical deforestation emissions. *Global*

Environmental Change, 56:1–10.

Pieper, K. J., Krometis, L.-A. H., Gallagher, D. L., Benham, B. L., and Edwards, M. (2015). Incidence of waterborne lead in private drinking water systems in Virginia. *Journal of Water and Health*, 13(3):897–908.

Poulsen, M. S., Rytting, E., Mose, T., and Knudsen, L. E. (2009). Modeling placental transport: Correlation of in vitro bewo cell permeability and ex vivo human placental perfusion. *Toxicology in Vitro*, 23(7):1380–1386.

Qaim, M. (2009). The economics of genetically modified crops. *Annual Review of Resource Economics*, 1:665–694.

Ransom, J. and Endres, G. (2020). Corn growth and management quick guide. `https://www.ndsu.edu/agriculture/ag-hub/publications/corn-growth-and-management-quick-guide`. Accessed at 01/31/2024.

Rendon-von Osten, J. and Dzul-Caamal, R. (2017). Glyphosate residues in groundwater, drinking water and urine of subsistence farmers from intensive agriculture localities: A survey in hopelchén, campeche, mexico. *International Journal of Environmental Research and Public Health*, 14(6).

Reynier, E. and Rubin, E. (2025). Glyphosate exposure and gm seed rollout unequally reduced perinatal health. *Proceedings of the National Academy of Sciences*, 122(3):e2413013121.

Richard, S., Moslemi, S., Sipahutar, H., Benachour, N., and Seralini, G.-E. (2005). Differential effects of glyphosate and roundup on human placental cells and aromatase. *Environmental Health Perspectives*, 113(6):716–720.

Roberts, M. J. and Schlenker, W. (2013). Identifying supply and demand elasticities of agricultural commodities: Implications for the US ethanol mandate. *American Economic Review*, 103(6):2265–95.

Rosinger, A. Y., Herrick, K. A., Wutich, A. Y., Yoder, J. S., and Ogden, C. L. (2018). Disparities in plain, tap and bottled water consumption among us adults: National health and nutrition examination survey (NHANES) 2007–2014. *Public Health Nutrition*, 21(8):1455–1464.

Rubin, S. J. (2013). Evaluating violations of drinking water regulations. *Journal AWWA*, 105(3):E137–E147.

Rum, I. A., Tukker, A., de Koning, A., and Yusuf, A. (2022). Impact assessment of the EU import ban on Indonesian palm oil: Using environmental extended multi-scale mrio. *Science of The Total Environment*, 853:158695.

Savitz, D. A., Arbuckle, T., Kaczor, D., and Curtis, K. M. (1997). Male Pesticide Exposure and Pregnancy Outcome. *American Journal of Epidemiology*, 146(12):1025–1036.

Searchinger, T., Heimlich, R., Houghton, R. A., Dong, F., Elobeid, A., Fabiosa, J., Tokgoz, S., Hayes, D., and Yu, T.-H. (2008). Use of U.S. croplands for biofuels increases greenhouse gases through emissions from land-use change. *Science*, 319(5867):1238–1240.

Searchinger, T., Peng, L., Zionts, J., and Waite, R. (2023). The global land squeeze: Managing the growing competition for land. Technical report, World Resources Institute, Washington, D.C.

Shoda, M. E., Baker, N. T., and Medalie, L. (2020). Glyphosate and aminomethylphosphonic acid (AMPA) in national water quality network streams and rivers in the U.S., water years 2015-2017. *U.S. Geological Survey data release*.

Sigman, H. (2005). Transboundary spillovers and decentralization of environmental policies. *Journal of Environmental Economics and Management*, 50(1):82–101.

Silver, M. K., Fernandez, J., Tang, J., McDade, A., Sabino, J., Rosario, Z., Vega, C. V., Alshawabkeh, A., Cordero, J. F., and Meeker, J. D. (2021). Prenatal exposure to glyphosate and its environmental degradate, aminomethylphosphonic acid (AMPA), and preterm birth: A nested case–control study in the PROTECT cohort (Puerto Rico). *Environmental Health Perspectives*, 129(5):057011.

Skidmore, M. E., Sims, K. M., and Gibbs, H. K. (2023). Agricultural intensification and childhood cancer in brazil. *Proceedings of the National Academy of Sciences*, 120(45):e2306003120.

Smith, A. and Taylor, J. E. (2017). *Essentials of Applied Econometrics*. University of California Press, 1 edition.

Smith, T., Krometis, L.-A. H., Hagedorn, C., Lawrence, A. H., Benham, B., Ling, E., Ziegler, P., and Marmagas, S. W. (2014). Associations between fecal indicator bacteria prevalence and demographic data in private water supplies in Virginia. *Journal of Water and Health*, 12(4):824–834.

S&P Global (2024). Biodiesel and renewable diesel. https://www.spglobal.com/content/dam/spglobal/ci/en/documents/products/pdf/CI_0325_Global_CEH_Biodiesel_and_Renewable_Diesel_Abstract.pdf. Accessed at 08/20/2025.

Squillace, P. J., Thurman, E. M., and Furlong, E. T. (1993). Groundwater as a nonpoint source of atrazine and deethylatrazine in a river during base flow conditions. *Water Resources Research*, 29(6):1719–1729.

Taheripour, F. and Tyner, W. E. (2020). US biofuel production and policy: implications for land use changes in Malaysia and Indonesia. *Biotechnology for Biofuels*, 13(1):11.

Tajai, P., Pruksakorn, D., Chattipakorn, S. C., Chattipakorn, N., and Shinlapawittayatorn, K. (2023). Effects of glyphosate-based herbicides and glyphosate exposure on sex hormones and the reproductive system: From epidemiological evidence to mechanistic insights. *Environmental Toxicology and Pharmacology*, 102:104252.

Teodoro, M. P., Haider, M., and Switzer, D. (2018). U.s. environmental policy implementation on tribal lands: Trust, neglect, and justice. *Policy Studies Journal*, 46(1):37–59.

Tiramani, M., Reich, H., Pfeil, R., Istace, F., and Crivellente, F. (2017). Glyphosate toxicity and carcinogenicity: a review of the scientific basis of the european union assessment and its differences with IARC. *Archives of Toxicology*, 91:2723–2743.

Triplett, R., Chatterjee, C., Johnson, C. K., and Ahmed, P. (2019). Perceptions of quality and household water usage: A representative study in jacksonville, FL. *International Advances in Economic Research*, 25:195–208.

Tropek, R., Sedláček, O., Beck, J., Keil, P., Musilová, Z., Šímová, I., and Storch, D. (2014). Comment on "high-resolution global maps of 21st-century forest cover change". *Science*, 344(6187):981–981.

Tudge, S. J., Purvis, A., and Palma, A. D. (2021). The impacts of biofuel crops on local biodiversity: a global synthesis. *Biodiversity and Conservation*, 30(11):2863–2883.

United States Department of Agriculture, Foreign Agricultural Service (2025). PSD Online: Production, supply, and distribution database. Accessed 2024/11/18/2024.

U.S. Bureau of Economic Analysis (2024). Gdp price deflator. Accessed 04/21/2024.

US Energy Information Administration (2025). Monthly biofuels capacity and feedstocks update. https://www.eia.gov/biofuels/update/. Accessed at 09/01/2025.

US Environmental Protection Agency (2016). Lifecycle greenhouse gas emissions for select pathways. https://www.epa.gov/sites/default/files/2016-07/documents/select-ghg-results-table-v1.pdf. Accessed at 7/5/2025.

USDA (2010). Field crops usual planting and harvesting dates. https://www.nass.usda.gov/Publications/Todays_Reports/reports/fcdate10.pdf. Accessed at 01/31/2024.

USDA (2024). European Union: Biofuels annual. https://www.fas.usda.gov/data/european-union-biofuels-annual-4. Accessed at 12/09/2024.

Useche, P., Barham, B. L., and Foltz, J. D. (2009). Integrating technology traits and producer heterogeneity: A mixed-multinomial model of genetically modified corn adoption. *American Journal of Agricultural Economics*, 91(2):444–461.

Uusitalo, V., Väisänen, S., Havukainen, J., Havukainen, M., Soukka, R., and Luoranen, M. (2014). Carbon footprint of renewable diesel from palm oil, jatropha oil and rapeseed oil. *Renewable Energy*, 69:103–113.

Van Stempvoort, D. R., Spoelstra, J., Senger, N. D., Brown, S. J., Post, R., and Struger, J. (2016). Glyphosate residues in rural groundwater, nottawasaga river watershed, ontario, canada. *Pest Management Science*, 72(10):1862–1872.

Viscusi, W. K., Huber, J., and Bell, J. (2015). The private rationality of bottled water drinking. *Contemporary Economic Policy*, 33(3):450–467.

Wang, T., Luri, M., Janssen, L., Hennessy, D. A., Feng, H., Wimberly, M. C., and Arora, G. (2017). Determinants of motives for land use decisions at the margins of the Corn Belt. *Ecological Economics*, 134:227–237.

Warnemuende, E. A., Patterson, J. P., Smith, D. R., and hua Huang, C. (2007). Effects of tilling no-till soil on losses of atrazine and glyphosate to runoff water under variable intensity simulated rainfall. *Soil and Tillage Research*, 95(1):19–26.

Warner, E., Zhang, Y., Inman, D., and Heath, G. (2014). Challenges in the estimation of greenhouse gas emissions from biofuel-induced global land-use change. *Biofuels, Bioproducts and Biorefining*, 8(1):114–125.

Weschenfelder, F., Lehmann, T., Schleussner, E., and Groten, T. (2019). Gestational weight gain particularly affects the risk of large for gestational age infants in non-obese mothers. *Geburtshilfe Frauenheilkd*, 79(11):1183–1190.

Wickerham, E. L., Lozoff, B., Shao, J., Kaciroti, N., Xia, Y., and Meeker, J. D. (2012). Reduced birth weight in relation to pesticide mixtures detected in cord blood of full-term infants. *Environment International*, 47:80–85.

Winter, T. C., Harvey, J. W., Franke, O. L., and Alley, W. M. (1998). Ground water and surface water: A single resource. *U.S. Geological Survey*.

Woittiez, L. S., van Wijk, M. T., Slingerland, M., van Noordwijk, M., and Giller, K. E. (2017). Yield gaps in oil palm: A quantitative review of contributing factors. *European Journal of Agronomy*, 83:57–77.

World Bank (2025). Commodity markets. Accessed 02/28/2024.

Xu, H., He, B., Guo, L., Yan, X., Dong, J., Yuan, W., Hao, X., Lv, A., He, X., and Li, T. (2024). Changes in the fine composition of global forests from 2001 to 2020. *Journal of Remote Sensing*, 4:0119.

Yang, E. and Faust, K. M. (2019). Human–water infrastructure interactions: Substituting services received for bottled and filtered water in us shrinking cities. *Journal of Water Resources Planning and Management*, 145(12):04019056.

Yang, Y., Tilman, D., Jin, Z., Smith, P., Barrett, C. B., Zhu, Y.-G., Burney, J., D'Odorico, P., Fantke, P., Fargione, J., Finlay, J. C., Rulli, M. C., Sloat, L., van Groenigen, K. J., West, P. C., Ziska, L., Michalak, A. M., the Clim-Ag Team, Lobell, D. B., Clark, M., Colquhoun, J., Garg, T., Garrett, K. A., Geels, C., Hernandez, R. R., Herrero, M., Hutchison, W. D., Jain, M., Jungers, J. M., Liu, B., Mueller, N. D., Ortiz-Bobea, A., Schewe, J., Song, J., Verheyen, J., Vitousek, P., Wada, Y., Xia, L., Zhang, X., and Zhuang, M. (2024). Climate change exacerbates the environmental impacts of agriculture. *Science*, 385(6713):eadn3747.

Yu, Q., You, L., Wood-Sichra, U., Ru, Y., Joglekar, A. K. B., Fritz, S., Xiong, W., Lu, M., Wu, W., and Yang, P. (2020). A cultivated planet in 2010 – part 2: The global gridded agricultural-production maps. *Earth System Science Data*, 12(4):3545–3572.

Zhao, R., Xu, L., Wu, M., Huang, S., and Cao, X. (2018). Maternal pre-pregnancy body mass index, gestational weight gain influence birth weight. *Women and Birth*, 31(1):e20–e25.